UNIVERSITÀ' DEGLI STUDI DI TRIESTE

XXVIII CICLO DEL DOTTORATO DI RICERCA IN

BIOLOGIA AMBIENTALE

MARINE COMMUNITIES OF BACTERIA AND PROTISTS, THEIR BIODIVERSITY AND INTERACTIONS

Settore scientifico-disciplinare: BIO/07

DOTTORANDO
LUCA ZOCCARATO

COORDINATORE
PROF. SERENA FONDA UMANI

SUPERVISORE DI TESI
PROF. ALBERTO PALLAVICINI
DOTT. MAURO CELUSSI

ANNO ACCADEMICO 2014 / 2015

RIASSUNTO

Ci sono più di 10^{30} batteri sul nostro pianeta, essi rappresentano quindi la forma di vita più abbondante, hanno infatti colonizzato tutti i tipi di ambiente dalle profondità oceaniche alle Dry Valleys in Antartide, sono in grado di sopravvivere in condizioni estreme come nei pressi dei vulcani sottomarini o in pozze e fiumi di natura effimera che si formano nelle distese di sale; concentrazioni relativamente alte sono state anche descritte di recente in atmosfera e questi procarioti potrebbero essere coinvolti nei processi di formazione delle nuvole. In aggiunta alla loro ubiquitarietà, i procarioti ricoprono anche ruoli chiave all'interno dei cicli biogeochimici e nel funzionamento degli ecosistemi. I procarioti marini sono numerosi quanto quelli terrestri (circa 1.2×10^{29}, 2.6×10^{29}, 3.5×10^{30}, e $0.25–2.5 \times 10^{30}$ rispettivamente negli oceani, nel suolo e nei sedimenti marini e terrestri) e sono coinvolti in diversi processi come i cicli dei nutrienti, il sequestro di CO_2 e la rimineralizzazione della materia organica. Essi rappresentano la base delle reti trofiche marine ponendosi come primo livello nei flussi di carbonio, e costituiscono inoltre la struttura portante della pompa biologica del carbonio.

Possiamo suddividere i procarioti marini nella frazioni fotoautotrofa ed eterotrofa anche se è stata recentemente dimostrata l'importanza di organismi dotati di strategie trofiche alternative come i fotoeterotrofi e i chemolitotrofi.

I procarioti fotoautotrofi sono tra i maggiori produttori primari degli oceani alimentando le reti trofiche pelagiche soprattutto in condizioni di oligotrofia. Così come il fitoplancton eucariotico, essi sono in grado di prelevare dall'ambiente nutrienti in forma inorganica e fissare la CO_2 per produrre nuova materia organica attraverso lo sfruttamento delle radiazioni solari. Grazie alle loro ridotte dimensioni (elevato rapporto superficie/volume) e alle loro cinetiche di assimilazione, questi procarioti sono in grado di surclassare organismi più grandi negli ambienti più poveri di risorse come le regioni pelagiche. La frazione eterotrofa dei procarioti raggruppa invece i principali consumatori

della materia organica (circa 14-20 volte la quantità di carbonio organico terrestre) contribuendo alla rimineralizzazione dei nutrienti.

All'interno del ciclo microbico, la biomassa dei procarioti viene continuamente riciclata tramite lisi virale che rilascia nell'ambiente i contenuti delle cellule incrementando temporaneamente il pool di materia organica disciolta. La biomassa dei procarioti può anche fluire verso i livelli trofici superiori canalizzata dalla predazione operata da nanoflagellati eterotrofi e piccoli ciliati. Mentre l'importanza della lisi virale è ancora in discussione a causa di risultati contrastanti emersi da studi effettuati in ambienti differenti, la pressione di grazing (predazione) è ampiamente riconosciuta come uno dei principali fattori che modellano le comunità di procarioti. Il ruolo dei grazers è dunque cruciale all'interno delle comunità planctoniche poiché influisce sul controllo della biomassa delle prede ed al contempo influenzano la biodiversità e la struttura delle loro comunità.

Il primo capitolo della mia tesi intitolato "Major contribution of prokaryotes in the pelagic microbial food webs in the Mediterranean Sea" si propone di studiare i flussi di carbonio nel mondo microbico in diverse aree del Mar Mediterraneo. Il focus è stato posto sulla pressione di predazione esercitata da protisti di 2-200 μm di diametro (nanoflagellati eterotrofi, ciliati e piccoli dinoflagellati eterotrofi) sui procarioti. Il lavoro è stato svolto con la finalità di stimare l'importanza della biomassa procariotica come fonte principale di carbonio a supporto delle reti trofiche pelagiche mediterranee in differenti condizioni di trofia.

L'ingestione di procarioti da parte dei predatori è stata valutata usando la tecnica delle diluizioni, ovverosia tramite esperimenti che permettono di determinare se le prede sono efficacemente controllate dai predatori. Nello studio abbiamo analizzato più di 80 esperimenti di diluizione portati a termine in 15 siti sparsi in tutto il Mar Mediterraneo, dal Mar Egeo all'oceano Atlantico. I procarioti hanno mostrato sempre i valori più elevati di biomassa ad eccezione delle situazioni di eutrofizzazione dove la biomassa del microfitoplancton era più alta (in concomitanza con eventi di

fioritura). L'ingestione di procarioti è risultata essere la via principale per il flusso di carbonio in condizioni oligotrofiche, mesotrofiche ed eutrofiche. Tale flusso è risultato essere significativo anche in situazioni di eutrofizzazione marcata, quando cioè prevaleva la rete trofica classica e l'ingestione di microfitoplancton. Analizzando l'efficienza delle reti trofiche è emerso come essa raggiunga i valori massimi in condizioni meso- eutrofiche, mentre durante gli eventi di eutrofizzazione la produzione potenziale dei procarioti e del fitoplancton eccede i tassi di ingestione dei predatori e l'efficienza risulta essere inferiore anche a quella stimata in condizioni di oligotrofia. Lo sbilanciamento tra produzione e consumo ha creato un surplus di biomassa che può aver favorito e supportato la crescita di predatori di taglia maggiore (> 200 μm) e/o può aver dato origine a sedimentazione ed export verso il fondo. L'ingestione dei procarioti è risultata essere una via efficiente per il trasferimento di carbonio verso i livelli trofici superiori anche nei domini meso- e batipelagici dove le nostre analisi hanno rilevato un'efficienza relativamente alta a supporto della teoria degli hot-spot. La distribuzione dei microrganismi nelle profondità oceaniche si ritiene infatti essere associata a micro particelle di materia organica in sprofondamento che vanno quindi a creare dei micro-hot spot di diversità.

Le comunità microbiche in tutti gli oceani sono caratterizzate da una variabilità spaziale e dalla presenza di pattern regionali. Diversi fattori locali e regionali possono esercitare un controllo bottom-up su questi popolamenti inducendone cambiamenti di abbondanza e di composizione nel corso del tempo. L'occorrenza o la co-occorrenza di variazioni di condizioni ambientali, di proprietà fisico-chimiche dell'acqua, di interazioni all'interno delle comunità, così come i limiti di dispersione degli organismi e le barriere idrografiche sono stati evidenziati come i maggiori fattori che modellano le comunità microbiche. Tuttavia, come evidenziato nel primo capitolo, anche la mortalità mediata dai virus e/o dai predatori può avere effetti considerevoli. La predazione infatti

esercita un controllo di tipo top-down sulle comunità microbiche ed è stata spesso identificata come la maggior causa di morte per i procarioti; alcuni esperimenti hanno inoltre evidenziato che il processo di predazione tende ad essere selettivo nei confronti di prede metabolicamente più attive. In queste dinamiche molto può dipendere dalla composizione specifica delle comunità dei predatori. Questi organismi sono principalmente protisti ed a seconda della tassonomia presentano differenti strategie di alimentazione (es. filtratori, a sedimentazione, ad intercettazione, cacciatori, a metabolismo osmotrofo).

Significativi passi avanti nella comprensione della diversità delle comunità di procarioti e di protisti sono stati raggiunti recentemente grazie al progresso tecnologico, uno su tutti l'avvento delle tecniche di sequenziamento di nuova generazione. Tali metodologie hanno permesso di superare i limiti precedenti (ad esempio l'incapacità di coltivare la maggior parte dei ceppi batterici ambientali, l'inadeguatezza delle analisi morfologiche e le limitazioni dei metodi chemotassonomici), e svariati studi sono stati portati a termine al fine di esplorare e rivelare la struttura delle comunità microbiche.

Il secondo capitolo della mia tesi intitolato "Water mass dynamics shape Ross Sea protist communities in meso- and bathypelagic layers" si prefigge di descrivere la biodiversità ancora sconosciuta delle comunità di protisti nel Mare di Ross.

Sono stati raccolti 13 campioni di comunità meso- batipelagiche di protisti durante la XXIX Spedizione Italiana in Antartide. Tutte le principali masse d'acqua profonde del Mare di Ross sono state campionate inclusa la High Salinity Shelf Waters (HSSW; masse d'acqua di piattaforma continentale ad elevata salinità), la Ice Shelf Water (ISW; masse d'acqua gelida di piattaforma), la Circumpolar Deep Water (CDW; corrente profonda circumpolare) e l'Antarctic Bottom Water (AABW; massa d'acqua profonda di origine antartica). L'approccio metodologico di analisi dei

campioni si è basato su tecniche di sequenziamento ad elevata resa eseguite con piattaforma Ion Torrent PGM.

L'analisi dei risultati ha evidenziato come le comunità di protisti siano modellate in relazione alla storia delle masse d'acqua: le HSSW di recente formazione presentavano comunità di protisti caratterizzate da un'elevata abbondanza relativa di organismi autotrofi; questi organismi in genere si sviluppano in superficie ma sono stati trovati a diverse centinaia di metri di profondità. Al contrario, CDW di più vecchia formazione hanno mostrato maggiori abbondanze di taxa come Excavata, Cercozoa (entrambi tipicamente batterivori), Radiolaria e Apicomplexa (generalmente parassiti). Risultati interessanti sono emersi dalle AABW, formatesi per inclusione di acque di piattaforma (HSSW e ISW) nella CDW; questa massa d'acqua infatti presentava firme genetiche eucariotiche tipiche di entrambe le masse d'acqua di origine.

In generale abbiamo rilevato un forte effetto di partizionamento sulle comunità di protisti generato dalle masse d'acqua; questo dato suggerisce come i fattori ambientali che rendono uniche le caratteristiche oceanografiche del bacino abbiano anche una profonda influenza sulle comunità di microorganismi presenti.

Lo stesso approccio molecolare di sequenziamento ad elevata resa è stato adottato anche per studiare le comunità procariotiche e le alterazioni indotte in esse dalla presenza di meduse. Il terzo e ultimo capitolo della tesi intitolato "*Aurelia aurita* ephyrae reshape a coastal microbial community" si prefigge infatti di fornire una descrizione comprensiva dell'influenza delle efire di *Aurelia aurita* a livello delle comunità microbiche pelagiche nel Golfo di Trieste.

Il capitolo getta luce sulle scarse conoscenze delle interazioni tra stadi giovanili delle meduse con protisti e procarioti marini. La scelta di *Aurelia aurita* come organismo modello per lo studio si è basata sui dati di notevole abbondanza e diffusione che caratterizzano questo taxon di scifozoi; negli

ultimi decenni si è inoltre assistito a incrementi nei trends di abbondanze e di bloom di questa medusa. L'intento del nostro lavoro nello specifico è stato quello di descrivere il duplice ruolo di *Aurelia aurita* come top-down e bottom-up controller sulle comunità microbiche.

Il disegno sperimentale si è basato su esperimenti di microcosmo prendendo in considerazione diversi parametri quali la biomassa delle prede, la produzione eterotrofa di carbonio (HCP), l'attività enzimatica extracellulare, la concentrazione del carbonio organico disciolto (DOC) e la pressione di grazing. L'approccio analitico combinava "tradizionali" osservazioni al microscopio con le nuove tecniche molecolari e con la stima delle alterazioni nelle funzionalità delle comunità procariotiche intese come produzione secondaria e processi di degradazione.

I risultati hanno evidenziato una predazione selettiva delle efire su diversi gruppi del microplancton correlata con l'abbondanza ed il livello di motilità delle prede; nessuna strategia di selezione invece è stata rilevata a livello di composizione tassonomica. La diversità delle comunità procariotiche sono risultate anch'esse sensibili alla presenza delle efire poiché sono stati rilevati incrementi significativi nelle abbondanze relative di taxa copiotrofi. La nostra ipotesi sulle ragioni alla base delle alterazioni rilevate sia rifà ai cambiamenti nella composizione del pool di DOC indotti da parte delle efire. Questi animali rilasciano infatti sostanze colloidali che hanno innescato un cambiamento nelle comunità procariotiche accompagnati tuttavia da ridotti incrementi di HCP; la ridotta produzione secondaria è probabilmente dovuta alla complessità ed alla scarsa biodisponibilità del DOC prodotto da queste meduse.

Il capitolo fornisce un nuovo approfondimento sugli effetti delle efire di *Aurelia* sulle comunità microbiche migliorando la nostra comprensione delle implicazioni ecologiche connesse ai bloom di meduse. Questi eventi stanno avendo un incremento costante negli ultimi anni legato probabilmente all'innalzamento della temperatura superficiale dei mari e ad altri fattori antropici, e potrebbero rappresentare un problema critico per tutti gli ecosistemi marini in un prossimo

futuro. Il lavoro rappresenta inoltre una visione integrata di come la pressione di predazione possa modificare le comunità microbiche attraverso un effetto diretto (sui protisti) ed indiretto (sui procarioti).

SUMMARY

There are more than 10^{30} bacteria on our planet, which represent the most abundant living form. They have colonized almost all environments from the deep oceans to the Dry Valleys in Antarctica. They are able to survive and live also in extreme environments such as thermal vents or ephemeral streams and ponds in salt plains; recently, relatively high concentrations have been assessed also in atmosphere where they might be involved in cloud formations. In addition to their ubiquity, prokaryotes act also as key players within biogeochemical cycles and in the ecosystem functioning. Marine prokaryotes are as numerous as terrestrial ones (almost 1.2×10^{29}, 2.6×10^{29}, 3.5×10^{30}, and $0.25–2.5 \times 10^{30}$ in the open ocean, in soil, and in oceanic and terrestrial subsurfaces, respectively) and they are involved in several processes like nutrient cycles, CO_2 sequestration and organic matter remineralization. They represent the base of marine trophic food webs being the first step of the carbon fluxes; moreover, they are the essential gears sustaining the biological carbon pump.

For the purpose of this thesis, we can divide marine prokaryotes in photoautotrophic and heterotrophic fractions although the relevance of organisms characterized by alternative life strategies, such as the photoheterotrophs and the chemolithotrophs, have been demonstrated.

Photoautotrophic prokaryotes are one of the major primary producers in the oceans fueling pelagic food webs especially in oligotrophic conditions. As well as the eukaryotic phytoplankton, they are able to uptake inorganic nutrient and fix carbon dioxide to produce new organic matter through the exploitation of solar irradiance. However, thanks to their small size (higher surface/volume ratio) and their uptake kinetics, these prokaryotes are able to outcompete larger organisms especially in environments poor of resources such as pelagic regions. The heterotrophic fraction of prokaryotes

represents instead the principal consumers of the organic matter (that represent 14 to 20 times the amount of terrestrial organic carbon) contributing to the remineralization of nutrients.

Inside the microbial loop, the biomass of all prokaryotes is continuously recycled via viral lysis that release in the environment the cell contents and thus temporarily increase the pool of dissolved organic matter. Prokaryotes biomass can also flow towards upper trophic levels channeled by grazing activity of heterotrophic nanoflagellates and small ciliates. While the relevance of viral lysis is still an open debate due to contrasting results emerged from studies on different environments, the grazing pressure is largely recognized as one of the major factor shaping prokaryote communities. The role of grazers is pivotal within plankton communities since they control the biomass of the prey while also affecting the biodiversity and structures of their assemblages.

The first chapter of my thesis entitled “Major contribution of prokaryotes in the pelagic microbial food webs in the Mediterranean Sea” was thus aimed to the study of carbon fluxes within microbial world in several areas of the Mediterranean Sea. The focus was set on the grazing pressure exerted by protists of 2-200 µm of size (i.e. heterotrophic nanoflagellates, ciliates and small heterotrophic dinoflagellates) on prokaryotes in order to assess the relevance of prey biomass as principal source of carbon supporting pelagic food webs among different trophic conditions in the Mediterranean Sea.

The ingestion of prokaryotes by grazers was assessed according with the dilution technique that allows to determine whenever prey communities are efficiently controlled by predators. In the study, I analyzed more than 80 dilution experiments carried out at 15 sites spread around the Mediterranean Sea from the Aegean Sea to the Atlantic Ocean. Prokaryotes showed always the highest biomasses with the exception of eutrophicated situations when microphytoplankton biomass was higher (concurrently with bloom events). Bacterivory resulted to be the major pathway for carbon flux in oligo-, meso- and eutrophic conditions although even in eutrophicated situations,

when herbivory prevailed, the carbon flux generated by ingestion on prokaryotes was still relevant. Analyzing the efficiency of those food webs emerged how it reached the maximum values in meso-eutrophic situations while during eutrophicated events the potential production of prokaryotes and of microphytoplankton exceeded grazer ingestion rates. This unbalance created a surplus of biomass that may have allowed the growth of larger predators population and/or may have generated sinking events with export toward the bottom. Prokaryotes' consumption still represented an efficient pathway for carbon transfer also in the meso- bathypelagic layers and the investigation, although targeted on shorted trophic food webs, highlighted relative high efficiencies supporting the theory of the marine deep hot spot. In fact, the distribution of microorganisms in deep ocean is believed to be associated with sinking micro particles of organic matter, which create micro-hot spots of diversity.

Spatial variability and regional patterns have been demonstrated to characterize the distribution of microbial communities in global oceans. Several local and regional factors can bottom-up control these population and induce changes in abundance and composition over time. The occurrence or co- occurrence of variations in environmental conditions, in physiochemical properties of the water mass, in community interactions, as well as organisms' dispersal limitation and the presence of hydrographic barriers were pointed out as major drivers shaping microbial communities. However, as assessed in the first chapter, also the mortality mediated by viruses and/or grazers can have remarkable effects. The predation activity– top-down control – was often identified as the main cause of prokaryotic loss and some experimental evidences support that feeding process tends to be more selective on metabolically active cells rather than inactive cells. Furthermore, also the composition of grazers' community might influence prey selection since bacterivores are mainly protists and different taxa are known to display different feeding strategies (e.g. filter-feeding,

sedimentation, interception feeding, raptorial, hosmotroph). Breakthrough advances in our comprehension of prokaryote and protist community compositions were recently achieved thanks to technological progress, one above all the advent of Next-Generation Sequencing (NGS) techniques. These methodologies significantly enhanced our understanding of the diversity of microorganisms and they allowed to overcome previous methodological limitations (i.e. un-cultivability of marine bacteria, unsuitability of morphological analysis and limitations of chemotaxonomic methods); several studies were carried out to explore and reveal the structures of microbial communities.

The second chapter of my thesis entitled "Water mass dynamics shape Ross Sea protist communities in meso- and bathypelagic layers" was aimed to describe the unknown diversity of protist communities in the Ross Sea.

Thirteen samples of protist communities were collected at meso- bathypelagic depths during the XXIX Italian expedition in Antarctica. All the principal deep water masses of the Ross Sea were sampled including the High Salinity Shelf Waters (HSSW), the Ice Shelf Water (ISW), the Circumpolar Deep Water (CDW) and the Antarctic Bottom Water (AABW). The molecular analysis was based on massive parallel high throughput sequencing techniques performed with an Ion Torrent PGM platform. The results highlighted as protist communities were shaped accordingly with the history of the water masses: young-newly formed HSSW presented protist communities characterized by high relative abundance of photoautotrophic organisms - which typically bloom at the surface - down to several hundred meters of depths. On the contrary, older CDW showed higher abundances of taxa as Excavata, Cercozoa (both typically bacterivorus), Radiolaria and Apicomplexa (parasites). Interestingly, the AABW, formed by the entrainment of shelf waters (HSSW and ISW) in CDW, maintained the eukaryotic genetic signatures typical of both parental water masses.

On overall, we revealed a strong partitioning effects on protist assemblage of the water masses suggesting how some of the environmental factors that characterized the unique oceanographic features of the basin have a deep influence on these organisms.

The same high throughput sequencing approach was adopted to study also the prokaryotic communities and in particular their modifications in response to the presence of Jellyfish. In fact, the third and last chapter of the thesis entitled "*Aurelia aurita* ephyrae reshape a coastal microbial community" was aimed to give a comprehensive description of *Aurelia aurita* ephyrae shaping effects on microbial communities of the Gulf of Trieste.

The chapter intended to shed light on the scarcely known interactions between juvenile jellyfish and marine protists and prokaryotes. *Aurelia aurita* was chosen as target organism since it is one of the most abundant and wide spread taxon of scyphozoans that during the last decades showed increasing trends of occurrence and blooming events. In particular we tried to describe the dual role of *A. aurita* ephyrae as top-down and bottom-up controller of microbial communities.

The experimental design was based on microcosm incubations where several parameters were taken into account such as the biomass of the prey, the heterotrophic carbon production (HCP), the extracellular enzyme activity, the dissolved organic carbon (DOC) concentration and the grazing pressures. The analytical approach combines 'traditional' microscopy observation with molecular techniques, and with the assessments of functional modifications of prokaryotic community in terms of secondary production and degradation processes.

The results highlighted a selective predation of the ephyrae on different groups of microplankton based on prey's abundance and motility while no selection was detected on the base of prey taxonomic composition. Prokaryotes assemblage composition changed as well within the ephyrae-treatments and copiotrophic taxa remarkably increased in relative abundance at the expense of

oligotrophic-related taxa. We hypothesized that the reason beyond the detected modification relies on changes in the composition of DOC pools due to the release of mucous-like substances by the ephyrae. The input trigged a reshaping of prokaryotic community although we detected small increases of HCP because of DOC likely complexity and low bio-availability.

The chapter provides a new insight into the effects of *Aurelia*'s ephyrae on marine microbes and it helps to better understand the ecological implications of jellyfish blooms; these events are displaying an increasing trend and they might become a more critical issue for all marine ecosystems in the near future. It represents also an integrated view of grazing pressure shaping microbial assemblages through a direct (on protists) and indirect (on prokaryotes) impacts.

Table of Contents

Chapter 1 - Major contribution of prokaryotes in the pelagic microbial food webs in the Mediterranean Sea.

Luca Zoccarato, Anna Malusà and Serena Fonda Umani

Laboratory of Marine Ecology, Department of Life Science, University of Trieste, via L. Giorgieri 10, 34127, Trieste (Italy).

Correspondence: Luca Zoccarato, Marine Ecology Laboratory, Department of Life Science, University of Trieste, via Giorgieri, 10 - 34127 Trieste, Italy, luca.zoccarato.88@gmail.com

Keywords:

pelagic food web, microzooplankton, microphytoplankton, prokaryotes, Mediterranean Sea, dilution protocol.

Advances in Oceanography and Limnology (2016) – in review

ABSTRACT

In this study, we analyzed more than 80 dilution experiments carried out at the surface and in the meso-bathypelagic layers at 15 Mediterranean sites that covered a wide range of trophic conditions. Our major aim was to test the hypothesis that prokaryotes, and particularly heterotrophic prokaryotes, are pivotal in sustaining not only nanoplankton but also microzooplankton energy requirements at all considered trophic states. Our results highlighted that bacterivory was the major pathway of organic carbon transfer in oligotrophic and meso-eutrophic environments. Microzooplankton mostly fed directly or indirectly (through nanoplankton exploitation) on prokaryotes instead that on microalgae. In eutrophicated conditions herbivory was the main trophic pathway; however heterotrophic prokaryotes always represented an important source of carbon. In this status we assessed the lowest food web efficiency (as the ratio between productivity at the highest trophic level and the productivity of the lower trophic levels), because of the possible grazers' satiation, which translated into an excess of autotrophic biomass available for export or transfer to higher trophic levels. Food web efficiency was higher in meso-eutrophic and oligotrophic conditions where the major pathway was bacterivory. In the meso-bathypelagic layers we assessed only nanoplankton predation on heterotrophic prokaryotes. Food web efficiency at these sites was relatively high. Nanoplankton seemed able to efficiently exploit the available biomass of heterotrophic prokaryotes.

1. INTRODUCTION

Food web efficiency can be defined as the ratio between the productivity of the highest trophic level and the productivity of the lower trophic levels (e.g. Rand and Stewart, 1998; Berglund et al., 2007). This value is influenced by the length and complexity of the food web because of energy loss during

each transfer from one level to the next. Since the early 1980's (Azam et al. 1983) the classic pelagic food web was substituted by a more comprehensive model that include the microbial loop and thus introducing more trophic interactions. These microbes are fundamental to ecosystem functioning and in the photic zone of oligotrophic systems (i.e. open ocean) picophytoplankton (cyanobacteria and picoeukaryote fractions) together with small autotrophic nanoplankton fix more carbon than microphytoplankton (i.e. diatoms) (e.g. Sommer *et al.*, 2002). The major grazers of prokaryotes are heterotrophic nanoplankton (NP; 2-10 μm) and, directly or indirectly, microzooplankton (MZP; 10-200 μm) that with their grazing activity play a critical role for the carbon transfer along the trophic food web and for remineralisation processes (Sherr and Sherr, 1994). Grazing pressure also structures the planktonic communities controlling their biomass, diversity (James and Hall, 1998, Lessard and Murrell, 1998), and primary productivity (Burkill *et al.*, 1995; Cotano *et al.*, 1998).

In the aphotic zone, despite the fact that it contains about 70% of the Earth's seawater volume, food webs are almost unexplored (Nagata *et al.*, 2010). Deep-water communities were generally considered bottom-up controlled because prokaryotes and grazers' abundance ratio decreases from the surface with a drastic reduction of the grazing pressure. However, prokaryotes display heterogeneous distribution because many of them are attached to sinking particles creating micro-hot spots, where prey-predator interactions take place (Azam, 1998; Herndl *et al.*, 2008; Arístegui *et al.*, 2009; Nagata *et al.*, 2010). Furthermore, Aristegui *et al.* (2009) found that the prokaryotes-grazers ratio only halves in meso-bathypelagic zones from the euphotic layers' ratio, thus re-evaluating the significance of grazing. Recently Pachiadaki *et al.* (2014) and Rocke *et al.* (2015) have measured the grazing impact on prokaryotic bathypelagic communities and found that the removal can be more than 30% of the initial standing stock. The relevance of viral-induced mortality is still unclear: Fonda Umani *et al.* (2010) found

that on average viral induced mortality of prokaryotes was 4 times lower compared to grazing loss, and Parada *et al.* (2007), despite that in the bathypelagic realm virus-host ratio increased by 10-times relative to the surface, suggested that viral induced mortality is not as relevant as expected.

The assessment of the predators' grazing pressure on prokaryotes is a key point in order to understand food web efficiency, not only in the oligotrophic marine systems, but also in the most eutrophic coastal systems (Sommer *et al.*, 2002). Recently, De Laender *et al.* (2010) using the linear inverse model approach, estimated that in microbial dominated trophic food webs bacteria are four time more important than phytoplankton in the protists' diet, while in herbivorous dominated food webs the diet of protists consist of similar amounts of bacteria and phytoplankton.

To test the hypothesis that prokaryotes, and particularly heterotrophic prokaryotes, are pivotal in sustaining not only NP but also MZP energy requirements over a wide range of trophic conditions, we compared the results of more than 80 dilution experiments (Landry and Hassett, 1982) carried out in the entire Mediterranean Sea.

2. MATERIALS AND METHOIDS

2.1 Studied area

The Mediterranean Sea is considered an oligotrophic basin due to the scarce presence of nutrients and chlorophyll *a* (Krom *et al.*, 1991; Antoine *et al.*, 1995). Oligotrophy exasperates moving eastwards as remarked by major decreasing gradients of nutrient concentrations (Krom *et al.*, 1993), primary production, autotrophic biomass, export of primary production (Danovaro *et al.*, 1999; Dolan *et al.*, 1999; Turley *et al.*, 2000) and chlorophyll concentration (Williams, 1998). On average, the most limiting nutrient is inorganic phosphorus (Sala *et al.*, 2002; Van Wambeke *et al.*, 2009) that deeply influences

microbial community of the Mediterranean Sea. The food webs in fact are predominantly microbial-dominated (Fogg, 1995) and while phytoplankton are both N and P limited, autotrophic prokaryotes are more sensitive to P limitation (Pitta *et al.*, 2005; Thingstad *et al.*, 2005; Zohary *et al.*, 2005). Only a few areas of the basin (close to river mouths, upwelling areas) are characterized by eutrophic conditions and present plankton communities where larger autotrophic and heterotrophic organisms become more representative.

Eighty-two dilution experiments were performed in the Mediterranean Sea at 15 sites located, from east to west, in the Aegean Sea (3 sites), the Ionian Sea (3 sites), the Otranto strait (1 site), the Adriatic Sea (3 sites), the Tyrrhenian Sea (1 site), the Ligurian Sea (1 site), the Balearic Sea (1 site), the Alboran Sea (1 site) and Atlantic Ocean (1 site) (Fig. 1). Sixty-eight experiments were carried out at the sub-surface level (0.5 m depth) and 14 in the meso-bathypelagic realm (between 670 m and 3860 m depth). Surface experiments were set up following two strategy: 34 were designed to assess MZP grazing rates (that include the effect of NP grazing; Stoecker et al., 2014) and 34 were designed to assess NP grazing rates on prokaryotes in absence of larger predators; the latter set of experiments were performed simultaneously and with the same sampled water used to set up the first set. Part of these results were already published and detailed references are reported in supporting information (Table S1, S2a and S2b for surface experiments and Table S3 for meso-bathypelagic experiments), while new experiments were carried out during OBAMA oceanographic cruise of the namesake project, from 24th of March to 06th of April 2011 on board of the R/V Urania, (5 sites between the Northern Ionian Sea and the Southern Adriatic Sea).

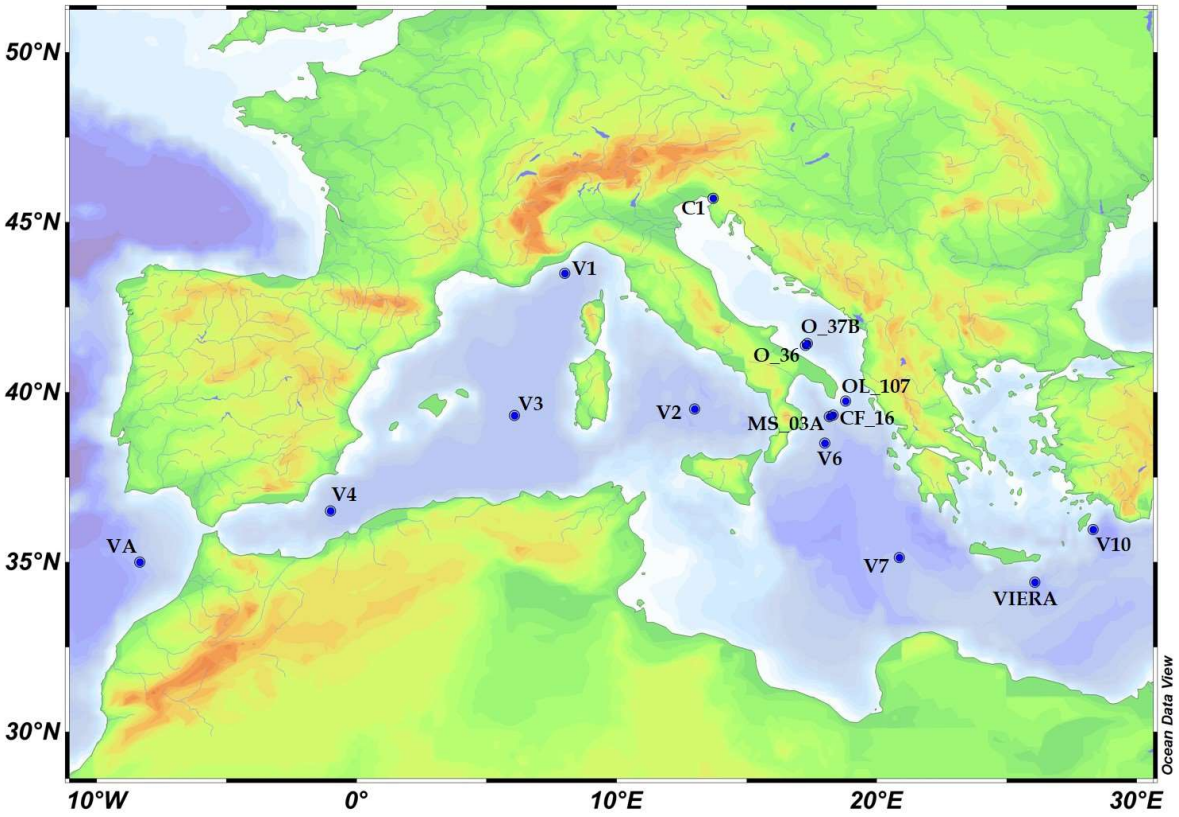

- **Fig. 1**: Map of the Mediterranean Sea with sampling sites marked by dots.

2.2 Dilution techniques

MZP-Dilutions experiment. Forty-eight liters of pre-screened (<200 µm) seawater collected at the surface layer was diluted with filtered (0.22 µm), particle free sea water from the same sample. Two identical bottle sets (2 L) of four dilutions each were made in the following proportions: 100% (whole sea water), 80%, 50% and 10% in three replicates each. The first set of dilutions (T_0) was immediately fixed with buffered and 0.2 µm filtered formaldehyde solution (2% final concentration). The second set of dilution (T_{24}) was incubated at *in situ* temperature for 24 hours on the deck (or on the shore) in 600 L tanks with sea-water circulation. Bottles were kept in movement by the flowing water and they were manually turned upside down each 3 - 4 hours. At the end of the incubation, the samples were fixed as the initial ones. Samples for MZP and microphytoplankton analyses were conserved in plastic bottles at

ambient temperature, while samples for nanoplankton and prokaryotes analyses were conserved in black plastic bottles, stored in the dark at 4°C, until laboratory analysis. In the oligotrophic Eastern Mediterranean microphytoplankton was not considered, because its abundance was below the detection limit (Di Pol et al., 2013). In the other experiments we assessed *in situ* phytoplankton growth rates with and without the addition of nutrients (5 µM $NaNO_3$ and 1µM KH_2PO_4) (Landry and Hassett, 1982).

NP-Dilutions experiment. Twelve liters of seawater were collected at the surface and in the meso-bathypelagic layers, pre-filtered immediately through a 200 µm mesh and then filtered through a 10 µm mesh to remove larger predators. Sets of dilutions were prepared as for MZP sets in 600 mL bottles. Sets for experiments with meso- and bathypelagic communities were incubated at *in situ* temperature for 24 hours in the dark in a portable refrigerator. Samples were fixed and stored as described before.

Sea water for both MZP and NP dilution experiments was simultaneously sampled from the same Niskin bottles. Based on the dilution method of Landry and Hassett (1982) as modified by Landry *et al.* (1995), we computed for several classes of prey (microphytoplankton, nanoplankton, heterotrophic and autotrophic prokaryotes): growth factor (µ), mortality factor (g), initial concentration of the prey (C_0), mean concentration of the prey during the experiment (1), ingestion rate (2) and potential production (3). In this review we considered only results with a significant ($r^2 > 0.6$) linear regression for the considered prey.

$$C_m = C_0\left(e^{(\mu-g)t} - 1\right)/\left(\mu - g\right) \qquad (1),$$

$$I = g \times C_m \qquad (2),$$

$$P_P = \mu \times C_m \qquad (3).$$

2.3 Microscopic analysis and cell to biomass conversion factors

Micro-plankton. Samples for microphytoplankton and microzooplankton (10 – 200 µm) were processed following the Utermöhl method (1958); organisms were enumerated and measured using an inverted optical microscope (Olympus IX51) equipped with an eyepiece scale. Taxonomic assignations, standardized geometrical formulas for volume conversion and carbon conversion factor were done following Strathmann (1967) and Smayda (1978) for microphytoplankton, Putt and Stoecker (1989) for microzooplankton.

Nanoplankton and prokaryotes. The assessment of prokaryotes (0.2 – 2 µm) and nanoplankton (2 – 10 µm) was performed according to the Porter and Freig protocol (1980) at the epifluorescence microscope. Aliquots of each sample were stained with a DAPI (4', 6-diamidino-2-phenylindole) solution, 1 µg mL^{-1} final concentration. Prokaryotes were collected on 0.22 µm black polycarbonate filters (Nucleopore, 25 mm) while nanoplankton on 0.8 µm black polycarbonate filters (Nucleopore, 25 mm). Counts were made using an epifluorescence microscope (Olympus BX 60 F5) at x1000 final magnification with UV filter set (BP 330–385nm, BA 420nm) for DAPI; green (BP 480–550 nm, BA 590 nm) and a blue (BP 420–480 nm, BA 515 nm) light sets for natural pigment fluorescence. More than 200 cells were counted for each prokaryotic and nanoplankton sample. Prokaryote samples were counted in triplicates. For the estimation of biomass, nanoplankton was divided into three dimensional classes: 2-3 µm, 3-5 µm and 5-10 µm as reported by Christaki *et al.* (2001). Cell abundance data were converted in biomass by applying the following conversion factors: 20 fg C $cell^{-1}$ for heterotrophic bacteria for surface samples (Ducklow and Carlson, 1992), 10 fg C $cell^{-1}$ for the meso-bathypelagic samples (Ducklow H., 2000) and 200 fg C $cell^{-1}$ for phototrophic bacteria (Caron *et al.*, 1995).

Nanoplanktonic organisms were approximated to spheres (diameter equal to the medium value of the each dimensional class) and the volume multiplied by 183 fg C μm^{-3} (Caron *et al.*, 1995).

2.4 Chlorophyll a

Chlorophyll *a* samples were collected from the same Niskin bottles sampled for the dilution experiments by filtering on board from 1 to 5 L of seawater through Whatman GF/F glass-fibre filters (45 mm diameter), the membranes were immediately frozen (-20°C) or stored in liquid nitrogen when available. The pigments extraction was run overnight in the dark at 4 °C with 90% acetone from the filter previously homogenized; concentrations were determined with the spectrofluorometer Perkin Elmer LS 50B (450 nm excitation and 665 nm emission wavelengths) measuring the chlorophyll *a* (Lorenzen and Jeffrey, 1980). The instrument calibration was made using pure Sigma chl *a* standards and computing a linear response for the considered range.

2.5 Elaborations

The overall ingestion efficiencies of grazer in different trophic conditions were visualized through box plots comparing the ingestion rate and the corresponding preys' potential production estimated in MZP-dilution experiments. Potential production is considered a good proxy for primary production (Calbet and Landry, 2004). Food web efficiency (FWE) was computed as the ratio of the highest trophic level production (in our truncated food webs it corresponded to microzooplankton at the surface and nanoplankton in the meso-bathypelagic layers) over the total potential production of all possible prey (see Berglund *et al.*, 2007). To investigate if the relations between ingestion rates of grazers with available biomasses of each kind of prey diverge from a linear response we tested three common models of functional response: Ivlev (4), Holling Type II or Disk Equation (5) and [, Holling Type III (6).

$$I = \alpha\left(1 - e^{-bC_0}\right) \qquad (4),$$

$$I = \alpha C_0 / (\beta + C_0) \quad (5),$$

$$I = \alpha C_0^2 / (\beta^2 + C_0^2) \quad (6),$$

where I and C0 are ingestion rates and biomasses estimated in each MZP-dilution experiment, α and β are constants and represent respectively the maximum rate of ingestion and the biomass values at which we have α/2. The values for α and β that minimize the residual sum-of-squares in each equation were computed with the Nonlinear Least Squares (nls) function implemented in the stats package of R. Only fitting models whose parameters were highly significant (p-values < 0.01) were considered and compared by the analysis of variance (ANOVA) and by the maximum likelihood to the same data (with the Akaike information criterion – AIC, and the Bayesian information criterion - BIC) to evaluate the fitting quality of the models.

3. RESULTS

3.1 Surface experiments

Fig. 2 shows the biomass of all primary producers and the chlorophyll *a* values assessed at the surface per each sampling event. We arbitrarily divided the increasing biomass values into three major groups: the first one with values for total autotrophic fraction < 6.44 µg C L^{-1} that we consider representative of oligotrophic condition (mean chl *a* 0.22 µg L^{-1}); the second one that can be considered meso-eutrophic with an autotrophic total carbon < 61.93 µg C L^{-1} and mean chl *a* of 0.60 µg L^{-1} and the last one which can be considered very eutrophic (or eutrophicated) with biomass largely exceeding 100 µg C L^{-1} and mean chl *a* of 2.60 µg L^{-1}. Groups presented significant differences among them (one-way Kruskal–Wallis test was highly significant, *p*-value << 0.01).

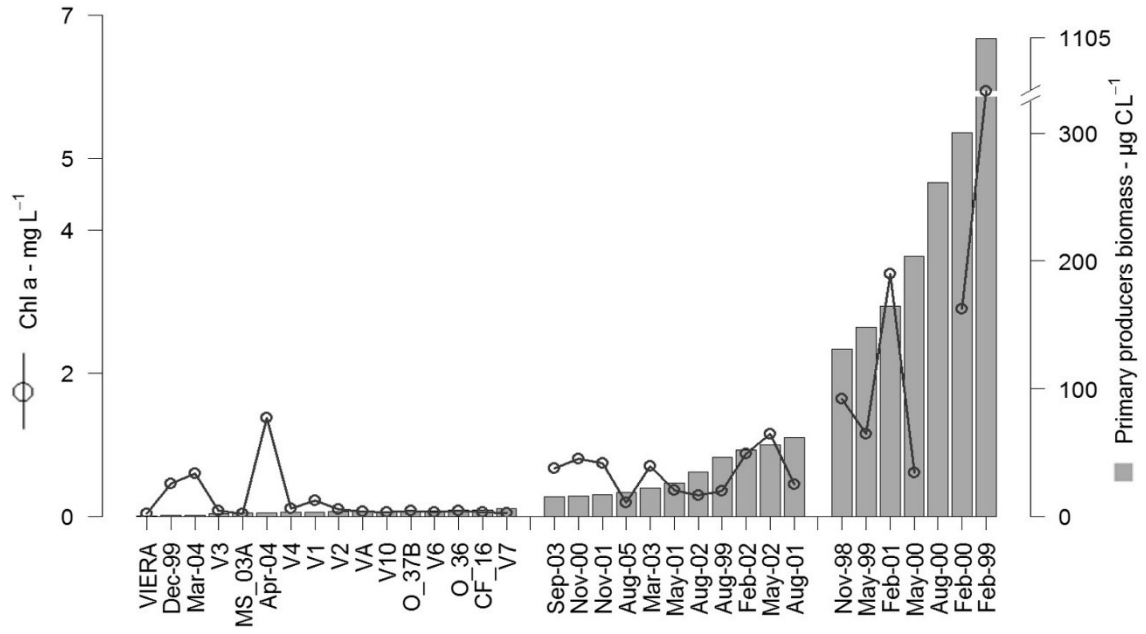

- **Fig. 2**: Primary producers' biomass and chlorophyll *a* distribution in sampling events.

Total biomass' composition (biomasses of all considered classes of organisms) assessed in each MZP-grazing experiments revealed significant differences among different groups of trophic condition as defined above. In oligotrophic and meso-eutrophic conditions NP and prokaryotes constituted on average almost 80% of total biomass (prokaryotes alone more than 60%) while MPP represented only a small fraction and mainly because of the presence of flagellates; furthermore in oligotrophic condition total biomass was mostly composed by NP and HP, on average 27.4% and 46.8% respectively whereas in meso-eutrophic condition mean total biomass was almost equally composed by MPP (28.8%), HP (33.7%) and AP (21.1%). In eutrophicated condition MPP dominated over microbial assemblages representing on average 91.1% of the total biomass and it was mainly composed of diatoms. MZP biomass was relatively high in meso-eutrophic condition (10.3%) but represented on average 4.8% and 2.5% in oligotrophic and eutrophicated conditions, respectively.

Assessing the grazing impact on available prey in MZP-dilution experiments we found as the daily amount of ingested carbon increased according to the trophic condition (Fig. 3). In oligotrophic condition grazers relied on HP (ingestion rates ranged from 1.19 to 23.86 µg C L^{-1} d^{-1}) and MZP predation on NP was detected (ingestion rates ranged from 0.77 to 16.71 µg C L^{-1} d^{-1}). In meso-eutrophic situations prokaryotes was subjected to the highest mortality rates with an average ingestion of 32.36 µg C L^{-1} d^{-1} for HP and 11.41 µg C L^{-1} d^{-1} for AP; MZP grazing on MPP occurred within a range from 0.56 to 23.78 µg C L^{-1} d^{-1}; an internal predation among grazer were detected in 7 cases out of 11 with estimated ingestion rates of MZP on NP ranging from 0.79 to 4.68 µg C L^{-1} d^{-1}. In eutrophicated condition ingestion rates of MZP on MPP were the highest ones ranging from 69.93 to 177.90 µg C L^{-1} d^{-1} (with relevant exception of February 1999 – see Fonda Umani *et al.,* 2012) followed by grazers' ingestion rates on HP (2.25 - 66.90 µg C L^{-1} d^{-1}), NP (0.58 - 7.43 µg C L^{-1} d^{-1}) and AP (0.08 - 5.58 µg C L^{-1} d^{-1}).

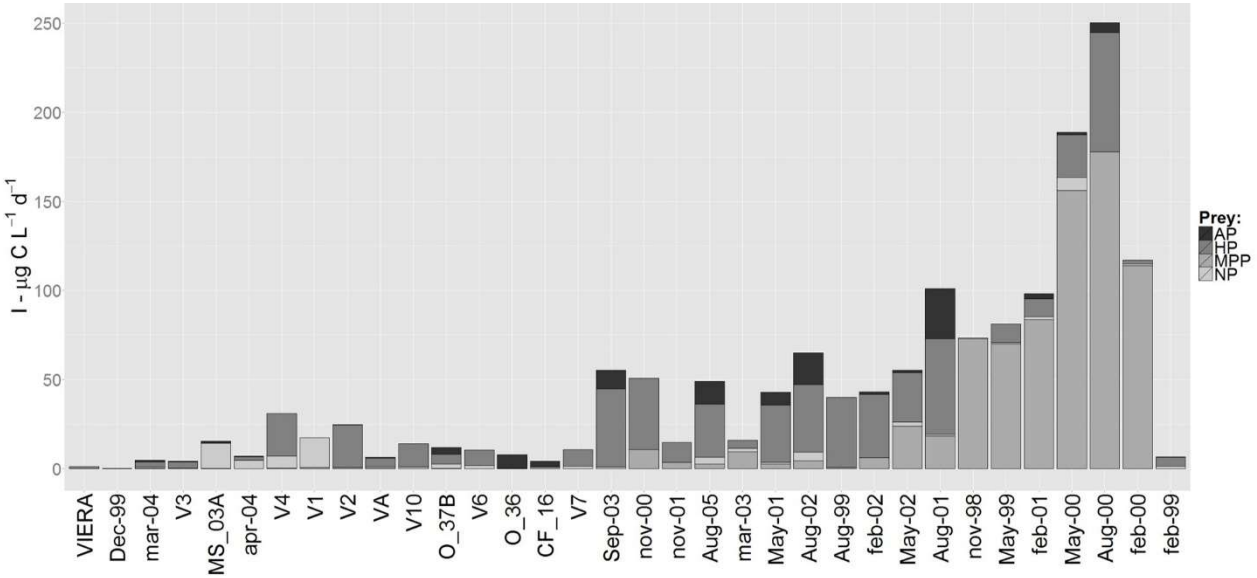

- **Fig. 3**: Ingestion rates of grazers in MZP-dilution experiments.

In the NP-dilution experiments, nanoplankton were the top predators (free from MZP grazing pressure) and their potential ingestion rates were estimated (Fig. 4). NP can only relied on prokaryotes biomass

and the heterotrophic fraction was the most exploited with values increasing from oligotrophic to meso-eutrophic conditions, lower values characterized experiments in eutrophicated conditions (mean ingestion rates were 5.30, 23.41, and 14.80 µg C L^{-1} d^{-1} respectively); ingestion rates for AP on average ranged from 1.87 µg C L^{-1} d^{-1} in oligotrophic state to 9.69 µg C L^{-1} d^{-1} in meso-eutrophic and 0.36 µg C L^{-1} d^{-1} in eutrophicated conditions.

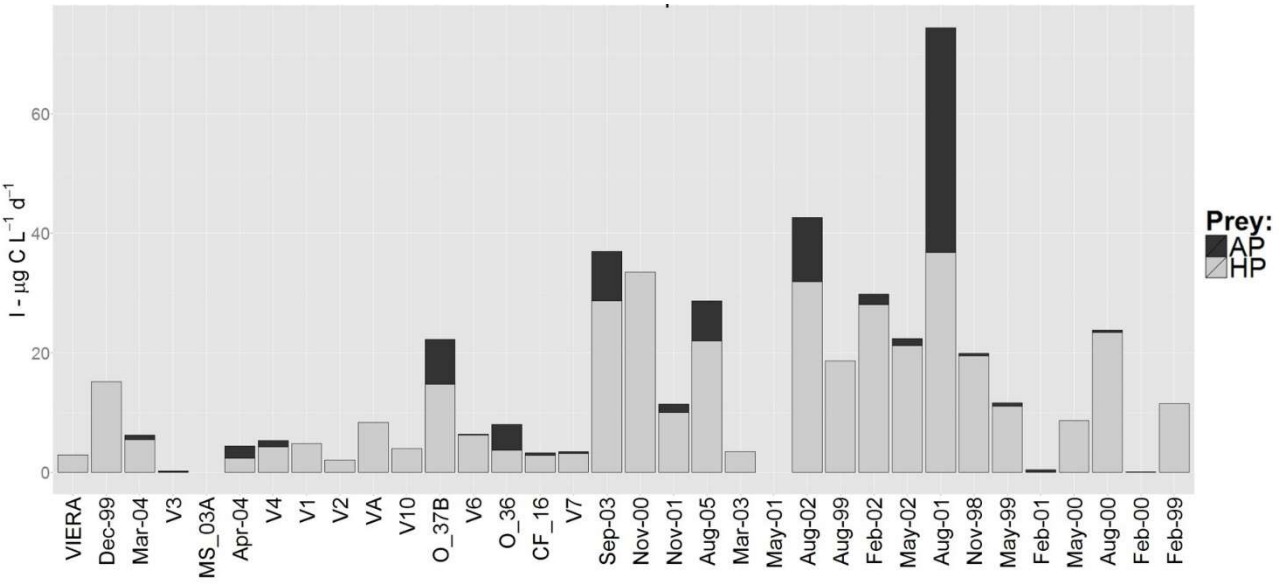

- **Fig. 4**: Potential ingestion rates of NP in NP-dilution experiments.

Fig. 5 reports the analysis of grazers ingestion efficiencies made through the comparison of ingestion rates and potential productions assessed in MZP-dilution experiments. Distributions of ingestion and PP values for each class of prey and for each trophic condition showed as although in some occasions ingestion rates exceeded PP on average the two rates were comparable; the ingestion efficiencies were thus close to 1. In some cases during eutrophicated condition PP of HP and especially of MPP were found to largely exceeded ingestion rates; these unbalance led to remarkable low ingestion efficiencies of grazers on MPP and HP prey when higher trophic state occurred.

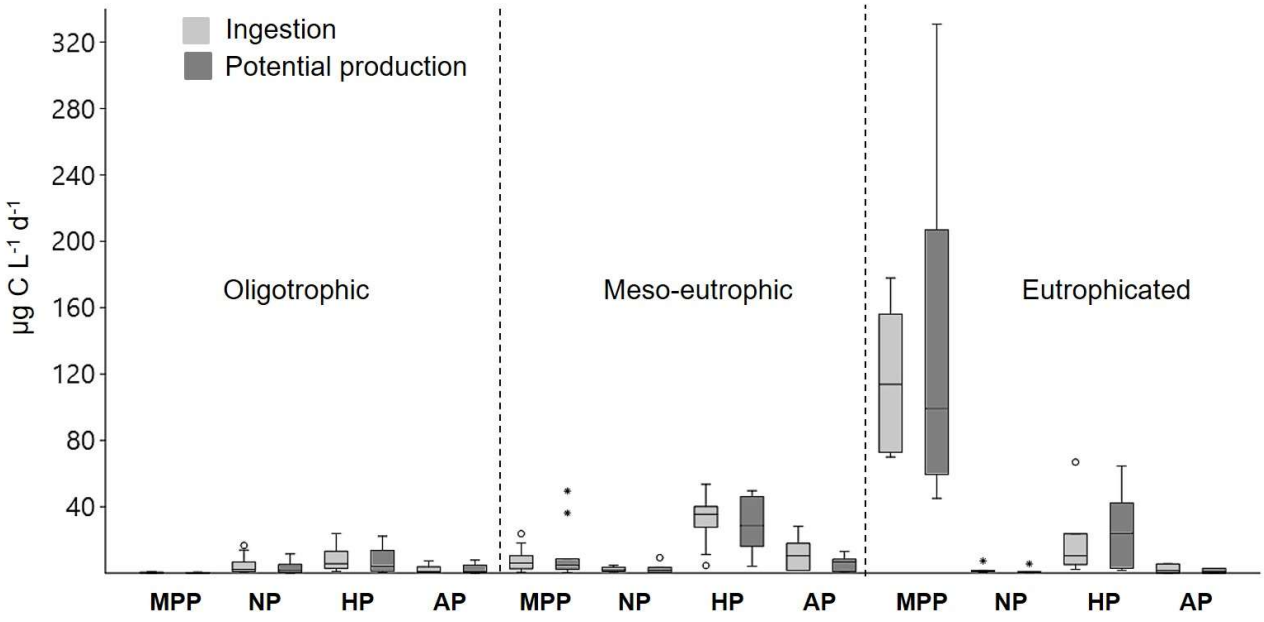

- **Fig. 5**: Box plot comparison of Potential Production and Ingestion values assessed in MZP-dilution experiments for all prey in all trophic conditions.

Among the functional response models tested on data collected from MZP-dilution experiments only Holling Type III (H3) gave significant fittings and only for HP, MPP and AP (Fig. 6). Although ANOVA test was never significant, differences emerged from statistical comparison of H3 with linear model (LM) among HP, MPP and AP: the LM was more explicative than H3 for AP (AIC 84.1 and 96.9 respectively, BIC 87.1 and 99.8 respectively); no difference was observed for HP (AIC 218.0 and 217.9 respectively, BIC 222.0 and 221.9 respectively), while for MPP H3 explained better than LM the data trend (AIC 224.8 and 232.5 respectively, BIC 228.7 and 236.4 respectively). The α coefficient of H3 indicated an upper threshold (α) for the ingestion rates on HP at 55.02 µg C L^{-1} d^{-1} and on MPP at 197.2 µg C L^{-1} d^{-1}. The β coefficient represented the available biomass at which the curve had the inflection point; after this point the ratio between ingestion and biomass starts to decrease. β was equal to 17.63 µg C L^{-1} for HP and to 159.71 µg C L^{-1} for MPP.

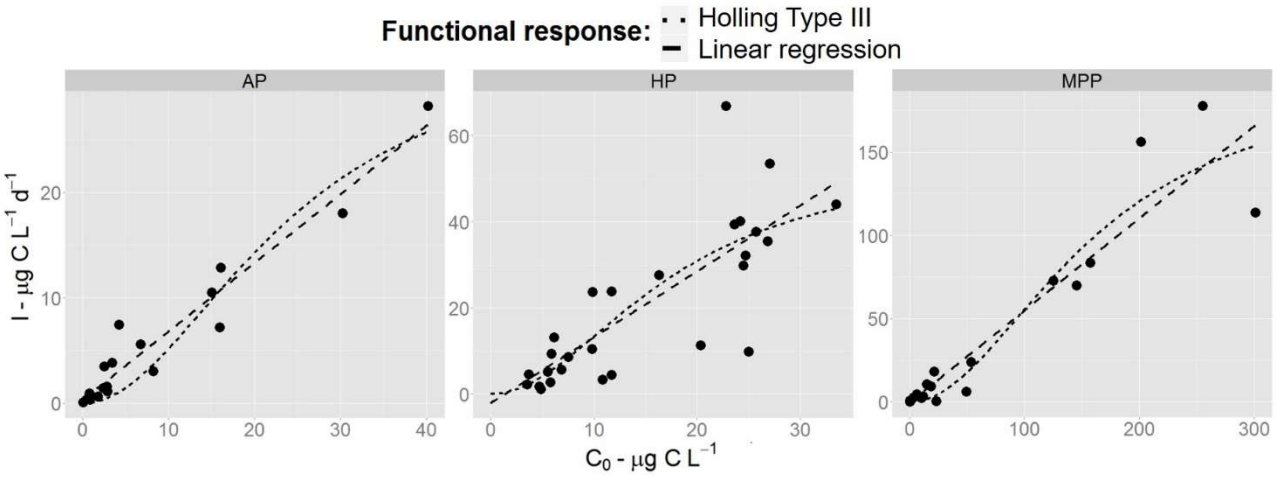

- **Fig. 6**: Comparison between ingestion rates and available biomass for MPP, NP, HP and AP. Functional responses models that provided a significant fitting are reported.

3.2 Meso-bathypelagic experiments

Fig. 7a reports HP biomasses estimated in the dilution experiments carried out in the meso- and bathypelagic layers where HP represented the only available prey for NP. HP biomass varied from 0.14 to 0.97 µg C L^{-1} with the exception of two mesopelagic (CF_16 and OL_107) stations with relatively high values (6.45 µg C L^{-1} and 7.24 µg C L^{-1}). Mean biomass of NP was 0.37 µg C L^{-1} with a standard deviation of ±0.31 µg C L^{-1} for all stations; however NP ingestion rates ranged between 0.05 and 3.2 µg C L^{-1} d^{-1} with the exception of the two mesopelagic stations in which ingestion rates were 13.29 µg C L^{-1} d^{-1} and 16.74 µg C L^{-1} d^{-1} respectively.

At bathypelagic layers, NP ingestion efficiency was close to 1 since PP and I were always comparable (Fig. 7b); an exception was found for the deepest station (VIERA) in which PP largely exceeded the ingestion. The two mesopelagic experiments were characterized by high PP and ingestion values with the ingestion rates that exceeded the potential production.

The functional response models were tested on bathypelagic dataset but no one gave a significant fitting, neither the linear regression (R^2 was <0.2).

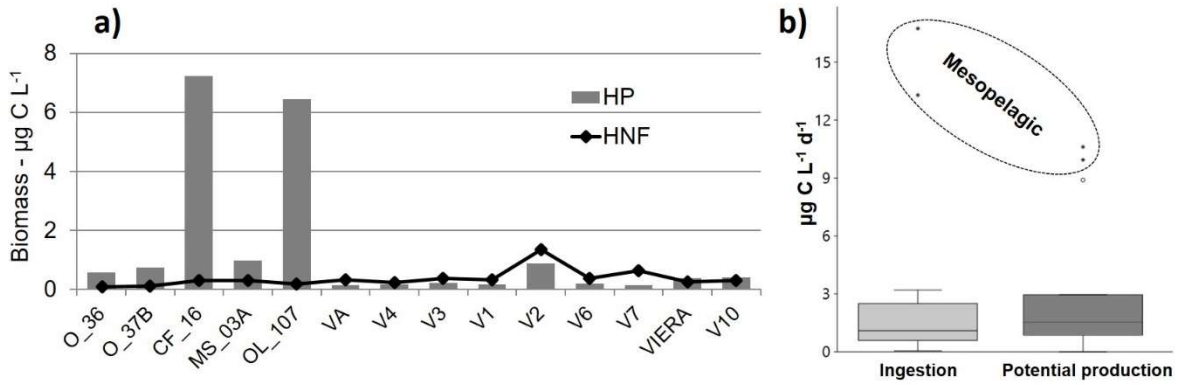

- **Fig. 7**: a) HP and NP biomasses for all dilution experiments carried out in the meso- and bathypelagic layers. b) Box plot comparison of Ingestion rates and Potential Production in meso- and bathypelagic NP-dilution experiments.

3.3 C-flux models

For all considered preys, mean ingestion rates assessed in MZP- and NP-dilution experiments, and mean values of biomasses were used to produce models of trophic carbon pathways for the three trophic conditions described at the surface and in the bathypelagic zones (Fig. 8). We reported the secondary production of MZP and the likely excesses of PP for MPP and HP pinpointed by ingestion efficiency values.

In eutrophicated condition the prevalent ingestion of MZP was on MPP (mean ingestion 112.35 µg C L^{-1} d^{-1}, mean MPP biomass 326.94 µg C L^{-1}) and of both grazers on HP (mean ingestion 19.72 µg C L^{-1} d^{-1}, mean biomass 17.78 µg C L^{-1}); NP in the experiments without MZP fed almost uniquely on HP (mean ingestion 14.80 µg C L^{-1} d^{-1}). In meso-eutrophic conditions, grazers mainly preyed on HP (mean ingestion 32.36 µg C L^{-1} d^{-1}, mean biomass 22.50 µg C L^{-1}), while lower mean ingestion rate was recorded on AP

(11.41 μg C L^{-1} d^{-1}) and only of MZP on MPP (8.15 μg C L^{-1} d^{-1}); in the experiments without MZP, NP intensely exploited HP (23.41 μg C L^{-1} d^{-1}) and the contribution of AP was also significant (9.69 μg C L^{-1} d^{-1}). In oligotrophic condition, grazers mostly ingested HP (8.92 μg C L^{-1} d^{-1} on mean biomass of 8.43 μg C L^{-1}) and MZP on NP (4.98 μg C L^{-1} d^{-1} on a mean biomass of 4.94 μg C L^{-1}). NP grazing on HP (5.30 μg C L^{-1} d^{-1}) in the experiments without MZP was higher than on AP (1.87 μg C L^{-1} d^{-1}). Comparing all the coupled MZP- and NP-dilution experiments, the HP mortality was always higher in MZP-experiments indicating a direct impact of MZP on HP. The mean production of MZP increased from 0.17 μg C L^{-1} d^{-1} in oligotrophic to 4.25 μg C L^{-1} d^{-1} in meso-eutrophic conditions and decreased to 1.02 μg C L^{-1} d^{-1} in eutrophicated state. Mean PP of MPP significantly exceeded the mean ingestion rate in eutrophicated condition producing an excess of biomass of 23.28 μg C L^{-1} d^{-1}; similar situation occurred also for HP with an excess of biomass of 4.89 μg C L^{-1} d^{-1}.

- **Fig. 8**: Carbon flux models computed for oligotrophic, meso-eutrophic and eutrophicated conditions at the surface and for the bathypelagic layers. Models are composed by mean ingestion rates of grazers (MZP and NP), mean potential ingestion rates of NP (dashed lines), MZP secondary production and mean biomasses for all classes of organisms. For eutrophicated condition possible exports of MPP and HP are reported.

The carbon flux for deep layers was elaborated using only bathypelagic data. NP could graze only on HP with a mean ingestion rate of 2.41 μg C L^{-1} d^{-1} on a mean biomass of 0.94 μg C L^{-1}. A production of 0.52 μg C L^{-1} d^{-1} was estimated for the NP.

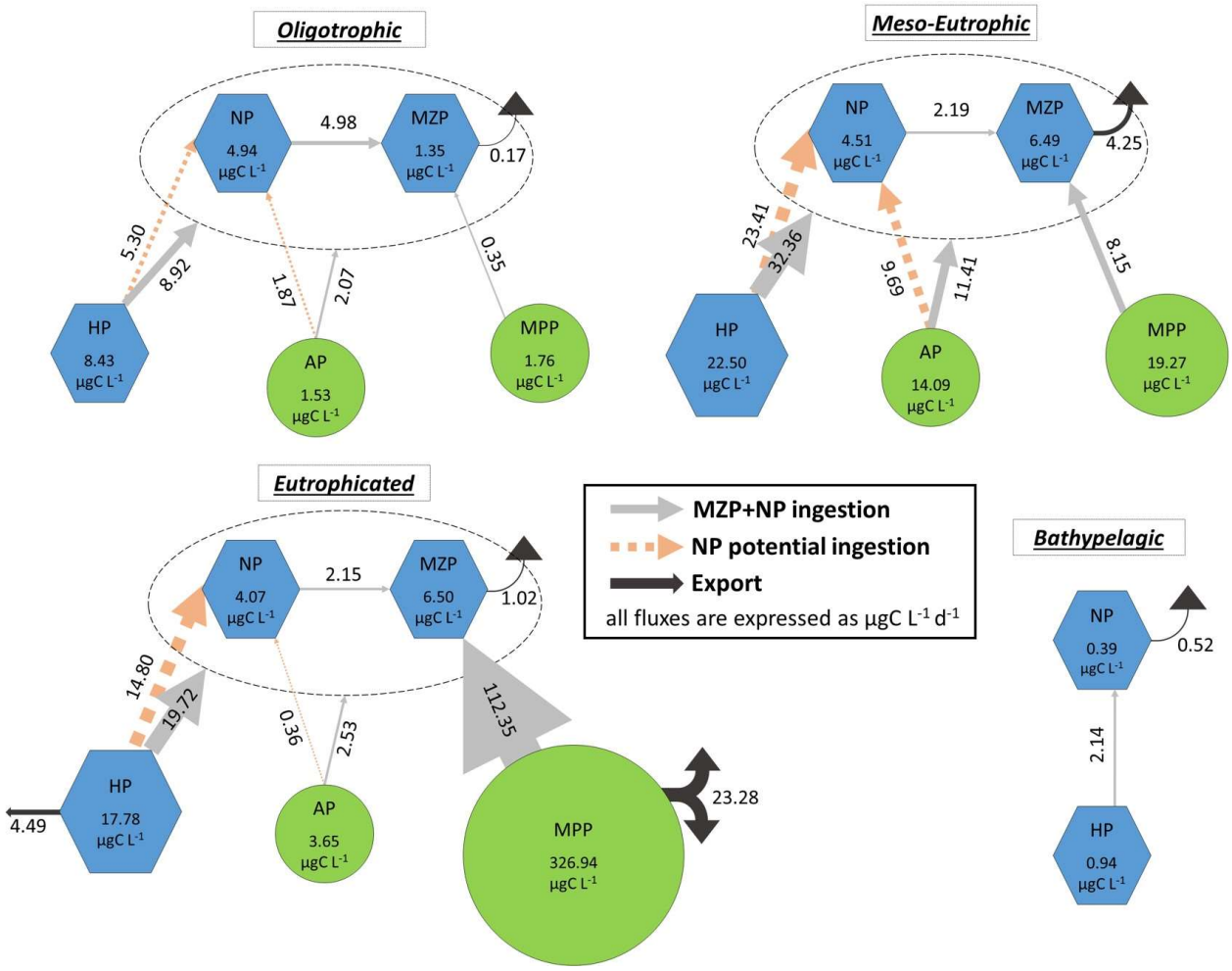

On average, in the surface experiments food web efficiency (i.e. the ratio between production at the highest level and production of all prey = MPP, NP, HP and AP) increased from oligotrophic to meso-eutrophic scenarios, being respectively 0.03 and 0.10, and decreased in eutrophicated conditions (0.01). In the meso-bathypelagic domain the food web efficiency computed considering NP as top predators was equal to 0.13.

4. DISCUSSION

4.1 Prokaryotes as major player at the surface

Our results highlighted as at the surface prokaryotes, and particularly HP, were grazed by MZP in all trophic conditions. Ingestion rates assessed in MZP-dilution experiments represented the concomitant predation impact of the two grazer communities of MZP and NP (e.g. Stoecker *et al.*, 2014). In order to partially solve this problem parallel MZP- and NP-dilution experiments were performed to estimate the mortality of each prey in presence of both grazers and of NP only. We are aware that results include also viral mediated prokaryotic mortality (Parada, 2007; Fonda Umani *et al.*, 2010; Di Pol *et al.*, 2013) but virus effect is expected to be the same in both MZP- and NP-dilution experiments since the same sea water was used to set up the parallel experiments.

The ingestion rates assessed in NP-dilution parallel experiments were not aimed to provide accurate estimation of NP grazing on prokaryotes communities; our intention was to compare these values with ingestion rates estimated in MZP-dilution experiments in order to clarify the role of MZP as direct grazer on prokaryotes. Through this comparison we can discriminate among three different situations (based on Fonda Umani and Beran, 2003) of grazers interaction with a prey: 1) a strong reduction of NP by MZP grazing that translates in not detectable grazing on HP in MZP experiments 2) partial reduction of NP biomass by MZP grazing, which lead to a lower HP mortality in MZP experiments 3) MZP directly feed on prokaryotes, and consequently ingestion rates obtained in MZP experiments are higher than for NP experiments

Situation 3 were detected for HP in several cases (65% of the experiments) and in all 11 experiments in meso-eutrophic condition. Thus the contribution of prokaryotes in the MZP diet, an aspect that is

seldom investigated, is instead noticeable. Situation 1 model corresponded to 15% of all experiments; situation 2 model in the remaining experiments.

The efficiency of grazers' ingestion (expressed as the ratio between ingestion and potential production rates of prey), with some precautions as suggested by Cáceres et al. (2013), could be a proxy for the carbon balance of the system and suggests the carrying capacity for higher trophic levels. In oligotrophic and meso-eutrophic conditions the ingestion efficiency was close to 1 indicating a good balance between production and loss; nevertheless this imply a low carrying capacity for higher trophic levels and translates in microbial dominated food webs where bacterivory is the major pathway of carbon flux. Indeed in these ecosystems, HP was on overall the most abundant and the most exploited stock. Ingestion rates on HP were higher than on MPP, NP and AP; solely in few experiments the predation on NP and AP were higher than on HP.

In eutrophicated condition, ingestion efficiency on HP was low and remarkably low was ingestion efficiency on MPP. The excess of MPP's production and biomass is the key factor supporting the growth of larger grazers in eutrophicated areas where herbivory represent the major path for carbon flux. Nevertheless we detected the highest mean ingestion rates on MPP and this prey represented more than 80% of MZP mean daily diet, grazing pressure affecting HP stock was not negligible either in eutrophicated state since they cover almost 14% of grazers' diet.

4.2 Food webs in meso- and bathypelagic layers

In the bathypelagic layers biomasses of MZP, NP and HP were lower than at the surface and values fell within ranges proposed by Nagata *et al.* (2010, and references therein). At two mesopelagic stations, HP biomasses were comparable with those found at the surface in oligotrophic conditions, although the biomass of NP was 10-times lower than at the surface. The higher biomasses might be correlated

with the role of circulation and/or to nutrient input from the upper euphotic layers, which enhanced HP production (Hansell and Ducklow, 2003). However ingestion rates exceeded PP and it might indicate the end or the ephemeral nature of the possible input events. The low ratio between HP and NP biomasses found at CF_16 and OL_107 agree with what reported by Pernice *et al.* (2015) that found how ratio of eukaryotes to prokaryotes biomasses was constantly lower in the mesopelagic rather than in bathypelagic layers all over the oceans.

Despite the fact that the mean biomass of HP in meso- and bathypelagic layers was 6 to 16% of the surface biomass, the ingestion rates were from 13 to 58% of the surface rates, suggesting a strong feeding adaptation of NP in high diluted-prey conditions as reported by Cho *et al.* (2000) in the East China Sea and recently by Pachiadaki *et al.* (2014) for the eastern Mediterranean Sea and by Rocke *et al.* (2015) for the North Atlantic Deep Water and the Antarctic Intermediate Water. All of them used fluorescently-labelled prokaryote tracing techniques that have been shown to produce comparable but lower results with respect to those obtained in dilution experiments (Vaqué *et al.*, 1994).

New feeding strategies have been hypothesized for micro-eukaryotes in the deep sea such as osmotrophy or parasitism (Pernice *et al.,* 2015), however the relatively high ingestion rates in face of low HP:NP abundance ratios emphasizes the importance of grazing to satisfy NP energetic requirements. HP biomass is thus essential to sustain NP communities in the dark realm of the Mediterranean Sea.

4.3 Food webs efficiency

At the surface, food web efficiency reflected the ingestion efficiencies estimated for each experiments being higher in oligotrophic and meso-eutrophic conditions where we observed a full exploitation of prey potential production by MZP and NP grazers. Conversely, in the eutrophicated condition a large

part of newly produced biomass was inefficiently exploited from grazers in the MZP-dilution experiments. We are aware that the considered food webs are truncated and mesozooplankton community, although consuming on average only 10% of daily global primary production (Calbet and Saiz, 2005), can significantly affect both MZP and MPP communities in meso-eutrophic and eutroficated conditions (e.g. Ohman and Runge, 1994; Rivkin *et al.,* 1996; Campbell *et al.,* 2009; Fonda Umani *et al.,* 2012). Most of the excess of MPP biomass can therefore be exploited by larger predators that however exhibit low ingestion efficiency since downward exports have been demonstrated in several areas such as the Gulf of Trieste (Fonda Umani *et al.,* 2012) and in the Bering Sea (Campbell *et al.,* 2015).

In the bathypelagic layers we could assess food web efficiency only considering nanoplankton as top predator. Also in this case food web efficiency, regardless of the diluted environment, was relatively high and nanoplankton seemed to be able to efficiently exploit the HP production.

Holling Type III (H3) model significantly described the correlation between ingestion rates and prey abundances for MPP and HP at the surface. In terms of goodness of fit and parsimony, H3 performed like linear model for HP while it resulted even more explicative for MPP. The model is based on a sigmoidal curve characterized by a low threshold, an inflection point and an upper threshold; these features allowed us to infer some relevant ecological implications.

The low threshold corresponded to low ingestion rates that have not paired slight biomass increases; these conditions were detected mainly in oligotrophic and meso-bathypelagic environments and might be explained by the dilution of available prey that reduce the prey-predator encounter rates (Wikner and Hagström, 1991; Pastor, 2008). In meso-and bathypelagic layers grazers evolved strategies to efficiently harvest even diluted prey (see Jürgens and Massana, 2008) but at the surface these adaptation might be energetically inconvenient; for instance in oligotrophic condition grazers relied on

more abundant NP and prokaryotes, rather than on MPP, to sustain their energetic requirements. H3 trend suggested the existence of lower threshold for MPP and HP and this is partially supported also by negative values of linear models' intercept; however we did not suggest any value for the lower threshold since we lack data of low ingestion rates; in the dilution method when the slope of the linear regression (g) is close to zero the grazing impact was commonly considered null and no ingestion rates is assessed (Calbet and Saiz, 2013; Schmoker *et al.,* 2013).

The high threshold (α) can be interpreted as the result of the individual inability to cope with higher prey availability as suggested by a modelling-approach study by Gentleman and Neuheimer (2008). A possible explanation is a delay in the match of grazers' growth with prey increases. The satiation thresholds suggested from Holling Type III for MPP and HP however were never reached in the analysed experiments but the comparison of their half saturation coefficients gave some interesting suggestions. The half saturation (β) coefficient indicate the point after which the rate between ingestion and available biomass starts to decrease; the β of MPP correspond to its available biomass of 159.71 μg C L^{-1} and this value was reached in eutrophicated condition within those experiment in which PP largely exceeded the ingestion; for HP the β value correspond to 17.63 μg C L^{-1} of available biomass that was exceeded in meso-eutrophic condition.

The ecological implication suggested by H3 model agreed with our interpretation of the result and we believe it could be even more informative performing the fitting analysis on a larger dataset.

5. CONCLUSION

We are aware of the limit of dilution experiments because they cannot fully represent natural conditions, however they can be used to compare different trophic situations when, as in our case, they are set up following the same protocol. The main results of our comparison were:

- Bacterivory was the major pathway of organic carbon in oligotrophic and meso-eutrophic surface conditions.
- In eutrophicated conditions herbivory was the main trophic pathway. However prokaryotes, represented a meaningful source of carbon.
- Pelagic food web efficiency was higher when bacterivory was the dominant pathway because herbivory was characterized by a lower efficiency.
- In the meso- and bathypelagic layers, NP ingestion rates on HP diminished but not at the same order of magnitude as their biomasses, thus determining a relative high efficiency of this truncated food web.

ACKNOWLEDGMENTS

We are grateful to all colleagues and SFU students who took part in the dilution experiments, to Giovanni Bacaro for his support with the statistical analysis, to Jack Koch for the review of the English grammar, to Mauro Celussi for his helpful feedbacks and to the crews of research vessels Urania and Universitatis.

FUNDING

This study was supported by the PERSEUS Project, managed by CONISMA, which provided the Ph. D. fellowship to LZ [grant numbers 287600].

REFERENCES

Antoine D, Morel A and André J-M, 1995. Algal pigment distribution and primary production in the eastern Mediterranean as derived from coastal zone color scanner observations. J. Geophys. Res., Wiley Online Library 100: 16193–16209.

Arístegui J, Gasol JM, Duarte CM and Herndl GJ, 2009. Microbial oceanography of the dark oceans pelagic realm. Limnol. Oceanogr. 54: 1501–1529.

Azam F, 1998. Microbial Control of Oceanic Carbon Flux: The Plot Thickens. Science (80-.)., American Association for the Advancement of Science 280: 694–696.

Azam F, Fenchel T, Field J, Gray J, Meyer-Reil L and Thingstad F, 1983. The Ecological Role of Water-Column Microbes in the Sea. Mar. Ecol. Prog. Ser. 10: 257–263.

Berglund J, Müren U, Båmstedt U and Andersson A, 2007. Efficiency of a phytoplankton-based and a bacterial-based food web in a pelagic marine system. Limnol. Oceanogr., Wiley Online Library 52: 121–131.

Burkill PH, Edwards ES and Sleight MA, 1995. Microzooplankton and their role in controlling phytoplankton growth in the marginal ice zone of the Bellingshausen Sea. Deep Sea Res. Part II Top. Stud. Oceanogr., Elsevier 42: 1277–1290.

Cáceres C, Taboada FG, Höfer J and Anadón R, 2013. Phytoplankton growth and microzooplankton grazing in the subtropical Northeast Atlantic. PLoS One 8: e69159. Calbet A and Landry MR, 2004. Phytoplankton growth, microzooplankton grazing, and carbon cycling in marine systems. Limnol. Oceanogr. 49: 51–57.

Calbet A and Saiz E, 2005. The ciliate-copepod link in marine ecosystems. Aquat. Microb. Ecol. 38: 157–167.

Calbet A and Saiz E, 2013. Effects of trophic cascades in dilution grazing experiments: from artificial saturated feeding responses to positive slopes. J. Plankton Res. 35: 1183–1191. Campbell RG, Ashjian CJ, Sherr EB, Sherr BF, Lomas MW, Ross C, Alatalo P, Gelfman C and Keuren D Van,

2015. Mesozooplankton grazing during spring sea-ice conditions in the eastern Bering Sea. Deep Sea Res. Part II Top. Stud. Oceanogr., Elsevier in press.

Cho BC, Na SC and Choi DH, 2000. Active ingestion of fluorescently labeled bacteria by mesopelagic heterotrophic nanoflagellates in the East Sea, Korea. Mar. Ecol. Prog. Ser. 206: 23–32.

Cotano U, Uriarte I and Villate F, 1998. Herbivory of nanozooplankton in polyhaline and euhaline zones of a small temperate estuarine system (Estuary of Mundaka): seasonal variations. J. Exp. Mar. Bio. Ecol. 227: 265–279.

Danovaro R, Dinet A, Duineveld G and Tselepides A, 1999. Benthic response to particulate fluxes in different trophic environments: A comparison between the Gulf of Lions-Catalan Sea (western-Mediterranean) and the Cretan Sea (eastern-Mediterranean). Prog. Oceanogr., Elsevier 44: 287–312.

De Laender F, Van Oevelen D, Soetaert K and Middelburg J, 2010. Carbon transfer in a herbivore- and microbial loop-dominated pelagic food webs in the southern Barents Sea during spring and summer. Mar. Ecol. Prog. Ser. 398: 93–107.

Di Poi E, Blason C, Corinaldesi C, Danovaro R, Malisana E and Fonda-Umani S, 2013. Structure and interactions within the pelagic microbial food web (from viruses to microplankton) across environmental gradients in the Mediterranean Sea. Global Biogeochem. Cycles 27: 1034–1045.

Dolan JR, Vidussi F and Claustre H, 1999. Planktonic ciliates in the Mediterranean Sea: Longitudinal trends. Deep. Res. Part I Oceanogr. Res. Pap., Elsevier 46: 2025–2039.

Ducklow H, 2002. Bacterial Production and Biomass in the Oceans. DL K (ed.), Microb. Ecol. Ocean, New York: Wiley-Liss.

Fogg GE, 1995. Some comments on picoplankton and its importance in the pelagic ecosystem. Aquat. Microb. Ecol., Inter-Research 9: 33–39.

Fonda Umani S and Beran A, 2003. Seasonal variations in the dynamics of microbial plankton communities: First estimates from experiments in the Gulf of Trieste, Northern Adriatic Sea. Mar. Ecol. Prog. Ser. 247: 1–16.

Fonda Umani S, Monti M, Bergamasco A, Cabrini M, De Vittor C, Burba N and Del Negro P, 2005. Plankton community structure and dynamics versus physical structure from Terra Nova Bay to Ross Ice Shelf (Antarctica). J. Mar. Syst. 55: 31–46.

Fonda Umani S, Malisana E, Focaracci F, Magagnini M, Corinaldesi C and Danovaro R, 2010. Disentangling the effect of viruses and nanoflagellates on prokaryotes in bathypelagic waters of the Mediterranean Sea. Mar. Ecol. Prog. Ser. 418: 73–85.

Fonda Umani S, Malfatti F and Del Negro P, 2012. Carbon fluxes in the pelagic ecosystem of the Gulf of Trieste (Northern Adriatic Sea). Estuar. Coast. Shelf Sci., Elsevier Ltd 115: 170–185.

Gentleman WC and Neuheimer a. B, 2008. Functional responses and ecosystem dynamics: How clearance rates explain the influence of satiation, food-limitation and acclimation. J. Plankton Res., Oxford Univ Press 30: 1215–1231.

Hansell D a. and Ducklow HW, 2003. Bacterioplankton distribution and production in the bathypelagic ocean: Directly coupled to particulate organic carbon export? Limnol. Oceanogr., Wiley Online Library 48: 150–156.

Herndl GJ, Agogué H, Baltar F, Reinthaler T, Sintes E and Varela MM, 2008. Regulation of aquatic microbial processes: The 'microbial loop' of the sunlit surface waters and the dark ocean dissected. Aquat. Microb. Ecol. 53: 59–68.

James MR and Hall JA, 1998. Microzooplankton grazing in different water masses associated with the Subtropical Convergence round the South Island, New Zealand. Deep Sea Res. Part I Oceanogr. Res. Pap., Elsevier 45: 1689–1707.

Jürgens K and Massana R, 2008. Protist grazing on marine bacterioplankton. 2nd ed. In: Kirchman D (ed.), Microb. Ecol. Ocean., Wiley-Liss, New York, pp. 383–441.

Krom MD, Kress N, Brenner S and Gordon LI, 1991. Phosphorus limitation of primary productivity in the eastern Mediterranean Sea. Limnol. Ocean., Wiley Online Library 36: 424–432.

Krom MD, Brenner S, Kress N, Neori a. and Gordon LI, 1993. Nutrient distributions during an annual cycle across a warmcore eddy from the E. Mediterranean Sea. Deep Sea Res. Part I Oceanogr. Res. Pap., Elsevier 40: 805–825.

Landry MR and Hassett RP, 1982. Estimating the grazing impact of marine micro-zooplankton. Mar. Biol. 67: 283–288.

Landry MR, Kirshtein J and Constantinou J, 1995. A refined dilution technique for measuring the community grazing impact of microzooplankton, with experimental tests in the central equatorial Pacific. Mar. Ecol. Prog. Ser. 120: 53–64.

Lessard EJ and Murrell MC, 1998. Microzooplankton herbivory and phytoplankton growth in the northwestern Sargasso Sea. Aquat. Microb. Ecol. 16: 173–188.

Lorenzen CJ and Jeffrey SW, 1980. Determination of chlorophyll in seawater. Unesco Tech. Pap. Mar. Sci. 35: 1–20.

Nagata T, Tamburini C, Arístegui J, Baltar F, Bochdansky AB, Fonda-Umani S, Fukuda H, Gogou A, Hansell D a., Hansman RL, Herndl GJ, Panagiotopoulos C, Reinthaler T, Sohrin R, Verdugo P,

Yamada N, Yamashita Y, Yokokawa T and Bartlett DH, 2010. Emerging concepts on microbial processes in the bathypelagic ocean - Ecology, biogeochemistry, and genomics. Deep. Res. Part II Top. Stud. Oceanogr., Elsevier 57: 1519–1536.

Ohman MD and Runge JA, 1994. Sustained Fecundity When Phytoplankton Resources are in Short Supply: Omnivory by Calanus finmarchicus in the Gulf of St. Lawrence. Limnol. Oceanogr., Wiley Online Library 39: 21–36.

Pachiadaki MG, Taylor C, Oikonomou A, Yakimov MM, Stoeck T and Edgcomb V, 2014. In situ grazing experiments apply new technology to gain insights into deep-sea microbial food webs. Deep Sea Res. Part II, Elsevier 112: 1–9.

Parada V, Sintes E, Van Aken HM, Weinbauer MG and Herndl GJ, 2007. Viral abundance, decay, and diversity in the meso- and bathypelagic waters of the North Atlantic. Appl. Environ. Microbiol. 73: 4429–4438.

Pastor J, 2008. Mathematical Ecology of Populations and Ecosystems. Oxford, UK.: Wiley-Blackwell.

Pitta P, Stambler N, Tanaka T, Zohary T, Tselepides A and Rassoulzadegan F, 2005. Biological response to P addition in the Eastern Mediterranean Sea. The microbial race against time. Deep. Res. Part II Top. Stud. Oceanogr., Elsevier 52: 2961–2974.

Putt M and Stoecker DK, 1989. An experimentally determined carbon : volume ratio for marine 'oligotrichous' ciliates from estuarine and coastal waters. Limnol. Oceanogr., Wiley Online Library 34: 1097–1103.

Rand PS and Stewart DJ, 1998. Prey fish exploitation, salmonine production, and pelagic food web efficiency in Lake Ontario. Can. J. Fish. Aquat. Sci., NRC Research Press 55: 318–327.

Rivkin R, Legendre L, Deibel D, Tremblay J, Klein B, Crocker K, Roy S, Silverberg N, Lovejoy C, Mesple F, Romero N, Anderson M, Matthews P, Savenkoff C, Vezina A, Therriault J, Wesson J, Berube C and Ingram R, 1996. Vertical Flux of Biogenic Carbon in the Ocean: Is There Food Web Control? Science, American Association for the Advancement of Science 272: 1163–6.

Rocke E, Pachiadaki MG, Cobban A, Kujawinski EB and Edgcomb VP, 2015. Protist Community Grazing on Prokaryotic Prey in Deep Ocean Water Masses. PLoS One 10: e0124505.

Sala MM, Peters F, Gasol JM, Pedrós-Alió C, Marrasé C and Vaqué D, 2002. Seasonal and spatial variation in the nutrient limitation of bacterioplankton growth in the northwestern Mediterranean. Aquat. Microb. Ecol. 27: 47–56.

Schmoker C, Hernández-León S and Calbet A, 2013. Microzooplankton grazing in the oceans: Impacts, data variability, knowledge gaps and future directions. J. Plankton Res., Oxford Univ Press 35: 691–

706.

Sherr EB and Sherr BF, 1994. Bacterivory and herbivory: Key roles of phagotrophic protists in pelagic food webs. Microb. Ecol., Springer 28: 223–235.

Sherr EB, Sherr BF and Hartz AJ, 2009. Microzooplankton grazing impact in the Western Arctic Ocean. Deep Sea Res. Part II Top. Stud. Oceanogr., Elsevier 56: 1264–1273.

Smayda TJ, 1978. From phytoplankters to biomass. In: Sournia A (ed.), Phytoplankt. Man., Paris: UNESCO Monographs on Oceanographic Methodology, pp. 273–279.

Sommer U, Stibor H, Katechakis A, Sommer F and Hansen T, 2002. Pelagic food web configurations at different levels of nutrient richness and their implications for the ratio fish production:primary production. In: Vadstein O, and Yngvar O (eds), Sustain. Increase Mar. Harvest. Fundam. Mech. New Concepts, Springer, pp. 11–20.

Stoecker DK, Weigel A and Goes JI, 2014. Microzooplankton grazing in the Eastern Bering Sea in summer. Deep Sea Res. Part II Top. Stud. Oceanogr. 109: 145–156.

Strathmann RR, 1967. Estimating the organic carbon content of phytoplankton from cell volume or plasma volume. Limnol. Oceanogr., Wiley Online Library 12: 411–418.

Strom SL, Miller CB and Frost BW, 2000. What sets lower limits to phytoplankton stocks in high-nitrate, low-chlorophyll regions of the open ocean? Mar. Ecol. Prog. Ser., Inter Research 193: 19–31.

Thingstad TF, Krom MD, Mantoura RFC, Flaten G a F, Groom S, Herut B, Kress N, Law CS, Pasternak A, Pitta P, Psarra S, Rassoulzadegan F, Tanaka T, Tselepides A, Wassmann P, Woodward EMS, Riser CW, Zodiatis G and Zohary T, 2005. Nature of phosphorus limitation in the ultraoligotrophic eastern Mediterranean. Science, American Association for the Advancement of Science 309: 1068–1071.

Turley CM, Bianchi M, Christaki U, Conan P, Harris JRW, Psarra S, Ruddy G, Stutt ED, Tselepides A and Van Wambeke F, 2000. Relationship between primary producers and bacteria in an oligotrophic sea - The Mediterranean and biogeochemical implications. Mar. Ecol. Prog. Ser. 193: 11–18.

Utermöhl H, 1958. Zur Vervollkommnung der quantitativen Plankton-Methodik. Mitt. Int. Ver. Theor. Angew. Limnol. 9: 1–38.

Van Wambeke F, Ghiglione J-F, Nedoma J, Mével G and Raimbault P, 2009. Bottom up effects on bacterioplankton growth and composition during summer-autumn transition in the open NW Mediterranean Sea. Biogeosciences, Copernicus GmbH 6: 705–720.

Vaque D, Gasol JM and Marrase C, 1994. Grazing rates on bacteria - The significance of methodology and ecological factors. Mar. Ecol. Prog. Ser., INTER-RESEARCH NORDBUNTE 23, D-21385

OLDENDORF LUHE, GERMANY 109: 263–274.

Wikner J and Hagström A, 1991. Annual study of bacterioplankton community dynamics. Limnol. Oceanogr., Wiley Online Library 36: 1313–1324.

Williams PJL, 1998. The balance of plankton respiration and photosynthesis in the open oceans. Nature, Nature Publishing Group 394: 55–57.

Zohary T, Herut B, Krom MD, Fauzi C. Mantoura R, Pitta P, Psarra S, Rassoulzadegan F, Stambler N, Tanaka T, Frede Thingstad T and Malcolm S. Woodward E, 2005. P-limited bacteria but N and P co-limited phytoplankton in the Eastern Mediterranean - A microcosm experiment. Deep. Res. Part II Top. Stud. Oceanogr., Elsevier 52: 3011–3023.

Supplementary – Tables S1 to S3

Details of the dilution experiments analyzed in the manuscript that were carried out at the surface and in meso-bathypelagic layers.

Samples V1, V2, V3, V4, V6, V7, V10, VA and VIERA were taken during VECTOR cruise and results have been published in Poi et al. (2013) and Fonda Umani et al. (2010).

Samples O_36, O_37B, CF_16, MS_03A and OL_107 were taken during OBAMA cruise.

All remaining samples were collected at the station C1 (13.710 E, 45.701 N, depth of 17 m) in the Gulf of Trieste - Northern Adriatic Sea from autumn 1998 to summer 2005. Results have been published in Fonda Umani et al. (2005) and Fonda Umani et al. (2012).

- **Table S1.** Chlorophyll a and biomasses values in all the dilution experiments carried out at the surface. Stations are grouped according to trophic conditions.

Trophic conditions:	**Oligotrophic**															
Station:	**VIERA**	**Dec-99**	**Mar-04**	**V3**	**MS_03A**	**Apr-04**	**V4**	**V1**	**V2**	**VA**	**V10**	**O_37B**	**V6**	**O_36**	**CF_16**	**V7**
Chl *a* - *mg L^{-1}*	0.04	0.46	0.60	0.08	0.04	1.37	0.11	0.22	0.10	0.07	0.06	0.08	0.06	0.08	0.06	0.05
Biomass - µg C L^{-1}																
MZP	0.59	3.47	1.21	0.38	0.51	8.80	0.34	0.22	0.18	0.78	0.43	1.02	0.47	2.22	0.52	0.49
MPP	0.04	0.13	0.12	1.68	0.23	1.01	2.53	2.73	2.75	3.24	3.30	0.13	3.76	0.34	0.28	5.89
NP	1.41	1.59	13.35	5.00	8.04	9.81	5.72	8.70	2.47	4.59	1.05	5.19	1.28	4.39	4.45	2.05
HP	4.87	21.02	5.84	10.85	4.71	5.13	11.70	13.15	9.84	11.70	6.14	5.80	7.49	6.32	4.49	5.89
AP	0.42	0.57	0.94	0.44	2.60	1.86	0.82	0.70	0.88	0.62	0.64	3.91	0.49	4.43	4.71	0.45

Trophic conditions:	**Meso-eutrophic**										
Station:	**Sep-03**	**Nov-00**	**Nov-01**	**Aug-05**	**Mar-03**	**May-01**	**Aug-02**	**Aug-99**	**Feb-02**	**May-02**	**Aug-01**
Chl *a* - *mg L^{-1}*	0.67	0.80	0.74	0.19	0.70	0.36	0.29	0.35	0.87	1.15	0.45
Biomass - µg C L^{-1}											
MZP	7.21	3.48	5.40	1.85	12.04	2.35	6.05	5.62	14.04	7.48	5.86
MPP	0.41	15.00	11.51	3.27	18.42	10.17	5.99	23.05	49.38	53.35	21.37
NP	6.24	2.86	2.63	6.53	3.64	4.13	2.91	3.25	3.55	10.11	3.81
HP	32.07	23.93	19.71	24.41	3.66	24.69	25.41	23.86	25.29	15.81	28.67
AP	14.91	0.69	5.76	15.37	3.93	15.97	28.85	23.34	2.78	2.79	40.56

Trophic conditions:	**Eutrophicated**						
Station:	**Nov-98**	**May-99**	**Feb-01**	**May-00**	**Aug-00**	**Feb-00**	**Feb-99**
Chl *a* - *mg L^{-1}*	1.64	1.15	3.39	0.61	-	2.90	5.94
Biomass - µg C L^{-1}							
MZP	6.43	7.84	4.38	4.69	4.08	8.49	9.62
MPP	124.95	145.25	157.17	201.17	255.09	300.68	1104.25
NP	0.86	3.33	2.83	10.71	3.79	4.20	2.75
HP	45.34	10.18	23.98	10.23	23.51	4.21	6.99
AP	5.79	2.79	7.70	2.47	6.66	0.02	0.15

Table 2a. **Ingestion and potential production rates estimated for MZP-dilution experiments and for NP-dilution experiments carried out in oligotrophic conditions.**

	Trophic condition:	Oligotrophic															
	Station:	**VIERA**	**dic-99**	**mar-04**	**V3**	**MS_03A**	**apr-04**	**V4**	**V1**	**V2**	**VA**	**V10**	**O_37B**	**V6**	**O_36**	**CF_16**	**V7**
MZP-dilution experiments	***Ingestion rates*** $\mu g\ C\ L^{-1} d^{-1}$																
	MPP	-	0.08	0.05	0.44	0.20	-	0.26	0.53	0.62	0.56	-	0.18	-	0.19	0.73	-
	NP	-	-	0.89	-	13.93	4.65	6.77	16.71	-	0.77	0.85	2.22	1.79	-	-	1.26
	HP	1.19	-	2.72	3.36	-	1.80	23.86	-	23.75	4.48	13.20	5.70	8.65	-	-	9.42
	AP	-	-	0.94	0.33	1.15	0.61	-	-	0.33	0.43	-	3.83	-	7.46	3.50	-
	Potential production rates $\mu g\ C\ L^{-1} d^{-1}$																
	MPP	-	0.08	0.01	0.40	0.57	-	0.24	0.48	0.43	0.19	-	0.14	-	0.42	0.11	-
	NP	-	-	0.54	-	9.28	5.22	3.48	11.59	-	0.15	0.56	1.63	1.11	-	-	1.87
	HP	11.63	-	4.28	0.47	-	2.44	2.74	-	22.29	1.22	16.60	1.16	13.76	-	-	11.17
	AP	-	-	0.85	0.26	0.84	0.68	-	-	0.14	0.75	-	4.67	-	7.86	2.95	-
NP-dilution experiments	***Ingestion rates*** $\mu g\ C\ L^{-1} d^{-1}$																
	HP	2.88	15.13	5.41	0.07	-	2.31	4.24	4.79	2.01	8.33	3.97	14.71	6.20	3.62	2.78	3.08
	AP	-	-	0.81	0.09	-	2.03	1.06	-	-	-	-	7.55	0.14	4.39	0.42	0.36

- **Table S2b.** Ingestion and potential production rates estimated for MZP-dilution experiments and for NP-dilution experiments carried out in meso-eutrophic and eutrophicated conditions.

	Trophic condition:	Mesotrophic											Eutrophic						
	Station:	set-03	nov-00	nov-01	ago-05	mar-03	mag-01	ago-02	ago-99	feb-02	mag-02	ago-01	nov-98	mag-99	feb-01	mag-00	ago-00	feb-00	feb-99
MZP-dilution experiments	***Ingestion rates μg C $L^{-1}d^{-1}$***																		
	MPP	-	10.52	3.38	2.60	9.39	2.43	4.53	0.56	6.06	23.78	18.22	72.82	69.93	83.63	156.08	177.90	113.78	-
	NP	0.79	-	-	3.65	1.86	1.09	4.68	-	-	2.25	0.99	0.58	0.88	1.71	7.43	-	1.01	1.27
	HP	44.04	40.12	11.34	29.82	4.59	32.17	37.77	39.43	35.47	27.64	53.54	-	10.47	9.83	23.71	66.90	2.25	5.16
	AP	10.48	-	-	12.87	-	7.21	18.01	-	1.55	1.59	28.18	-	-	3.02	1.43	5.58	-	0.08
	Potential production rates μg C $L^{-1}d^{-1}$																		
	MPP	-	3.01	2.20	8.53	4.71	4.02	5.93	0.33	1.69	49.53	36.25	45.05	99.15	59.52	330.87	72.32	206.88	-
	NP	0.33	-	-	2.17	0.70	0.39	9.33	-	-	1.65	3.58	0.30	0.33	0.74	5.71	-	0.48	0.43
	HP	28.60	49.58	4.11	16.10	4.70	35.60	24.22	46.14	23.38	30.28	47.14	-	24.06	2.99	42.33	64.53	1.55	9.79
	AP	6.71	-	-	8.38	-	2.27	7.06	-	0.85	0.83	13.13	-	-	2.86	0.93	1.12	-	0.04
NP-dilution experiments	***Ingestion rates μg C $L^{-1}d^{-1}$***																		
	HP	28.67	33.49	9.95	21.98	3.42	-	31.88	18.63	28.06	21.19	36.80	19.50	11.01	-	8.65	23.38	-	11.46
	AP	8.30	-	1.45	6.69	-	-	10.75	-	1.78	1.19	37.66	0.38	0.61	0.38	-	0.42	0.01	-

- **Table S3**. Biomass, ingestion and potential production rates estimated in the NP-dilution experiments carried out in meso-bathypelagic layers.

	Mesopelagic					Bathypelagic								
Station:	**O_36**	**O_37B**	**CF_16**	**MS_03A**	**OL_107**	**VA**	**V4**	**V3**	**V1**	**V2**	**V6**	**V7**	**VIERA**	**V10**
Biomass - µg C L^{-1}														
NP	0.08	0.11	0.31	0.30	0.19	0.32	0.24	0.38	0.34	1.35	0.36	0.65	0.26	0.30
HP	0.57	0.75	7.24	0.97	6.45	0.14	0.16	0.23	0.17	0.89	0.18	0.14	0.38	0.41
Ingestion rates µg C $L^{-1}d^{-1}$														
HP	0.19	1.02	16.74	1.10	13.29	0.05	0.20	0.91	1.00	3.20	0.59	1.27	2.51	1.18
Potential production rates µg C $L^{-1}d^{-1}$														
HP	-	0.84	10.61	1.49	9.94	0.00	0.14	0.87	1.22	2.57	1.52	2.96	8.90	2.28

Chapter 2 - Water mass dynamics shape Ross Sea protist communities in meso- and bathypelagic layers

Luca Zoccarato[1], Alberto Pallavicini[1], Federica Cerino[2], Serena Fonda Umani[1] and Mauro Celussi[2].

[1]Marine Ecology Laboratory, Department of Life Science, University of Trieste, Trieste, Italy.

[2]Oceanography Division, OGS (Istituto Nazionale di Oceanografia e di Geofisica Sperimentale), Trieste, Italy.

Scientific Reports (2016) – submitted

Abstract

Deep-sea environments are dominated by microbes and represent the last largely unexplored and poorly known ecosystems on Earth. The Ross Sea is characterized by unique oceanographic dynamics and harbors several water masses deeply involved in cooling and ventilation of deep oceans. In this study a forefront molecular technique was adopted to sequence the V9 region of the 18S ribosomal DNA gene and unveil differences in protist communities correlated with physicochemical properties. The analyzed samples were significantly different in terms of environmental parameters and community composition outlining significant structuring effect of temperature and salinity. Overall, meso- and bathypelagic layers were dominated by the groups Alveolate (especially Dinophyta), Stramenopiles and Excavata; nonetheless, protist communities were shaped accordingly to the history of the water masses (advection effect and mixing events). Newly-formed High Salinity Shelf Waters (HSSW) were characterized by high relative abundance of phototrophic organisms, which typically bloom at the surface during the austral summer. Older Circumpolar Deep Waters (CDW) showed higher abundance of Excavata taxa that are typical bacterivores in deep water masses. At the shelf-break, Antarctic Bottom Water (AABW), formed by the entrainment of shelf waters in CDW, maintained the eukaryotic genetic signature typical of both parental water masses.

1. Introduction

The Ross Sea is located in the southwestern continental margins of the Southern Ocean and for 98.8% of its extension the bathymetry exceeds the limit of epipelagic waters[1]. In this cold and dark environment the formation of the Antarctic Bottom Water (AABW) takes place, strongly influencing cooling and ventilation processes of deep oceans. AABW is generated from vertical mixing events occurring between the modified Circumpolar Deep Water (mCDW) and the Shelf Water (SW). In turn the SW derives from winter buoyancy loss of superficial waters due to sea-ice formation process (either Antarctic Surface Waters or mCDW) that produces dense and salty water masses (HSSW) as well as smaller amount of super cooled Ice Shelf Water (ISW)[2].

The Ross Sea represents one of the most biologically productive areas in the Southern Ocean[1] and all its water masses are intimately linked with the thermohaline conveyor belt[3] fueling deep oceans with dissolved oxygen and inorganic and organic carbon[4]. The ecosystems of the basin, as well as all the Antarctic aquatic environments, are dominated by microorganisms which play critical roles in biogeochemical cycles and in the biological carbon pump[5,6]. The prokaryotic fraction is essential for the ecosystems functioning in the dark realms where approximately 75 % and 50 % of its biomass and its production, respectively, are retained. Nevertheless also protist communities play critical roles in the ecosystems acting as primary producers, consumers, decomposers, and trophic links in aquatic food webs[7,8].

During the last decades technological progress significantly enhanced our understanding of the diversity of microorganisms, one above all the possibility offered by the DNA barcode parallel and massive sequencing. Several studies have been carried out to explore and reveal the structures of microbial communities in different areas, but, although particular focus was placed on Bacteria and Archaea (for example[9–11]), only few researches included or targeted protists[12,13]. Recently, remarkable breakthrough on a comprehensive knowledge of microbes distribution originated from

two global sampling surveys [14,15] and some of the dynamics that shape and control the diversity of microbial communities in the epipelagic realm have been unveiled pinpointing possible abiotic and biotic constraining factors[16]. For the meso- bathypelagic communities there are evidences that highlight as the composition of prokaryotic assemblages of the North Atlantic[10], the Arctic[17] and the Southern Oceans[18,19] changed among different water masses while communities of the same water mass were found to be similar even at thousands kilometers of distance. Similar data are still scarce for protists although few studies demonstrated a strong correlation of eukaryotes assemblage composition with the basin of origin[20] or even with the water mass[21]. Which one between the physicochemical composition and the history of the water mass have to be considered as the pivotal factor for the structuring of the communities is still an open question. Notwithstanding these achievements, the Antarctic marine microbial communities are still poorly explored[11] and no data on protist assemblages inhabiting its deep biosphere are available in the literature.

The present study is focused on the Ross Sea that represents a changing, heterogeneous environment that harbors several water masses characterized by great variability in terms of physicochemical parameters[2]. Few data are available about dynamics and drivers concerning protist communities in the principal water masses[22] and, to the best of our knowledge, a comprehensive description at a fine taxonomic level is still missing. The aim of this study is thus to assess the diversity of protist communities describing shifts in composition among the main water masses (HSSW, ISW, AABW and CDW). The research provides a new insight into the poorly known meso-bathypelagic assemblages of protists of the Southern Ocean; it seeks for physicochemical environmental control effects on the diversity and the partitioning of protist communities highlighting the advection effects and traces of mixing events in AABW formation.

2. Methods

2.1 Sampling strategy

Thirteen water samples for the analysis of meso- bathypelagic protist communities were collected during the 2014 XXIX Italian Expedition in Antarctica on the R/V Italica. The sampler carousel was equipped with a SBE 9/11 Plus CTD profiler and sampling depths were chosen accordingly to physicochemical characterization of water column (potential temperature and salinity). Sampling sites were located along the Ross Sea (see Figure 1 and Supplementary Table S1). At each site, 20 liters of sea water were directly pre-filtered with a 200 µm mesh to remove larger zooplankton and then filtered on 2 µm pore size PCTE membrane (Sterlitech) using a peristaltic pump (Millipore®). The membranes were placed in sterile vials and frozen at -80 °C until molecular analysis.

Dissolved macronutrient concentrations were determined in pre-filtered (Whatman GF/F) and frozen (-20°C) samples, by means of a QuAAtro automated flow analyzer (SEAL Analytical), according to Koroleff and Grasshof[23].

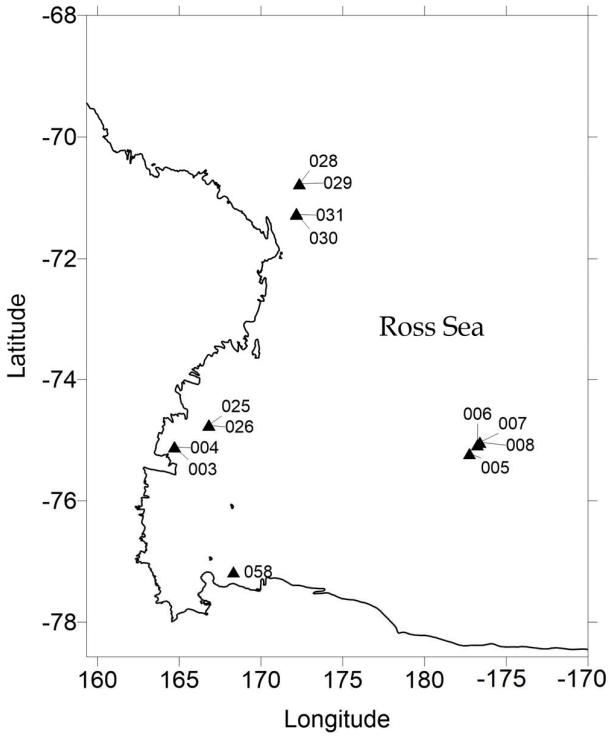

- **Figure 1: Sampling stations in the Ross Sea.**

2.2 Metabarcoding Amplicon Sequencing

DNA extraction was performed using PowerSoil DNA Isolation Kit (MOBIO) customized with two improvements in the protocol: the membrane was completely dissolved in chloroform during DNA extraction step to increase DNA recovery avoiding issues related with folding and scrubbing of the filter; the chloroform was successively removed increasing to 5' the time of the first centrifugation step and recovering the upper water phase.

Metabarcoding analysis was based on hyper variable 9 region (V9) of the rRNA 18S gene amplified with primers pair 1391F (*5'*-GTACACACCGCCCGTC-*3'*) and EukB (*5'*-TGATCCTTCTGCAGGTTCACCTAC-*3'*)[12].To limit over-cycling of targeted region, amplification was led in real time and each samples amplification was stopped when plateau was reached. The primary qPCR was performed in 10 µL reaction with 0.5U of KAPA 2G HiFi Taq, 1X KAPA 2G Buffer HiFi, 0.3 µM dNTPs, 1X EvaGreen (Biotium), 0.3 µM of each primer, 2 µL of DNA template and RNasi free water up to the final volume. Thermocycling conditions were set to: 1' at 95°C, 28-31 cycles of 15" at 95°C, 10" at 60°C, 4" at 72°C, and 3' of final elongation at 72°C. Negative controls with RNase free water instead of DNA template were amplified to ensure absence of contaminations. Sequencing adapters were attached to amplicons with a secondary PCR performed in 25 µL with same reagents, concentrations and cycling conditions of the primary PCR (9 cycles). No significant amplifications rise in the negative controls.

Amplified samples were normalized using SequalPrep Normalization kit (Thermo Fisher), pooled together, processed with Ion PGM Hi-Q OT2 kit and Ion PGM Hi-Q Sequencing kit (Life Technologies). The sequencing was carried out with an Ion Torrent PGM running Ion 314 chip v2. For 3 random samples the extraction, amplification and sequencing steps were carried out in triplicate; moreover we sequenced also a PCR negative control to allow a better detection and removal of any environmental DNA contaminations (eg. from the laboratory) during bioinformatics steps of sequences' analysis.

2.3 Amplicon sequences analysis

Sequences' dataset was exported raw from Torrent Server in fastq format. Demultiplex and forward primer removal was done with fastq_strip_barcode_relabel2.py script (USEARCH package, available at http://drive5.com/usearch drive5.com) while reverse primer was trimmed with Cutadapt 1.9.1[24]. Per-base average quality scores of reads (sequences) were checked with FastQC to ensure the absence of quality drops. Trimmed reads were length and quality filtered with USEARCH v8.1 setting the minimum length threshold at 70 b (expected amplicon length of 120-130 b) and the quality threshold to a maximum allowed expected errors of 1 nucleotide each 100 bases[25]. Reads were dereplicated and chimeras were removed performing d*e-novo* chimera detection with UCHIME algorithm[26] and also during clustering step with UPARSE-REF algorithm[27]; assignation to different operational taxonomic units (OTUs) was carried out with a threshold dissimilarity level of 3% on the global alignment length. The global alignment search strategy implemented in the ggsearch36 program (FASTA package available at http://faculty.virginia.edu/wrpearson/fasta/CURRENT/) was adopted to perform taxonomic assignation of the most abundant reads of each OTUs against V9_PR2 reference database; up to 20 hits were considered per each OTUs and it was retained only the best reference (identity score and e-value) or, in case of equality, the taxonomic assignation was kept at the level of the last common ancestor[20,28].

The OTUs table was manually cleaned from prokaryotic taxa since V9 primers can potentially amplify regions of 16S rDNA[29] (those sequences were included into V9_PR2 reference database) and Metazoa taxa as the sampling method were not representative for these groups. Furthermore only OTUs that occurred in at least 2 different samples were included[20]. From this final table two version were then created: (i) containing the 3 samples (006, 030 and 031) with related replicates and (ii) with 13 distinct samples.

2.4 Statistical analysis

Alfa- and beta-diversity analyses were performed in R with the package Vegan (linear regression, rarefaction curves, Shannon index, non-metric multidimensional scaling (NMDS), distance-based Redundancy Analysis (dbRDA), PERMANOVA test, ANOSIM) and VennDiagram. For community comparison, the differences in sequencing depth among samples were minimized by subsampling at 3512 reads each samples with rrarefy command (Vegan); the rarefied dataset resulted to be highly representative of full dataset when compared with a Mantel test based on Pearson correlation (R = 0.98 and p-value < 0.001). OTU abundance values were log transformed to diminish the effect of the most abundant OTUs[30] before computing Bray-Curtis dissimilarity matrix while environmental variables were normalized making the sum of squares equal to one and dissimilarity matrix was based on Euclidean distance.

3. Results

3.1 Characterization of water masses

Samples were collected within four specific water masses (Fig. 2), identified as follows, according to Orsi and Wiederwohl[2]: 1) High Salinity Shelf Water (HSSW) showing salinity values > 34.73 and temperatures near the surface freezing point; 2) Ice Shelf Water (ISW) identified by temperatures lower than the surface freezing point and salinity = 34.62; 3) Circumpolar Deep Water (CDW) corresponding to neutral density anomalies between 27.98 and 28.27 and potential temperature > 0°C ; 4) Antarctic Bottom Water (AABW) with densities > 28.27 and temperatures lower than 0°C. Details information on samples along with measured physicochemical parameters are available as Supplementary Table S1.

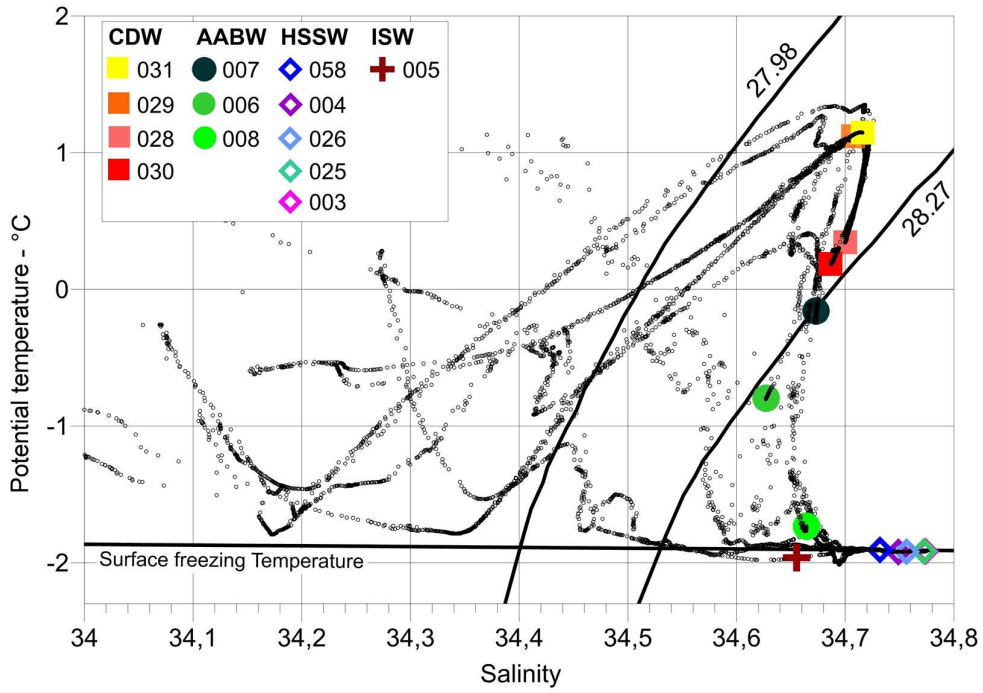

- **Figure 2: θ/S diagram of the water column at each station.** The legend indicates the name of the stations grouped accordingly with water masses' characteristic.

3.2 Sequencing considerations

OTUs table obtained after all cleaning steps was composed by 153,816 18S ribosomal RNA gene sequences with sample fractions that ranged from 3,512 to 13,315 reads (mean 8,096). Similarity threshold of 97 % for OTUs' clustering was chosen in order to fully be consistent and comparable with the few existent studies on meso- and bathypelagic protist communities carried out with massive parallel sequencing techniques[29,21,31]. Our molecular strategy was based on Ion Torrent sequencing and to test the reproducibility of applied extraction, amplification and sequencing protocols and methodologies, we compare a subset of 3 samples, each of them made in triplicate. The explorative approach was those proposed by Massana et al.[30]: each pairwise of replicates was compared plotting their OTU abundances in a scatterplot and performing a linear regression; all R^2 coefficients and slopes were then ordinated and plotted according with reads ratio of each pairwise. Figure 3a shows as R^2 statistics were always high (0.92 on average) and not correlated with reads

ratio while slopes values tended to decrease at low reads ratio but no significant correlation was found. Analyzing the percentage of shared OTUs among all pairwise (Fig. 3b), we obtained relatively low values, ranging from 56 % to 70 %, although the percentages of shared reads were high (from 89 % to 97 %).

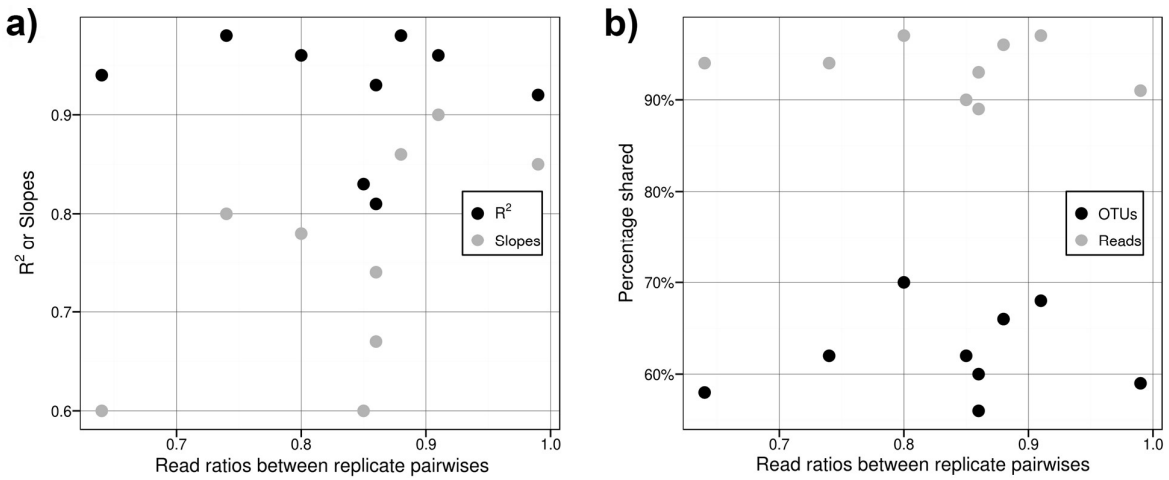

- **Figure 3: Concise comparison of Ion Torrent replicates (n=9).** R^2 coefficients (black dots) and slope values (white dots) from linear regressions of all pairwise of replicates(a); percentage of shared OTUs (black dots) and percentage of shared reads of each pairwise (b); all statistics are plotted against reads ratio of replicates.

The rarefaction curves reported in Figure 4a related the number of detected OTUs with sequencing effort; OTUs richness ranged from 271 to 731 (478 mean) and the majority of samples showed curves that approached saturation phase. A significant difference (t = 3.62, *p*-value < 0.01) emerged comparing curves and OTUs richness of samples representing HSSW (green curves; 366 mean) and samples of other water masses (> 530 means). Also the Shannon index confirmed the existence of different alpha-diversity levels among water masses; the maximum value was found in CDW samples with mean (± s.d.) value of 4.23 ± 0.32, followed by AABW samples with 3.94 ± 0.46, ISW sample with 3.42 and HSSW samples with 2.49 ± 0.72. A total rarefaction curve was performed pooling together the reads of all samples (Fig. 4b) to give an estimate of the total richness of meso-

bathypelagic realm; this curve achieved the plateau and the maximum number of OTUs reached was 1743.

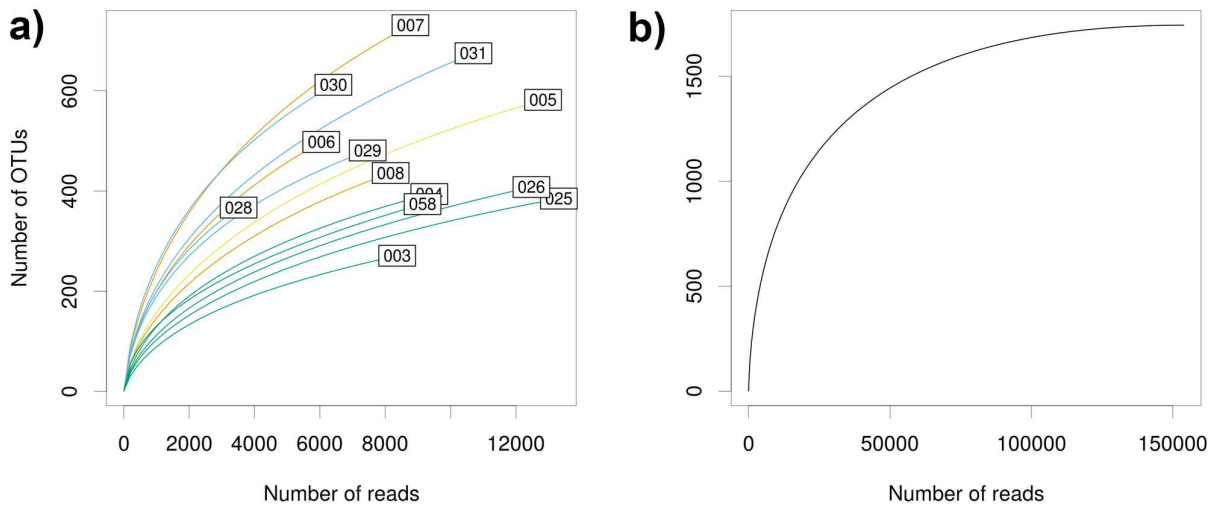

- **Figure 4: rarefaction curves overview.** Comparison between OTUs richness and sequencing depth per each samples (a) and pooling all samples together (b). Colors represent HSSW (green), ISW (yellow), AABW (orange) and CDW (blue).

3.3 Links between environmental and genomic data

Figure 5 shows the nMDS ordination plots based on environmental distance (a) and OTUs taxonomic distance (b); in both cases samples clustered according to water masses and results were supported by the analysis of similarity (ANOSIM; R = 0.61, P =0.01 and R = 0.68, P =0.001 respectively). The investigation of the taxonomic distance constrained by environmental variables were performed through the distance-based redundancy analysis (dbRDA). The plot in Figure 5c shows how the physicochemical parameters arranged samples by the first two axes: dbRDA1 that explained 42.6 % of fitted and 32.6 % of total variations, and dbRDA2 that explained 19.2 % of fitted and 13.8 % of total variations. All variables had a moderate correlation (r > 0.5) with one of those two axes although dbRDA1 was strongly correlated with temperature (r = 0.86), salinity (r = -0.68) and DO (r = -0.93), while dbRDA2 was related with phosphate (r = -0.62). Exceptions were represented by

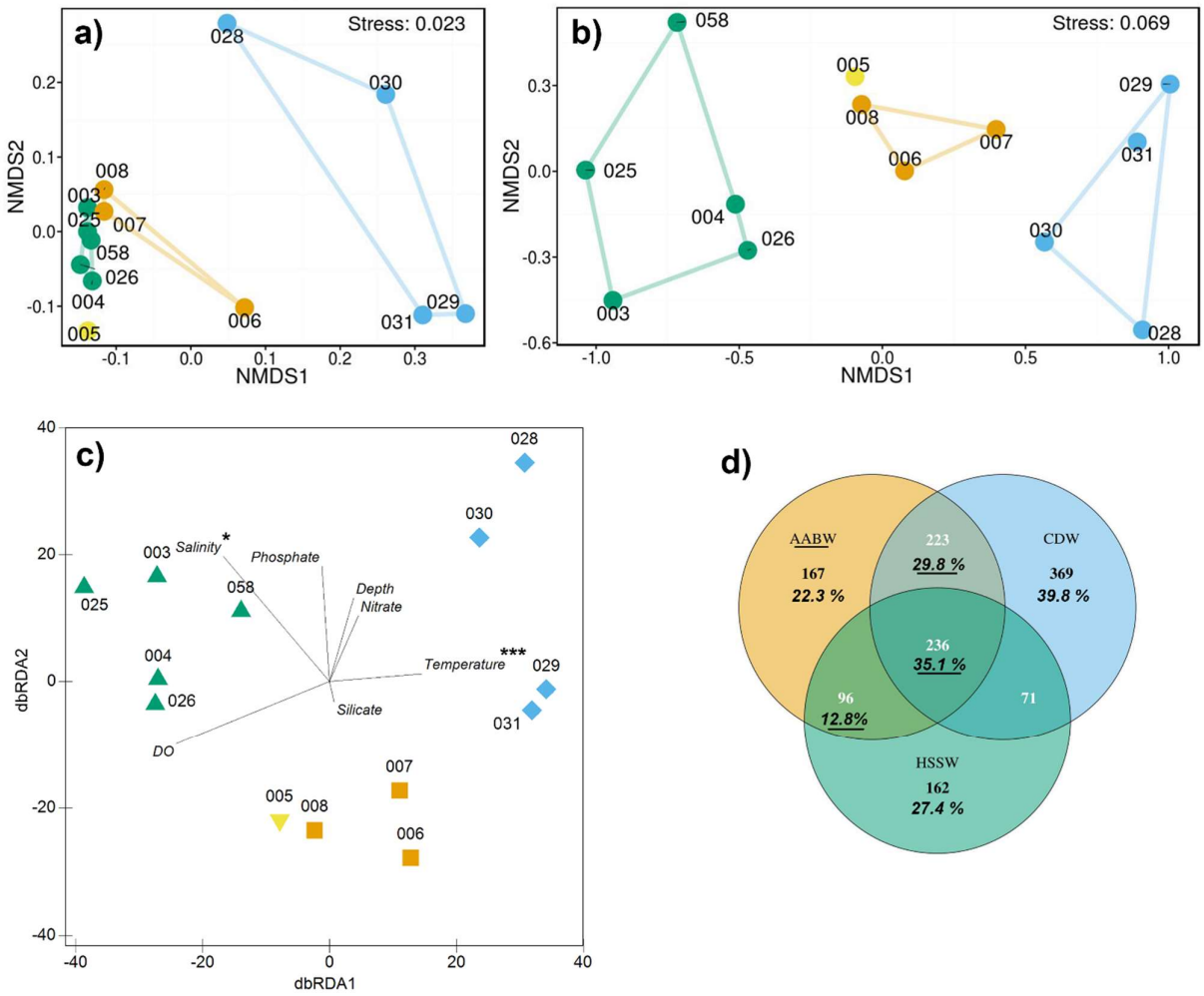

- **Figure 5: Comparison of beta-diversity among meso-bathypelagic protist communities.** nMDS ordination based on environmental Euclidean dissimilarity matrix of normalized environmental variables (a), and nMDS ordination based on Bray-Curtis dissimilarity matrix of square root transformed OTUs abundance (b). In the distance based Redundancy Analysis (dbRDA) vectors with a significant statistic based on PERMANOVA test are marked with asterisks (* for $P < 0.5$, *** for $P < 0.001$) (c). Venn diagram of OTUs partitioning among AABW, CWD and HSSW; percentage of unique OTUs in each water mass are reported, as well as percentage of OTUs that AABW shared with the other water masses or with both of them (d). Colors represent HSSW (green), ISW (yellow), AABW (orange) and CDW (blue).

depth that correlated with dbRDA3 (r = -0.90) and silicate that correlated with dbRDA4 (r = 0.83) (see Supplementary Figure S2).

Analyzing the OTUs partitioning among water masses (Fig. 5d; ISW was excluded because described by only one sample), CDW harbored higher unique diversity (369 OTUs, 39.8 % of its total OTUs richness) than HSSW (162 OTUs, 27.4 %) and AABW (167 OTUs, 22.3 %); CDW shared only 71 OTUs (7.7 %) with HSSW while AABW shared 29.8 % of OTUs with CDW and 12.8 % OTUs with HSSW and 35.1 % with both.

3.4 Protist taxonomy in deep Ross Sea water masses

In order to highlight possible differences in taxonomic composition among meso- bathypelagic communities, the relative contribution of the 8 most abundant groups of protists were investigated. The analysis of the local diversity were conducted in terms of relative number of reads and relative number of OTUs averaged per each water mass (Fig. 6). Apicomplexa, Ciliophora and Dinophyta – divisions of the Super-group Alveolata – dominated in all water masses with an average 57.0 % of reads (5.0 %, 2.6 % and 49.4 % for each division respectively) and an average 51.9 % of OTUs (2.6 %, 6.7 % and 42.6 %). Excavata reads were remarkably abundant in CDW (20.4 %; mean 5.4 % in the other water masses) although its contribution in OTUs was high in all water masses (11.0 % in HSSW, 17.7 % in ISW, 17.8 % in AABW and 25.5 % in CDW). Cercozoa and Radiolaria divisions are reported for the Super-group Rhizaria; Cercozoa contribution was on average 4.8 % of reads (range from 1.5 % in CDW to 7.5 % in AABW) and 7.1 % of OTUs (range from 3.7 % in CDW to 11.0 % in HSSW); Radiolaria reads were abundant only in CDW (9.7 %; mean 2.5 % in the other water masses) while OTUs contribution averaged 7.9 % considering all water masses (5.1 % in HSSW, 6.7% in ISW, 8.8 % in AABW and 11.0 % in CDW). Hacrobia was on average 0.6 % of reads and 2.6 % of OTUs. Stramenopiles reads contribution was on average 14.2 % among all water masses with the exception of 43.7 % in HSSW although OTUs contribution ranged from 7.7 % in CDW to 18.0 % in HSSW.

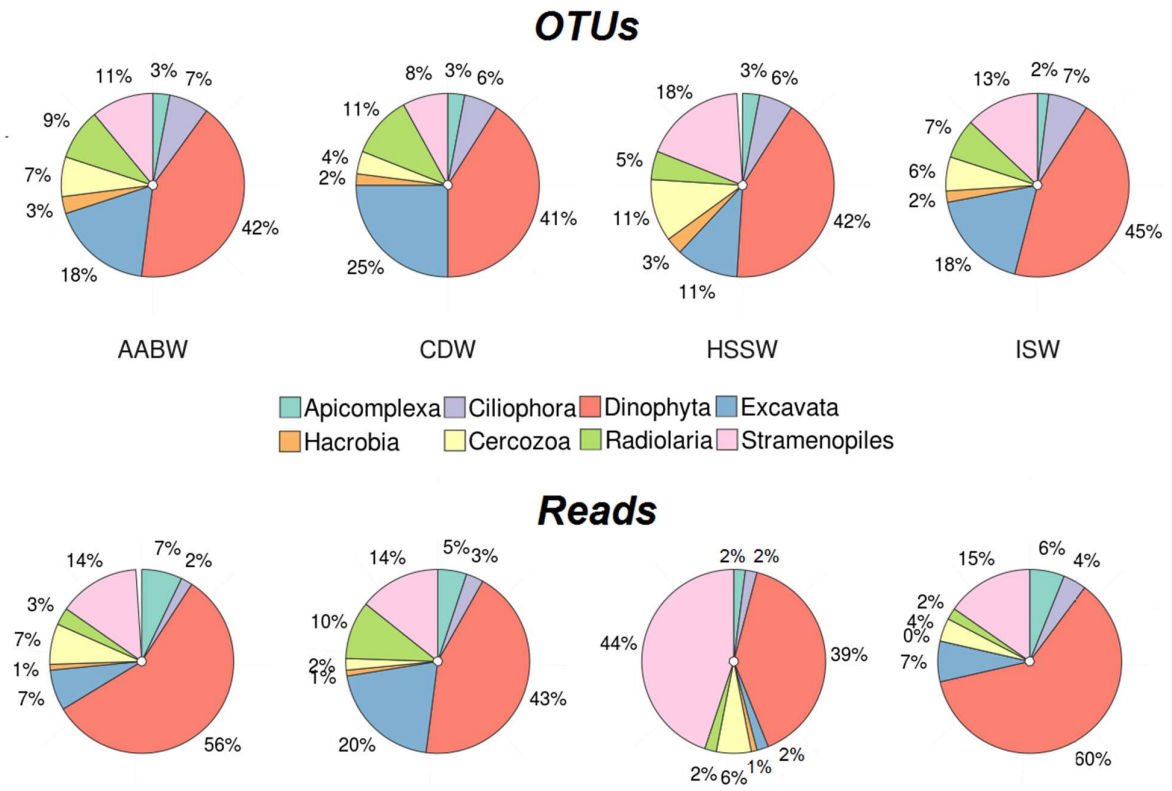

- **Figure 6: Relative composition of the most abundant protist groups among the investigated water masses.** For each groups are reported the percentage contribution in terms of OTUs (top pane) and reads (bottom pane); values of each sample are averaged accordingly to the water mass.

The relative abundance (RA) of each OTU was cross-compared among samples (Fig. 7) to support and further explore the differences in protist community composition in the different water masses. The insight was performed for OTUs with RA > 0.5 % and from the analysis 3 groups of OTUs emerged: Group I that harbored OTUs with comparable high RA among all samples, Group II which showed OTUs with similar RA in HSSW, ISW and AABW samples, and Group III that was characterized by OTUs with higher RA in CDW samples rather than in the other water masses. The groups had also different taxonomic composition: Group I was mainly composed of Alveolata such as Dinophyceae (39.1 %), Gregarines (0.9 %) and Syndiniales (0.5 %); Stramenopiles like Bacillariophyta (17.4 %) and

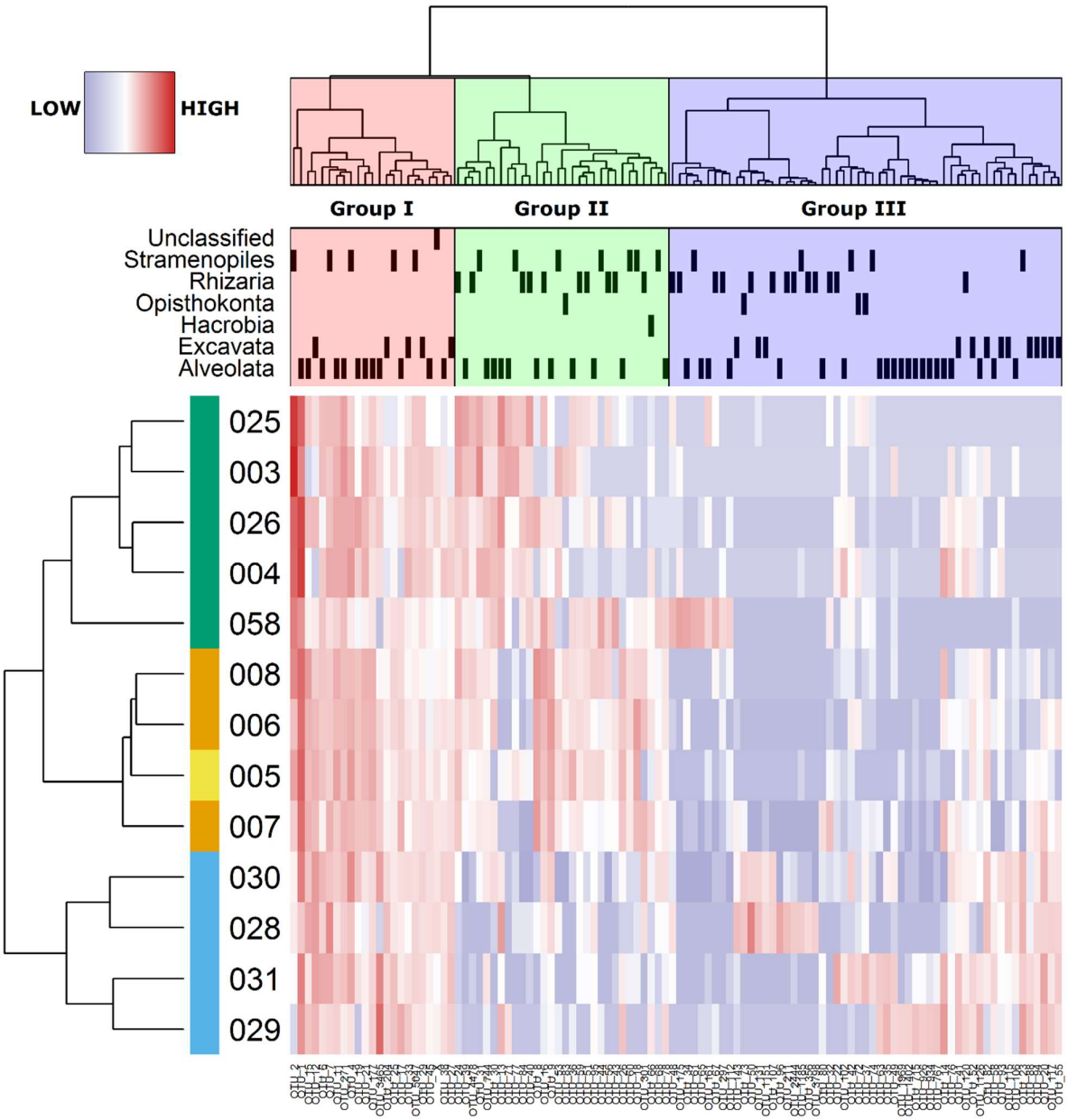

- **Figure 7: Cross-comparison of RA of most abundant OTUs in all samples.** Heat maps comprehends OTUs with RA > 0.5 % and it shows in which samples the highest RA were detected for each OTU. The color bar on the y-axis represents the color code of the water masses: HSSW is green, ISW is yellow, AABW is orange and CDW is blue.

MAST-1 (0.5 %), and the Excavata's class Euglenozoa (13.0 %). Group II comprised Filosa-Thecofilosea (30.0 %, Rhizaria), Dinophyceae (20.0 %), Bacillariophyta (20.0 %) and few OTUs of

Spirotrichea and Gregarines (both Alveolata); Group III included Dinophyceae (21.4 %), Polycystinea (14.3 %, Rhizaria) and Euglenozoa (12.5 %) as well as few OTUs of Syndiniales, Gregarines and Litostomatea (all Alveolata), Acantharea (Rhizaria) and MAST-1 (Stramenopiles).

A basin scale overview of the diversity of protist in meso- bathypelagic layers of the Ross Sea was conducted mainly at class-level and is reported in Supplementary Table S3. The analysis revealed that 66 different class-levels were taxonomically assigned however more than 90 % of the total number of reads belonged to the first 8 entries: Dinophyceae (Alveolata, 44.1 %), Bacillariophyta (Stramenopiles, 24.9 %), Discoba unclassified (Excavata, 4.8 %), Filosa-Thecofilosea (Rhizaria, 4.6 %), Apicomplexa (Alveolata, 4.5 %), Euglenozoa (Excavata, 4.5 %), Syndiniales (Alveolata, 3.0 %) and Polycystinea (Rhizaria, 2.5 %); those classes belonged to four different Super-groups although with a prevalence of Alveolata. Interestingly, in our survey the presence of Fungi was almost negligible (Ascomycota 0.4 %, Ichthyosporea 0.1 % and Basidiomycota 0.1 % of total reads).

The degree (%) of novelty found within each taxa group were expressed as proposed by Pernice et al.[21]: we estimated per each taxon the average similarity of its OTUs against the reference sequences and the averaged similarity of its OTUs weighed on the respective numbers of reads. Overall, only 23.2 % of taxa showed OTUs similarity > 97 % while 55.1 % were above 90 % of similarity, 18.8 % above 80 % and only 2.9 % of taxa shown lower similarity levels; the reads weighted similarity values show in general a comparable distribution except for a higher percentage of > 97 % cutoff (34.8 %, 39.1 %, 23.2 % and 2.9 % respectively) indicating that the OTUs with lower similarity in the reference database were those found with lower abundances. Among the most represented classes Dinophyceae and Bacillariophyta had relatively high level of similarity (> 96.3 % for OTUs and > 99.0 % for Reads) while the other groups might harbored higher level of novelty with mean OTUs similarity of 94.5 % and mean reads similarity of 95.7 %.

An insight investigation (see Supplementary Table S4), conducted at the order-level (5th rank of PR2 reference database taxponomy), revealed that more than half of the reads of Dinophyceae class (contribution 42.3 %) belonged to the Dinophyceae Uncultured_18 order (contribution 22.7 %) that had a strong match with the full 18S rDNA sequence of dinoflagellate phylotype SL163A10 (99% identity and *e*-value of $0.4*10^{-65}$); this taxon was exceptionally abundant in samples 004 and 026 (both HSSW). Bacillariophyta at the order-level had a missing taxonomy in the adopted reference database although at family-level the taxon split predominantly into two groups: Polar-centric-Mediophyceae and Raphid-pennate with average contributions of 12.0 % and 5.4 % respectively; these taxa had remarkable high abundance in samples 003, 025 and 058 (all HSSW). Such findings for Bacillariophyta are in agreement with visual microscopy analysis as detailed in the Supplementary Section S5. For the other abundant class-level groups emerged that each one of them were mostly represented by just one order-level: for Filosa-Thecofilosea (4.6 %) the Cryomonadida (3.4 %), for Apicomplexa (contribution 4.5 %) was the Gergarines (contribution 4.5 %), for Euglenozoa (4.5 %) the Diplonemea (4.4 %), for Syndiniales (3.0 %) the MALV-I (2.3 %) and for Polycystinea (2.6 %) the Collodaria-Nassellarida (2.3 %).

4. Discussion

The results clearly support a significant diversity among protist communities inhabiting different water masses in the deep realm of the Ross Sea (Fig. 5). Each water mass was characterized not just by unique physicochemical properties but also from dissimilar community compositions due to the presence of exclusive OTUs. HSSW and CDW harbored the most dissimilar assemblages while AABW was characterized by a genetic signature typical of both parental water masses in agreement with what conceivable for oceanography dynamics[2]. The ISW, while more similar to HSSW for the measured physiochemical parameters (Supplementary table S1, Fig. 5a), grouped with AABW when

protist community composition was taken into account; such result has to be related to the site of AABW retrieval that occurred at the shelf break where ISW typically overflows (i.e. at the mouth of the Glomar Challenger trough). Among the measured environmental factors, temperature, salinity and dissolved oxygen were the most explicative variables of protist distribution, in agreement with what reported by Willkins et al.[32] for the Southern Ocean and within the global view provided by Tamames et al.[33]. Moreover several studies found how different water masses harbored distinct microbial communities[9,10,17,18,21] although it is still unclear whether local (i.e. environmental conditions, physiochemical properties of the water mass, community interactions) or regional factors (i.e. organisms dispersal limitation, hydrographic barriers) acted as major drivers leading to these β-diversity patterns (see Lindström and Langenheder[34]).

The dynamics and the mechanisms that underlie to the spatial partitioning of microbial communities are the core topics of biogeography studies[35] and have been largely investigated in the last decade. Our results cannot be used to disentangle the effects of local and regional factors since the samples of each water mass were collected within short distances (few hundred kilometers). The prevalence of advection-derived shaping effects and distance factors have been recently demonstrated to occur in CDW and AABW by Willkins et al.[32] who analyzed the composition of prokaryotic communities in several water masses of the Southern Ocean. Instead, to our consideration, the environmental conditions had a pivotal role shaping the protist communities of shelf waters (HSSW and ISW) since in these samples we detected remarkable contributions of photoautotrophic Bacillariophyta and Dinophyceae classes that dominated in terms of sequences these deep protist communities. The 18S rDNA genetic signature of these taxa could be biased by differential rDNA copy numbers among species that leads to overestimations, although the evidences for Bacillariophyta taxa were supported by microscopy analysis (Supplementary Section S5) that revealed the presence of *Pseudo-nitzschia* spp., pennate diatoms (both Raphid-pennate) and *Chaetoceros* spp. spores (Polar-centric-

Mediophyceae) in samples 003, 025 and 058, as well as the presence of dinoflagellate phylotype SL163A10 in sample 004 and 026.

The spore of *Chaetoceros* as a resisting form might originate from relatively old sinking events since their presence in Antarctic deep layers has already been reported in the literature[36,37]. However their involvement in recent phytoplanktonic dynamics are suggested by the co-occurrence with *Pseudo-nitzschia,* pennate diatoms and phylotype SL163A10, and all of them might be part of blooms that recurred each year from November to February in the Ross Sea[38]. Sinking events have been demonstrated to rapidly export to deep layers blooms of *Phaeocystis antartica*[39] and of diatoms[40]; furthermore evidences were provided on the fact that the senescence of the organisms are not a prerequisite for the process. Intact phytoplanktonic cells were found under the Ross Ice Shelf likely transported by advection process involving modified HSSW[31]. Agusti et al.[41] lately showed that, on a global scale, the sinking of healthy phytoplankton cells occurs, stating that the velocity of sinking mechanisms and the abundance of the exported cells are significant and the assemblage composition of sunk cells is directly influenced by the superficial community from which they originate.

Overall protist communities of the deep realm in Ross Sea included about 1700 OTUs and 66 class-level groups that might represents interesting values in comparison with the 2500 OTUs and 46 class-level groups assessed for the global bathypelagic realm; although this represents just a descriptive comparison since Pernice et al.[21] based their investigation on a different high-throughput sequencing approach and targeted a diverse region of 18S rDNA gene. The dominant taxonomic groups were Dinophyta (division of Alveolata), Stramenopiles, Excavata and Rhizaria (Cercozoa and Radiolaria divisions), in agreement with similar studies based on high-throughput sequencing methods[21]. Dinophyta dominated the assemblages with > 50 % of OTU and read abundances; this taxon holds one of the most diverse lineage of marine plankton, characterized by

various and heterogeneous life strategies, although still poorly described in terms of taxonomy and ecological significance (see Le Bescot et al.[42]). The phylotype SL163A10 was abundant (meant as > 0.5 of RA in each sample) in all samples but showed the highest values in Shelf Waters. SL163A10 was firstly identified by Gast et al.[43] that reported it as an abundant taxon in sea water and pack-ice meltwater communities of the Ross Sea; recently Torstensson et al.[44] confirmed as the dinoflagellate comprised 63% of total sequences in sea-ice samples. The ecology of this taxa is still unknown but, as the pigmented Bacillariophyta found in deep Shelf Water, they will eventually die[41] becoming a new source of organic matter that contributes to support the high prokaryotic metabolic rates in the deep ocean[45].

The second most represented group of protists was the Stramenopiles; this taxon was mainly composed by Bacillariophyta, class that was found in all water masses with remarkable abundance in HSSW. The MArine STramenopiles (MAST), one of the major class of phagotrophs in the surface ocean[46], represented only a small fraction of protist communities in the meso- bathypelagic regions analyzed here (1.4 % of total reads) and its scarcity has been reported in the Ross Sea also at the surface[13]. However other heterotrophic taxa such as Excavata and Cercozoa (Rhizaria) were found to be abundant in protist assemblages and especially in CDW. The Excavata is usually well represented in deep waters and includes several bacterivours forms as the heterotrophic flagellates clade Diplonemea[47]; in our study Excavata was one of the most OTUs-rich groups, especially abundant in CDW samples and it was almost uniquely composed of Diplonemea; this order recorded also for the highest grade of novelty among the abundant groups (94.4 % and 94.0 % of similarities for OTUs and reads). The Cercozoa gathers a large variety of gliding, free-swimming and parasites protists characterized by amoeboid- and flagellate-like body form (see Howe et al.[48]). In our samples, Cryomonadida represented a dominant order of Cercozoa that in turn was mainly composed by Protaspa and Cryothecomonas lineages (see Supplementary Table S5). Protaspa is

usually described as gliding phagotrophs biflagellates[49] while Cryothecomonas exhibit feeding strategies such as parasitism[50] and grazing on bacteria and phytoplankton[51]; the latter lineage has already been reported in polar/cold environments although Thaler et al.[52] found no evidence of parasitic forms but rather all Cryothecomonas appeared to be free-living. The other division of Rhizaria, the Radiolaria, was mainly represented by Collodaria; this order includes colonial and naked species of Radiolaria[53] which although have been described to bear photosynthetic endosymbionts[54] and to dominate in the global bathypelagic realm[21], information on their ecology in deep ocean are still missing. Apicomplexa is another well represented taxon of Alveolata and it was almost uniquely composed by Gergarines order; little is known about the ecology of this group albeit its presence was recorded in hydrothermal vents[55] and it is usually ascribed as parasite of planktonic invertebrates (such as polychaetes, amphipods, hyperiids, mysids, mollusks, and tunicates)[56]; the cycle of Gergarines includes also a resisting stage (oocysts) that therefore implies a likely inactive ecological role. Interestingly in our survey the contribution of Fungi was almost negligible in dissent with finding for global deep oceans[21]. This would suggest a geographic/environmental confinement for these organisms at low/mid latitudes.

We here briefly point out some methodological remarks that have to be kept in mind considering the data provided in this study. Our investigative approach was based on PCR-amplifications that can alter the ratio among abundant and rare taxa. We therefore tried to limit this issue performing the DNA barcode amplification step on a real time PCR machine to monitor and to reduce at minimum the number of amplification cycles. To avoid concerns about reproducibility random samples have been processed in triplicates; replicates resulted to be very similar ($R^2 > 0.81$) and shared the same abundant OTUs supporting the suitability of the molecular strategy to obtain consistent beta-diversity and taxonomic analyses. The number of represented OTUs might have been reduced with the rarefaction but this step is essential to overcome differences induced by

uneven sequencing depth; furthermore Caporaso et al.[57] highlighted as for analysis of community comparison 2,000 reads are enough to capture the same relationships among samples expressed by their full datasets of hundreds thousands of sequences. Finally we keep in mind that the V9 region of the 18S rRNA lacks in resolution within the Ciliate group[58] and is not indicated to perform fine taxonomical comparison (eg. Species level) although similar conclusion arose for β-diversity analysis of global protist community in comparison with comparing full-length Sanger sequences[59].

In summary the high-throughput sequencing approach adopted to investigate protist communities in the deep layers of the Ross Sea revealed a strong partitioning effects of the water masses suggesting how some of the environmental factors that characterized the oceanographic features of the basin have a deep influence on Shelf Water and in turn to AABW protist assemblage. Relevant signatures of photoautrophic organisms were found in these water masses while whereas in CDW was remarkable the contribution of phagotropic/bacterivorous and parasite taxa. This study provided the first comprehensive insight into protist diversity of this unique habitat unveiling the remarkable importance of Dinophyta, Bacillariophyta, phagotrophs (Diplonemea, Cryomonadida) and parasites (Gergarines) within these microbial communities; the analysis highlight also some groups with unexplained ecological functions (Collodaria), while the presence of fungal signature was almost irrelevant.

References

1. Smith, W. O., Sedwick, P., Arrigo, K. R., Ainley, D. & Orsi, A. The Ross Sea in a Sea of Change. *Oceanography* **25,** 90–103 (2012).
2. Orsi, A. H. & Wiederwohl, C. L. A recount of Ross Sea waters. *Deep. Res. Part II Top. Stud. Oceanogr.* **56,** 778–795 (2009).
3. Baines, P. G. & Condie, S. in *Ocean, Ice, and Atmosphere: Interactions at the Antarctic Continental Margin* (eds. Jacobs, S. S. & Weiss, R. F.) **75,** 29–49 (American Geophysical

Union, Washington, D. C., 1998).

4. Honjo, S. Particle export and the biological pump in the Southern Ocean. *Antarct. Sci.* **16,** 501–516 (2004).
5. Wilkins, D. *et al.* Key microbial drivers in Antarctic aquatic environments. *FEMS Microbiol. Rev.* **37,** 303–35 (2013).
6. Cavicchioli, R. Microbial ecology of Antarctic aquatic systems. *Nat. Rev. Microbiol.* **13,** 691–706 (2015).
7. Massana, R. Eukaryotic picoplankton in surface oceans. *Annu. Rev. Microbiol.* **65,** 91–110 (2011).
8. Caron, D. A., Countway, P. D., Jones, A. C., Kim, D. Y. & Schnetzer, A. Marine protistan diversity. *Ann. Rev. Mar. Sci.* **4,** 467–493 (2012).
9. Galand, P. E., Casamayor, E. O., Kirchman, D. L. & Lovejoy, C. Ecology of the rare microbial biosphere of the Arctic Ocean. *Proc. Natl. Acad. Sci. U. S. A.* **106,** 22427–22432 (2009).
10. Agogué, H., Lamy, D., Neal, P. R., Sogin, M. L. & Herndl, G. J. Water mass-specificuty of bacterila communities in the North Atlantic revealed by massively parallel sequencing. *Mol. Ecol.* **20,** 258–274 (2011).
11. Yu, Z., Yang, J., Liu, L., Zhang, W. & Amalfitano, S. Bacterioplankton community shifts associated with epipelagic and mesopelagic waters in the Southern Ocean. *Sci. Rep.* **5,** 12897 (2015).
12. Stoeck, T. *et al.* Multiple marker parallel tag environmental DNA sequencing reveals a highly complex eukaryotic community in marine anoxic water. *Mol. Ecol.* **19,** 21–31 (2010).
13. Wolf, C., Frickenhaus, S., Kilias, E. S., Peeken, I. & Metfies, K. Protist community composition in the Pacific sector of the Southern Ocean during austral summer 2010. *Polar Biol.* **37,** 375–389 (2013).
14. Bork, P. *et al.* Tara Oceans studies plankton at planetary scale. *Science (80-.).* **348,** 873–875 (2015).
15. Duarte, C. M. Seafaring in the 21St Century: The Malaspina 2010 Circumnavigation Expedition. *Limnol. Oceanogr. Bull.* **24,** 11–14 (2015).
16. Lima-Mendez, G. *et al.* Determinants of community structure in the global plankton interactome. *Science (80-.).* **348,** 1262073 (2015).
17. Galand, P. E., Potvin, M., Casamayor, E. O. & Lovejoy, C. Hydrography shapes bacterial biogeography of the deep Arctic Ocean. *ISME J.* **4,** 564–576 (2010).

18. Celussi, M., Bergamasco, A., Cataletto, B., Umani, S. F. & Del Negro, P. Water masses bacterial community structure and microbial activities in the Ross Sea, Antarctica. *Antarct. Sci.* **22,** 361–370 (2010).
19. Wilkins, D. *et al.* Biogeographic partitioning of Southern Ocean microorganisms revealed by metagenomics. *Environ. Microbiol.* **15,** 1318–1333 (2013).
20. de Vargas, C. *et al.* Eukaryotic plankton diversity in the sunlit ocean. *Science (80-.).* **348,** 1261605 (2015).
21. Pernice, M. C. *et al.* Large variability of bathypelagic microbial eukaryotic communities across the world's oceans. *ISME J.* 1–14 (2015). doi:10.1038/ismej.2015.170
22. Fonda Umani, S. *et al.* Plankton community structure and dynamics versus physical structure from Terra Nova Bay to Ross Ice Shelf (Antarctica). *J. Mar. Syst.* **55,** 31–46 (2005).
23. Koroleff, F. & Grasshof, K. in *Methods of Seawater Analyses* (eds. Grasshoff, K., Kremling, K. & Ehrhardt, M.) 125–188 (Verlag Chemie, 1983). doi:10.1002/9783527613984
24. Martin, M. Cutadapt removes adapter sequences from high-throughput sequencing reads. *EMBnet.journal* **17,** 10–12 (2011).
25. Edgar, R. C. & Flyvbjerg, H. Error filtering, pair assembly and error correction for next-generation sequencing reads. *Bioinformatics* **31,** 3476–3482 (2015).
26. Edgar, R. C., Haas, B. J., Clemente, J. C., Quince, C. & Knight, R. UCHIME improves sensitivity and speed of chimera detection. *Bioinformatics* **27,** 2194–2200 (2011).
27. Edgar, R. C. UPARSE: highly accurate OTU sequences from microbial amplicon reads. *Nat. Methods* **10,** 996–998 (2013).
28. Guillou, L. *et al.* The Protist Ribosomal Reference database (PR2): A catalog of unicellular eukaryote Small Sub-Unit rRNA sequences with curated taxonomy. *Nucleic Acids Res.* **41,** 597–604 (2013).
29. Pawlowski, J. *et al.* Eukaryotic Richness in the Abyss: Insights from Pyrotag Sequencing. *PLoS One* **6,** e18169 (2011).
30. Massana, R. *et al.* Marine protist diversity in European coastal waters and sediments as revealed by high-throughput sequencing. *Environ. Microbiol.* **17,** 4035–4049 (2015).
31. Vick-Majors, T. J. *et al.* Biogeochemistry and microbial diversity in the marine cavity beneath the McMurdo Ice Shelf, Antarctica. *Limnol. Oceanogr.* in press (2015). doi:10.1002/lno.10234
32. Wilkins, D., van Sebille, E., Rintoul, S. R., Lauro, F. M. & Cavicchioli, R. Advection shapes

Southern Ocean microbial assemblages independent of distance and environment effects. *Nat. Commun.* **4,** 1–7 (2013).

33. Tamames, J., Abellán, J. J., Pignatelli, M., Camacho, A. & Moya, A. Environmental distribution of prokaryotic taxa. *BMC Microbiol.* **10,** 1–14 (2010).
34. Lindström, E. S. & Langenheder, S. Local and regional factors influencing bacterial community assembly. *Environ. Microbiol. Rep.* **4,** 1–9 (2012).
35. Lomolino, M. V., Riddle, B. R., Whittaker, R. J. & Brown, J. H. *Biogeography*. (Sinauer Associates, Inc., 2010).
36. Crosta, X., Pichon, J. J. & Labracherie, M. Distribution of Chaetoceros resting spores in modern peri-Antarctic sediments. *Mar. Micropaleontol.* **29,** 283–299 (1997).
37. Ferrario, M. E., Sar, E. A. & Vernet, M. Chaetoceros resting spores in the Gerlache Strait, Antarctic Peninsula. *Polar Biol.* **19,** 286–288 (1998).
38. Peloquin, J. A. & Smith, W. O. Phytoplankton blooms in the Ross Sea, Antarctica: Interannual variability in magnitude, temporal patterns, and composition. *J. Geophys. Res. Ocean.* **112,** 1–12 (2007).
39. DiTullio, G. R. *et al.* Rapid and early export of Phaeocystis antarctica blooms in the Ross Sea, Antarctica. *Nature* **404,** 595–598 (2000).
40. Smetacek, V. *et al.* Deep carbon export from a Southern Ocean iron-fertilized diatom bloom. *Nature* **487,** 313–319 (2012).
41. Agusti, S. *et al.* Ubiquitous healthy diatoms in the deep sea confirm deep carbon injection by the biological pump. *Nat. Commun.* **6,** 7608 (2015).
42. Le Bescot, N. *et al.* Global patterns of pelagic dinoflagellate diversity across protist size classes unveiled by metabarcoding. *Environ. Microbiol.* (2015). doi:10.1111/1462-2920.13039
43. Gast, R. J. *et al.* Abundance of a novel dinoflagellate phylotype in the Ross Sea, Antarctica. *J. Phycol.* **42,** 233–242 (2006).
44. Torstensson, A. *et al.* Physicochemical control of bacterial and protist community composition and diversity in Antarctic sea ice. *Environ. Microbiol.* **17,** 3869–3881 (2015).
45. Herndl, G. J. & Reinthaler, T. Microbial control of the dark end of the biological pump. *Nat. Geosci.* **6,** 718–724 (2013).
46. Massana, R., del Campo, J., Sieracki, M. E., Audic, S. & Logares, R. Exploring the uncultured microeukaryote majority in the oceans: reevaluation of ribogroups within stramenopiles.

ISME J. **8,** 854–866 (2014).

47. Lara, E., Moreira, D., Vereshchaka, A. & López-García, P. Pan-oceanic distribution of new highly diverse clades of deep-sea diplonemids. *Environ. Microbiol.* **11,** 47–55 (2009).
48. Howe, A. T. *et al.* Novel cultured protists identify deep-branching environmental DNA clades of cercozoa: New Genera Tremula, Micrometopion, Minimassisteria, Nudifila, Peregrinia. *Protist* **162,** 332–372 (2011).
49. Hoppenrath, M. & Leander, B. S. Dinoflagellate, Euglenid, or Cercomonad? The ultrastructure and molecular phylogenetic position of Protaspis grandis n. sp. *J. Eukaryot. Microbiol.* **53,** 327–342
50. Drebes, G., Kühn, S. F., Gmelch, A. & Schnepf, E. Cryothecomonas aestivalis sp. nov., a colourless nanoflagellate feeding on the marine centric diatomGuinardia delicatula (Cleve) Hasle. *Helgoländer Meeresuntersuchungen* **50,** 497–515 (1996).
51. Thomsen, H. A., Buck, K. R., Bolt, P. A. & Garrison, D. L. Fine structure and biology of Cryothecomonas gen. nov. (Protista incertae sedis) from the ice biota. *Can. J. Zool.* **69,** 1048–1070 (1991).
52. Thaler, M. & Lovejoy, C. Distribution and diversity of a protist predator Cryothecomonas (Cercozoa) in Arctic marine waters. *J. Eukaryot. Microbiol.* **59,** 291–299 (2012).
53. Ishitani, Y., Ujiié, Y., de Vargas, C., Not, F. & Takahashi, K. Phylogenetic relationships and evolutionary patterns of the order collodaria (radiolaria). *PLoS One* **7,** 1–8 (2012).
54. Stoecker, D. K., Johnson, M. D., De Vargas, C. & Not, F. Acquired phototrophy in aquatic protists. *Aquat. Microb. Ecol.* **57,** 279–310 (2009).
55. Moreira, D. & López-García, P. Are hydrothermal vents oases for parasitic protists? *Trends Parasitol.* **19,** 556–558 (2003).
56. Théodoridès, J. Parasitology of Marine Zooplankton. *Adv. Mar. Biol.* **25,** 117–177 (1989).
57. Caporaso, J. G. *et al.* Global patterns of 16S rRNA diversity at a depth of millions of sequences per sample. *Proc. Natl. Acad. Sci. U. S. A.* **108,** 4516–4522 (2010).
58. Dunthorn, M., Klier, J., Bunge, J. & Stoeck, T. Comparing the hyper-variable V4 and V9 regions of the small subunit rDNA for assessment of ciliate environmental diversity. *J. Eukaryot. Microbiol.* **59,** 185–187
59. Lie, A. A. Y. *et al.* Investigating Microbial Eukaryotic Diversity from a Global Census: Insights from a Comparison of Pyrotag and Full-Length Sequences of 18S rRNA Genes. *Appl. Environ. Microbiol.* **80,** 4363–4373 (2014).

Acknowledgements

This study was supported by the DEEPROSSS (DEEP ROSS Sea ecosystem functioning: new insights on the role of ventilation on microbial metabolism and diversity) project in the framework of the Italian Program for Research in Antarctica (PNRA: project n. 2013/AN1.01). We are grateful to G. De Carolis (CNR), R. Geletti (OGS) and the crew of R/V Italica for their help during sampling. M. Kralj (OGS) provided nutrient data. The precious comments of A. Bergamasco (CNR-ISMAR) and G. Budillon (Univ. Parthenope) helped in water masses identification.

Author Contributions

LZ and MC collected the samples during the oceanographic cruise. LZ performed the molecular analysis (from DNA extraction to high-throughput sequencing) and the bioinformatics elaborations; AP supplied molecular facilities and gave his contribution on high-throughput sequencing data interpretation; FC carried out the insight on phytoplanktonic taxa at the microscope; SFU and MC supervised the research. All authors contributed in writing the manuscript.

Additional Information

Accession codes: All sequences from this study were deposited in GenBank (NCBI; www.ncbi.nlm.nih.gov/genbank/) under the BiomProject accession numbers PRJNA312643.

Competing financial interests: The authors declare no competing financial interests.

Supplementary

Table S1: Detailed information of sampling sites. Abbreviation: DO, dissolved oxygen.

Site	Collection date	Lat_N	Long_E	Bottom depth	Sampling depth (m)	Water mass	Potential temperature (°C)	Salinity	DO (mg L^{-1})	Nitrate (µM)	Phosphate (µM)	Silicate (µM)
003	1/11/13	-75.1099	164.6848	1080	1066	HSSW	-1.89	34.77	7.36	30.74	1.89	77.24
004	1/11/13	-75.1121	164.7091	1080	700	HSSW	-1.90	34.75	7.54	30.67	1.73	77.87
005	1/13/13	-75.2207	-177.2428	495	410	ISW	-1.96	34.64	7.33	31.37	1.64	76.41
006	1/13/13	-75.0758	-176.7683	563	558	ABW	-0.78	34.63	6.47	31.41	1.54	77.24
007	1/15/13	-75.0357	-176.6252	1095	1058	ABW	-1.72	34.66	6.91	29.36	1.76	77.24
008	1/15/13	-75.0339	-176.6214	1095	1080	ABW	-1.73	34.66	6.93	31.19	1.69	108.39
025	1/21/13	-74.7509	166.8090	957	944	HSSW	-1.89	34.77	7.52	31.75	1.90	89.66
026	1/21/13	-74.7559	166.7998	957	700	HSSW	-1.90	34.76	7.63	29.53	1.92	102.70
028	1/23/13	-70.7655	172.3536	1769	1743	CDW	-0.93	34.70	4.99	33.04	2.01	93.32
029	1/23/13	-70.7687	172.3554	1769	450	CDW	0.71	34.71	4.77	31.92	1.58	102.70
030	1/24/13	-71.2575	172.1657	1401	1380	CDW	0.26	34.69	5.29	32.16	2.03	102.70
031	1/24/13	-71.2708	172.1682	1401	400	CDW	0.38	34.58	5.42	31.89	2.20	93.32
058	2/1/13	-77.1704	168.3131	899	888	HSSW	-1.88	34.73	7.17	29.98	2.11	93.32

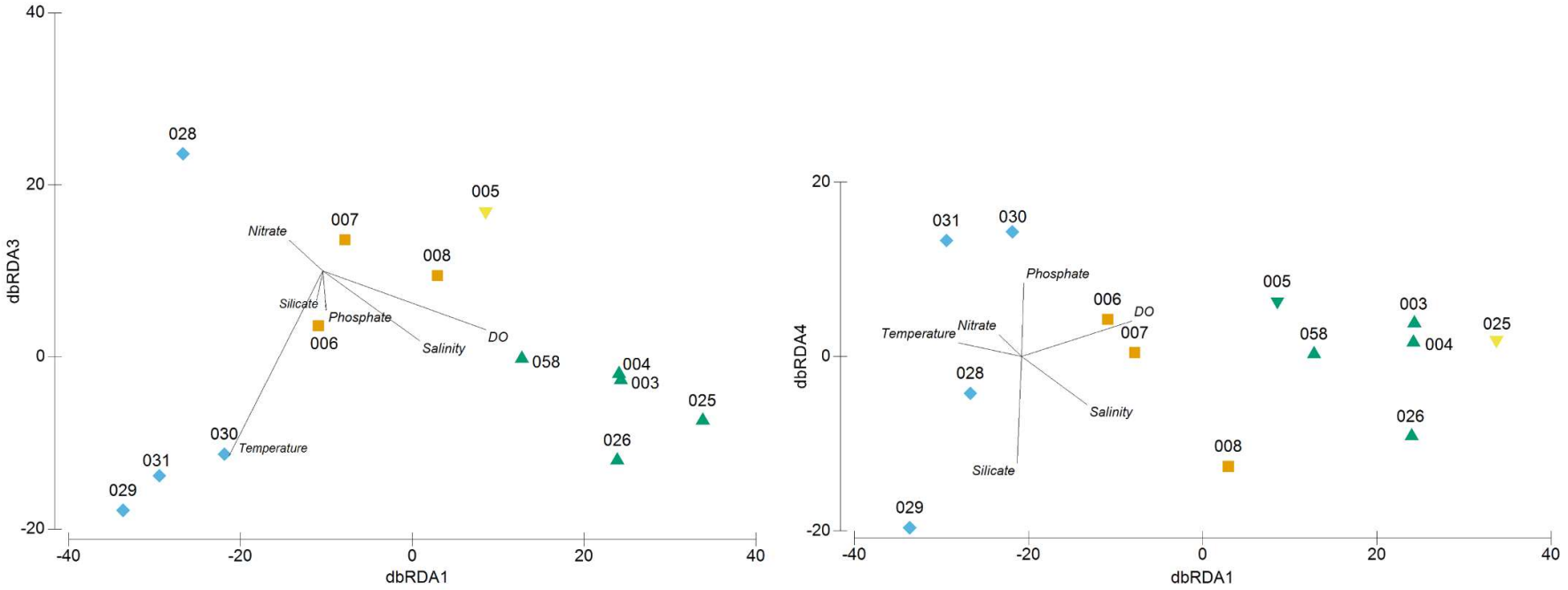

Figure S2: distance based Redundancy Analysis (dbRDA) comparison of meso-bathypelagic protist communities. dbRDA3 and dbRDA4 are plotted versus dbRDA1. dbRDA3 explain 14.0 % of fitted and 9.3 % of total variations, and dbRDA4 explain 7.8 % of fitted and 5.2 % of total variations. Vectors with a significant statistic based on PERMANOVA test are marked with asterisks (* for $P < 0.5$, *** for $P < 0.001$). Abbreviation: DO Dissolved Oxygen.

Table S3: Overview of protist taxonomic groups reported mainly at class level. Table reports per each group the number of OTUs, the number of reads, the reads percentage contribution on total number, the average similarity of correlated OTUs with the reference sequences (%) and the average similarity weighted on the read numbers of each OTU. Reported taxonomic groups refer to the 4th rank in the reference database that mainly correspond to class level; when the taxonomy for that level was missing it is provided the taxonomy of the 3rd rank (*). Entries are ordered accordingly to reads number.

Supergroup	***Taxonomic group***	**OTUs**	**Reads**	**Contribution (%)**	**Avg. similarity (%)**	
					OTUs	**Reads**
Alveolata	Dinophyceae	323	51394	44.099	96.3	99.4
Stramenopiles	Bacillariophyta	84	29017	24.898	96.5	99.0
Excavata	Discoba*	178	4617	4.792	95.1	97.3
Rhizaria	Filosa-Thecofilosea	61	5528	4.637	95.1	96.8
Alveolata	Apicomplexa*	46	5098	4.467	93.8	95.6
Excavata	Euglenozoa	135	4478	4.461	94.3	94.5
Alveolata	Syndiniales	276	3147	3.027	93.8	95.5
Rhizaria	Polycystinea	38	1785	2.549	95.0	94.9
Alveolata	*Spirotrichea*	44	1334	1.145	94.5	97.3
Stramenopiles	*MAST*	45	1209	1.037	96.7	99.0
Rhizaria	*Acantharea*	34	957	0.821	92.7	97.4
Rhizaria	*RAD-B*	34	927	0.795	93.9	94.1
Stramenopiles	*Bolidophyceae-and-relatives*	5	723	0.62	93.2	95.6
Alveolata	*Litostomatea*	12	722	0.62	95.2	93.9
Opisthokonta	*Choanoflagellatea*	20	654	0.561	94.1	94.9
Opisthokonta	*Ascomycota*	18	434	0.372	99.4	99.9
Hacrobia	*Prymnesiophyceae*	10	336	0.288	93.2	97.6
Hacrobia	*Telonemia**	14	319	0.274	93.6	88.5
Rhizaria	*RAD-C*	10	288	0.247	90.7	92.5
Alveolata	*Oligohymenophorea*	35	280	0.24	92.5	93.4
Stramenopiles	*Opalinata*	1	265	0.227	84.0	84.0
Excavata	*Discoba*	13	245	0.21	89.6	88.4
Archaeplastida	*Mamiellophyceae*	13	209	0.179	96.0	97.3
Picozoa	*Picomonadida*	10	177	0.152	96.4	97.0
Opisthokonta	*Ichthyosporea*	5	129	0.111	92.0	89.5
Alveolata	*Colpodea*	14	117	0.1	93.1	93.0
Rhizaria	*Filosa-Imbricatea*	11	112	0.096	90.4	93.6
Alveolata	*Dinophyta*	10	108	0.093	91.3	89.8
Rhizaria	*RAD-A*	10	99	0.085	90.6	91.9
Rhizaria	*Radiolaria**	4	99	0.085	92.3	95.8
Rhizaria	*Filosa-Phaeodarea*	3	97	0.083	92.3	94.8
Opisthokonta	*Basidiomycota*	16	73	0.063	96.8	98.4
Alveolata	*Phyllopharyngea*	4	68	0.058	93.0	97.2
Archaeplastida	*Pyramimonadales*	6	66	0.057	97.3	97.4
Hacrobia	*Cryptophyceae*	6	65	0.056	90.7	90.1
Rhizaria	*Endomyxa-Ascetosporea*	11	56	0.048	84.1	84.8
Stramenopiles	*Labyrinthulea*	8	44	0.038	91.7	86.3
Hacrobia	*Katablepharidaceae*	2	30	0.026	90.0	94.3

Table S3: continued.

Supergroup	*Taxonomic group*	OTUs	Reads	Contribution (%)	Avg. similarity (%)	
					OTUs	Reads
Stramenopiles	*Chrysophyceae-Synurophyceae*	3	23	0.02	96.3	94.6
Rhizaria	*Rotaliida*	6	22	0.019	96.8	98.3
Stramenopiles	*MOCH*	3	21	0.018	94.7	97.1
Stramenopiles	*Stramenopiles***	2	15	0.013	96.0	97.5
Rhizaria	*monothalamids*	7	15	0.013	96.4	95.7
Stramenopiles	*Pinguiophyceae*	2	10	0.009	84.0	84.2
Amoebozoa	*Variosea*	1	9	0.008	87.0	87.0
Archaeplastida	*Streptophyta*	2	9	0.008	84.0	85.1
Alveolata	*Dinophyta**	2	8	0.007	93.0	90.5
Archaeplastida	*Nephroselmidophyceae*	2	7	0.006	86.5	86.7
Stramenopiles	*Pelagophyceae*	3	7	0.006	98.0	98.1
Rhizaria	*Novel-clade-10-12*	1	6	0.005	81.0	81.0
Stramenopiles	*Bicoecea*	1	6	0.005	85.0	85.0
Stramenopiles	*Dictyochophyceae*	2	6	0.005	99.5	99.8
Archaeplastida	*Embryophyceae*	3	5	0.004	94.0	89.6
Rhizaria	*Filosa-Metromonadea*	2	5	0.004	85.5	85.8
Apusozoa	*Planomonadida*	1	4	0.003	90.0	90.0
Alveolata	*Ciliophora-5*	1	4	0.003	100.0	100.0
Archaeplastida	*Trebouxiophyceae*	3	4	0.003	95.7	94.5
Alveolata	*Prostomatea*	1	4	0.003	97.0	97.0
Alveolata	*Ellobiopsidae*	1	2	0.002	100.0	100.0
Rhizaria	*Filosa-Granofilosea*	1	2	0.002	84.0	84.0
Rhizaria	*Miliolida*	1	2	0.002	98.0	98.0
Archaeplastida	*Zygnemophyceae*	1	2	0.002	88.0	88.0
Opisthokonta	*Nucleariidea*	1	2	0.002	86.0	86.0
Rhizaria	*Textulariida*	1	1	0.001	95.0	95.0
Archaeplastida	*Rhodellophyceae*	1	1	0.001	69.0	69.0
Opisthokonta	*Fonticulea*	1	1	0.001	89.0	89.0

Section S5: Microscopy analysis targeted on phytoplanktonic microorganisms.

Methods. For each sample, 5 L of seawater were were slowly and gently poured through a 10 µm mesh to obtain samples of 250 mL[1] that were fixed with buffered formaldehyde solution (2% final concentration) and stored in dark bottles at 4°C. Aliquots of 100 mL were processed following Utermöhl[2]. Cell counts were performed along transects (1-2), counting a minimum of 200 cells, using an inverted light microscope (LEICA BMI3000B) equipped with phase contrast, at a magnification of 400x. Phytoplanktonic cells were identified to the lowest taxonomic rank, following Rines and Hargraves[3], Tomas[4], Scott and Marchant[5].

Results: Samples belonging to deep (> 700 m) High Salinity Shelf Water (HSSW) were analyzed at light microscope in order to support the remarkable abundances of phototrophic groups detected with the molecular approach. Two taxa of Bacillariophyta (Polar-centric-Mediophyceae and Raphid-pennate) represented together 77.7 %, 60.5 % and 28.8 % of relative abundances in samples 003, 025 and 058 respectively.

The microscopy analysis revealed a dominance of *Chaetoceros* spp. spores in samples 003 and 025 (18.4×10^3 and 11.3×10^3 cells L^{-1}, respectively), and lower abundance was detected in the sample 058 (1.0×10^3 cells L^{-1}); this taxon belongs to the Polar-centric-Mediophyceae group. *Pseudo-nitzschia* spp. (ranging from 0.5 to 1.5 x 10^3 cells L^{-1}) and undetermined pennate diatoms > 20µm in size were also observed (ranging from 0.1 to 0.8 x 10^3 cells L^{-1}), both of taxa belong to the Raphid-pennate group.

These data support and agree with the relative abundances estimated for the same taxa in the molecular analysis.

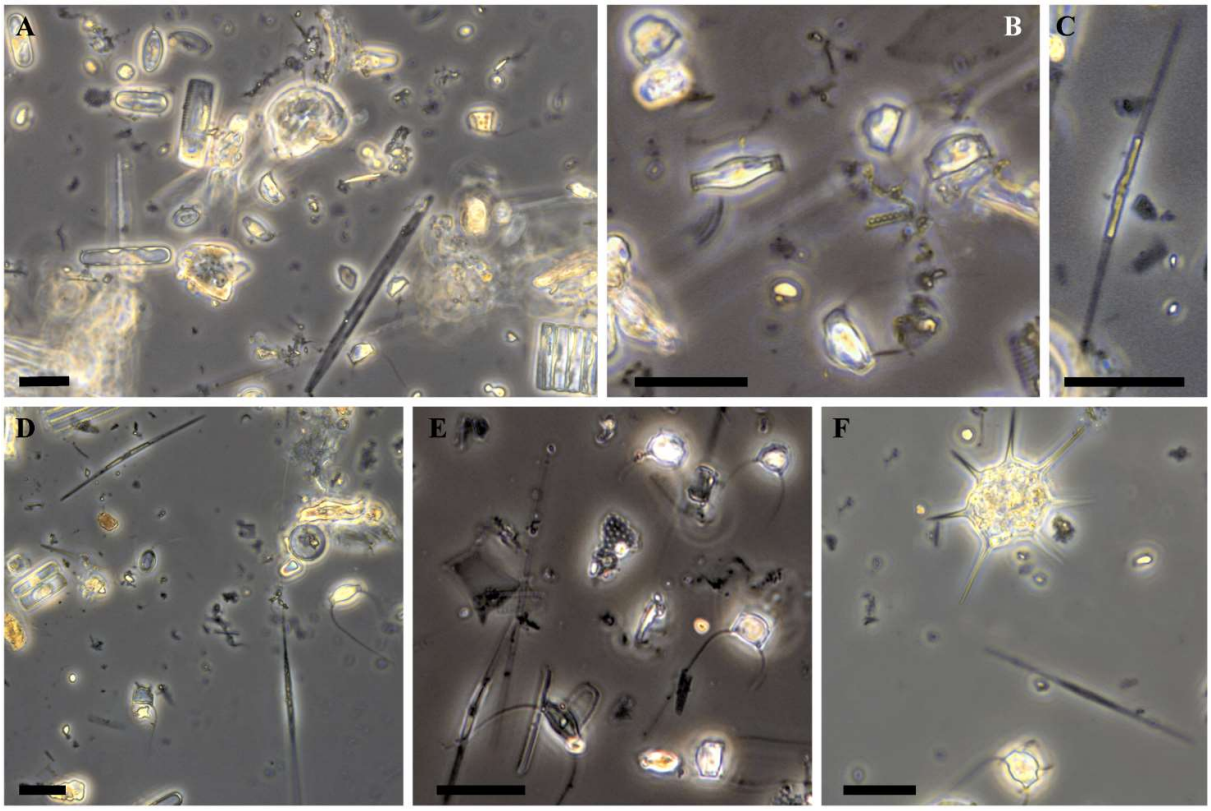

Figures: Micrographs in light microscopy of Bacillariophyta taxa identified in samples 005 (A-C), 025 (D-E) and 058 (F). A) Undetermined pennate diatoms (black arrowheads) and *Chaetoceros* spp. spores (white arrows); B) *Chaetoceros* spp. spores; C) *Pseudo-nitzschia* sp.; D) Undetermined pennate diatoms (black arrowheads), *Chaetoceros* spp. spores (white arrow) and *Pseudo-nitzschia* sp. (black arrow); E) *Chaetoceros* spp. spores; F) *Chaetoceros* spp. spores (white arrow) and *Pseudo-nitzschia* sp. (black arrow). Scale bar: 20 µm.

References:

1. Fonda Umani, S., Monti, M., Cataletto, B. & Budillon, G. Tintinnid distributions in the Strait of Magellan (Chile). *Polar Biol.* **34,** 1285–1299 (2011).
2. Utermöhl, H. Zur Vervollkommnung der quantitativen Plankton-Methodik. *Mitt. Int. Ver. Theor. Angew. Limnol.* **9,** 1–38 (1958).
3. Rines, J. E. B. & Hargraves, P. E. *The Chaetoceros Ehrenberg (Bacillariophyceae) Flora of*

Narragansett Bay, Rhode Island, U.S.A. (J. Cramer, Berlin, Stuttgart, 1988).

4. Tomas, C. & Haste, G. *Identifying marine phytoplankton*. (Academic Press, San Diego, CA, 1997).

5. Scott, F. J. & Marchant, H. J. *Antarctic marine protists*. (ABRS, Canberra and AAD, Hobart, 2005).

Chapter 3 - Aurelia aurita ephyrae reshape a coastal microbial community

Luca Zoccarato[1*], Mauro Celussi[2], Alberto Pallavicini[1] and Serena Fonda Umani[1]

[1]Marine Ecology Laboratory, Department of Life Science, University of Trieste, Trieste, Italy.

[2]Oceanography Division, OGS (Istituto Nazionale di Oceanografia e di Geofisica Sperimentale), Trieste, Italy.

***Correspondence**: Luca Zoccarato, Marine Ecology Laboratory, Department of Life Science, University of Trieste, via Giorgieri, 10 - 34127 Trieste, Italy, luca.zoccarato.88@gmail.com

Keywords: *Aurelia aurita*, ephyrae, microplankton, protists, prokaryotes, NGS, community reshaping

Frontiers in Microbiology (2016) – in review

Abstract

During last decades, increasing attention has been paid to the impact of jellyfish blooms on marine communities. *Aurelia aurita* is one of the most studied Scyphozoans and several studies were carried out to describe its role as top-down controller within classical food web; by now, although, scarce data are available to define the effects of these medusae on microbial communities. The aims of this study were to describe the predation impact of *Aurelia aurita*'s ephyrae on a natural microplanktonic assemblage, and seeking for any reshaping effects on bacterial community composition and functioning. Surface costal water was used to set up a grazing experiment in microcosms which were incubated for 24 hours. Samples were taken to assess biomass of prey, heterotrophic carbon production (HCP), extracellular enzyme activity and grazing pressures. A next-generation sequencing technique was choose to investigate biodiversity shifts among bacterial and protist communities though SSU rRNA tag approach.

Our results showed that *Aurelia aurita* ephyrae were responsible for remarkable decreases in the abundances of more motile groups of microplankton such as tintinnids, dinoflagellates and aloricate ciliates while Bacillariophyceae and Mediophyceae experienced smaller reductions; no evidence of selective predation emerged analyzing communities' diversity down to family level compositions. Among prokaryotes, the heterotrophic fraction significantly increased in biomass (up to +45%) with increment also of HCP and leucine aminopeptidase activity (+40%); significant modifications were detected in community compositions since some classes of Gammaproteobacteria and Flavobacteriia displayed higher relative abundances while a net decrease was found for Alphaproteobacteria. Overall, this study provides a new insight about the effect of jellyfish on the microbial community underling their selective predation towards more motile groups of microplankton and their impact on prokaryotes community favoring blooms of copiotrophic taxa.

1. INTRODUCTION

During the last decades jellyfish abundance and jellyfish blooms have been showing increasing trends (Brotz et al., 2012) likely related to human activities such as overfishing, eutrophication and the increasing availability of new substrate (marine constructions) suitable for benthic stage setting (Richardson et al., 2009). Furthermore several data have highlighted as the global warming is positively correlated with jellyfish abundance (Decker et al., 2007; Kogovšek et al., 2010; Lynam et al., 2011; Purcell, 2012). Some of the consequences arisen from jellyfish increases are well known although not all the ecological impacts have been unveiled. This study is focused on the scyphomedusa *Aurelia aurita* for which the increasing trend of blooms (Kogovšek et al., 2010) and the overall increment in abundance (Mills, 2001) are well documented. Thanks to its ability to adapt over a wide range of salinity and temperature values, *A. aurita* is quite common in the Adriatic Sea (Bonnet et al., 2012) where it forms dense aggregations especially during spring and summer (Avian and Rottini, 1994; Di Camillo et al., 2010).

A. aurita has been largely studied as top-down controller within the classical food web assessing its ingestion or clearance rates on rotifers, *Artemia salina*, mollusk larvae, fish larvae, copepods and copepod nauplii (Båmstedt, 1990; Elliott and Leggett, 1997; Hansson et al., 2005; Titelman and Hansson, 2006; Møller and Riisgård, 2007; Riisgård and Madsen, 2011). The predation kinetics for these prey are known: *Aurelia* is capable to consume up to 28,230-54,000 prey ind^{-1} d^{-1} (Omori et al., 1995) with ingestion rates that increase according to jellyfish's size and to the seawater temperature (Båmstedt, 1990; Møller and Riisgård, 2007). Moreover the size of the jellyfish and of the prey have deep implications on the capturing efficiency (Riisgård and Madsen, 2011) but in literature few studies tackled these issues thus far. One of the first studies reporting the presence of dinoflagellates and ciliates in its gut content was performed by Båmstedt (1990). Despite the low concentrations detected for those prey (that were no significant in medusa diet) the author, in

agreement with results of Stoecker et al., (1987), proposed how different species might have a different vulnerability to jellyfish grazing. However few studies addressed the feeding activity on microplanktonic organisms, and they were either focused on few taxa (Uye and Shimauchi, 2005; Zheng et al., 2015) or considering microzooplankton group as a whole (Malej et al., 2007).

Jellyfish are also known to be an important source of dissolved organic matter (DOM) that could support carbon demand of marine Bacteria (Blanchet et al., 2014). The DOM originated from medusae can integrate or compensate the DOM produced by phytoplankton (by primary production and exudation) especially in oligotrophic environments or during jellyfish outbreaks. This process is still scarcely investigated and few data are available. Turk et al. (2008) pointed out that a fraction of the released DOM is labile since they detected significant shifts in term of bacterial biomass and production during field experiments. The excretions of jellyfish contain inorganic nutrient (principally ammonium and phosphate) and DOM rich in primary ammines and amino acids, suggesting a tight coupling with bacteria activities and hence an influence of carbon, nitrogen and phosphorus cycling (Pitt et al., 2009). Recently, Tinta et al. (2012) and Blanchet et al. (2014) demonstrated the bioavailability of jellyfish-derived matter (homogenate of the bodies) that due to its protein-rich composition, triggers fast modifications of bacteria communities favoring taxa specialized in the degradation of organic compounds.

The aim of our work was thus to test if small medusae as the ephyrae of *Aurelia aurita* can predate and determine an impact on major groups of microplankton within a natural assemblage. A special effort was addressed to the description of communities' composition at a fine taxonomic resolution in order to highlight possible selective ingestion. We also aimed to describe the influence of ephyrae on bacterial community composition and its functioning.

2. Material and methods

2.1 Ephyrae collection and sea water sampling

During last week of September 2014, *Crassostrea gigas* oysters bearing *Aurelia* polyps were collected by SCUBA diving from dock pillars in the Port of Koper (Slovenia). They were stored in containers filled with seawater collected at the sampling site and transported to Marine Biology Station laboratory (Piran, Slovenia). Polyps were kept in 0.45 µm sieved sea-water, in the dark within a thermostatic chamber and fed twice per week with freshly hatched *Artemia* nauplii ad libitum; sea-water was replaced 3 hours after feeding. The acclimation temperature was 19°C while strobilation was induced by lowering temperature to 14°C. Ephyrae were fed with freshly collected zooplankton (50 µm net) until 36 hours before the setup of the experiment to limit contaminations with eukaryotic DNA from the medium. Once ephyrae reached the desired average size of 5 mm of diameter (27th of October 2014) they were immediately transferred at the Laboratory of Marine Ecology (University of Trieste, Italy). Sea water to set up the experiments was simultaneously collected at the surface in the bay of Aurisina (Trieste, Italy) few meters far from the coastline and it was immediately filtered on a 200 µm mesh to remove any organisms larger than microplankton.

2.2 Ephyrae – grazing experiment

Screened sea water was immediately transferred to the laboratory and it was used to prepare 6 microcosms in 2.2 L transparent Nalgene® bottles: 3 bottles were the controls and 3 bottles were the treatment: in each of them 5 ephyrae were added. Microcosms were then placed into an aquarium with flowing water and incubated for 24 hours replicating *in-situ* PAR irradiance (26 µmol m^{-2} s^{-1}) and temperature (16.8-17.5 °C); irradiance follow also the natural circadian cycle. To avoid sedimentation, in addition to the flow within the aquarium, bottles were gently turned upside-down each hour. Ephyrae impact on natural microbial communities were assessed considering several classes of microbes: pigmented and heterotrophic nanoplankton, autotrophic and heterotrophic

prokaryotes. Samples for assessing the abundance and biomass of each class, the leucine aminopeptidase exoenzymatic activity, the heterotrophic carbon production and the diversity of microplankton and of prokaryotes through Next-Generation Sequencing technique were taken at the beginning (T0) and at the end of the incubation (T24). Samples at the beginning of the experiment were taken directly from the screened sampled sea water in 3 replicates while samples at the end of the incubation were taken from each microcosm. During the incubation other samples were taken for estimating nanoplankton and prokaryotic abundance, leucine aminopeptidase activity and heterotrophic carbon production. According to the protocol of Frost (1972), abundance and biomass values at the beginning and at the end of microcosm incubations were used to estimate growth and grazing coefficients, the average growth and the grazing coefficient from each ephyrae-treated microcosm were used to calculate the ingestion rates. The abundances and biomasses of microplankton were estimated at the finest taxonomic level reachable from the operator at the optical microscopy (such as family, genus or species). When a taxon was missing at T24 within an ephyrae-treated microcosm the arbitrary value of 1 was given in order to allow formula calculation. Only ingestion rates higher than 2 times their own standard deviation were considered.

2.3 Microscopic analysis –abundance and biomass

Micro-plankton. For each sample an aliquot of 0.5 L of sea water was fixed with buffered formaldehyde solution (2% final concentration) and stored in a dark bottle at 4°C. The whole volume was processed following Utermöhl (1958). Using an inverted optical microscope (Olympus IX51) the organisms were taxonomically assigned, enumerated and measured with an eye piece. Geometrical formulas summarized in Olenina et al. (2006) were used to estimate biovolumes of dinoflagellates, Coccolithophyceae, Coscinodiscophyceae, Fragilariophyceae, Dictyochophyceae, Mediophyceae and Bacillariophyceae; for aloricate ciliates, tintinnids and metazoans the biovolumes were

calculated from equivalent geometrical shapes (Edler 1979). Equations from Menden-Deuer and Lessard (2000) were then used to obtain organic carbon quotas.

Nanoplankton and Prokaryotes. Samples of 20 mL and 3 mL were taken to assess the abundance of nanoplankton and prokariotic fractions, respectively. Samples were fixed with buffered formaldehyde solution (prefiltered through 0.2 µm Acrodisc syringe filter), stored in sterile dark bottles at 4°C and processed following Porter and Feig protocol (1980); each sample of prokaryotes was processed in 3 replicates. Aliquots of each sample were stained with a DAPI (4', 6-diamidino-2-phenylindole) solution, 1 µg mL^{-1} final concentration and placed in the dark for 15 minutes. After staining, prokaryotes were collected on 0.22 µm black polycarbonate filters (Nucleopore, 25 mm) while nanoplankton on 0.8 µm black polycarbonate filters (Nucleopore, 25 mm). The filters were immediately placed on slides between two drops of immersion non fluorescent oil (Olympus) and kept at -20°C in the dark. The counts were made using an epifluorescence microscope (Olympus BX 60 F5) at x1000 final magnification with UV filter set (BP 330–385nm, BA 420nm) for DAPI; green (BP 480–550 nm, BA 590 nm) and a blue (BP 420–480 nm, BA 515 nm) light sets for natural pigment fluorescence. More than 300 cells were counted for prokaryotes and nanoplankton in each sample; non pigmented cells were considered as heterotrophic. For biomass estimation of nanoplankton it was divided into three dimensional classes: 2-3 µm, 3-5 µm and 5-10 µm as reported by Christaki et al. (2001). Cell abundances were converted in biomass by applying the following conversion factors: 20 fg C $cell^{-1}$ for heterotrophic prokaryotes (Ducklow and Carlson, 1992), 200 fg C $cell^{-1}$ for *Synechococcus* (Caron et al., 1991). The nanoplanktonic organisms were approximated to spheres (diameter equal to the medium value of the each dimensional class) in order to multiply their volumes for the conversion factor of 183 fg C μm^{-3} (Caron et al., 1995).

2.4 Heterotrophic Carbon Production (HCP)

HCP was estimated by incorporation of ^{3}H-leucine (Leu) (Kirchman et al. 1985). At each sampling event duplicate 1.7-mL aliquots and one killed controls (90 µL 100% trichloroacetic acid – TCA) were collected from each microcosm, amended with 20 nM radiotracer (s.a. 52.9 Ci mmol^{-1}) and incubated at 16.8-17.5 °C in the dark. Incubations were stopped with TCA (5% f. c.) after 1 h. The extraction with 5% TCA and 80% ethanol was carried out using the microcentrifugation method (Smith and Azam 1992). Activity in the samples was determined using a β-counter (Tri-Carb 2900 TR Liquid Scintillation Analyzer) after the addition of 1 mL scintillation cocktail (Ultima Gold MV; Packard). Incorporation of ^{3}H-leucine was converted into carbon produced via prokaryotic protein production according to Simon and Azam (1989), assuming a two-fold isotope dilution for leucine.

2.5 Leucine aminopeptidase activity

Leucine aminopeptidase activity was assayed using the fluorogenic substrate analogue (Hoppe, 1993) leucine-7-amino-4-methyl-coumarin (Sigma-Aldrich). The enzyme activity was expressed in terms of the rate of 7-amino-4-methyl-coumarin (AMC) production over time. Hydrolysis was measured by incubating triplicate 2 mL sub-samples collected at each time point from every bottle with 200 µM substrate (saturating concentration; Celussi and Del Negro, 2012) for 1 h in the dark at experimental temperature. Fluorescence increase due to AMC hydrolyzed from the model substrate was measured by a Shimadzu RF-1501 spectrofluorometer (380-nm excitation and 440-nm emission). Triplicate standard AMC solutions (Sigma-Aldrich) were used to produce calibration curves. Duplicate blanks without fluorogenic substrate were used for determining the natural fluorescence increase in the samples not attributable to the tested enzyme. In order to test degradation processes performed by the prokaryotic consortium associated to the animals, at T24 3 ephyrae were collected alive and placed in 3 vials with 1 mL of seawater from the same bottle. Vials were added with 9 mL of 0.2 µm-filtered seawater yielding to a 1:10 dilution. These aliquots

were treated as described above to estimate leucine aminopeptidase activity with a 200 µM final substrate concentration. Degradation processes ascribable to animal-associated prokaryotes were then computed by correcting results for dilution (10X) and subtracting hydrolysis rates measured in animal-free seawater.

2.6 Next-Generation Sequencing: samples collection and processing

Molecular diversity description were based on metabarcoding analysis performed with a PGM Ion Torrent platform. For microplankton community the hyper variable 9 region of the rRNA 18S gene was targeted with primers pair 1391F and EukB (Stoeck et al., 2010). Samples were collected filtering 1 L per each sample on 2 µm PCTE membrane (Sterlitech) and the membranes were immediately frozen at -80°C. Extraction of the DNA was performed using PowerSoil DNA Isolation Kit (MOBIO) customized with two improvement in the protocol: the membrane was completely dissolved in chloroform during DNA extraction step to increase DNA recovery avoiding issues related with folding and scrubbing of the filter; the chloroform was successively removed increasing to 5' the time of the first centrifugation step and recovering the upper water phase. To limit over-cycling amplification of targeted region was led in real time and each samples amplification was stopped when plateau was reached. The primary qPCR was performed in 10 µL reaction with 0.5U of KAPA 2G HiFi Taq, 1X KAPA 2G Buffer HiFi, 0.3 µM dNTPs, 1X EvaGreen (Biotium), 0.3 µM of each primer, 2 µL of DNA template and RNasi free water up to the final volume. Thermocycling conditions were set to: 1' at 95°C, 28-31 cycles of 15" at 95°C, 10" at 60°C, 4" at 72°C, and 3' of final elongation at 72°C. Negative controls with RNase free water instead of DNA template were amplified to ensure absence of contaminations. Sequencing adapters were attached to amplicons with a secondary PCR performed in 25 µL with same reagents, concentrations and cycling conditions of the primary PCR (9 cycles). No significant amplifications rise in the negative controls.

For prokaryotic community, the hyper variable 4 region of the rRNA 16S gene was targeted. Samples were collected filtering 0.5 L per each sample on 0.2 µm cellulose acetate membrane (Sterlitech) in order to collect the organisms and the membranes were then immediately frozen at -80°C. Extraction of the DNA was performed with PowerSoil DNA Isolation Kit (MOBIO) and following the original protocols. PCR amplification strategy was the same used for microplankton. Primers for the primary qPCR were 515F (S-*-Univ-0515-a-S-19) and a combination of 806R (S-D-Bact-0787-b-A-20) with 802R (S-D-Bact-0785-b-A-18) (Claesson et al., 2010; Walters et al., 2011). The PCR reaction was performed in 10 µL with 1X HotMasterMix (5 PRIME), 1X EvaGreen (Biotium), 0.3 µM of forward primer and 0.15 + 0.15 µM of reverse primers, 2 µL of DNA template and RNasi free water up to the final volume. Thermocycler conditions were set to: 2' at 94°C, 26-34 cycles of 20" at 94°C, 20" at 55°C, 40" at 65°C, and 2' of final elongation at 65°C. The secondary qPCR was performed in 25 µL with same reagents, concentrations and cycling conditions of the primary PCR (9 cycles); dilution of DNA template and primers pair for secondary PCR were the same as for microplankton secondary PCR.

Amplified samples were normalized using SequalPrep Normalization kit (Thermo Fisher), pooled together, processed with Ion PGM Hi-Q OT2 kit and Ion PGM Hi-Q Sequencing kit (Life Technologies). The sequencing was carried out with an Ion Torrent PGM running Ion 314 chip v2 for microplankton samples and Ion 316 chip v2 for prokaryotes samples.

2.7 Bioinformatics' analysis

Reads' dataset was exported raw from Torrent Server in fastq format. Demultiplex and forward primer removal was done with fastq_strip_barcode_relabel2.py script (USEARCH package, available at http://drive5.com/usearch drive5.com) while reverse primers and reverse adaptors were trimmed with cutadapt 1.8.3 (Martin, 2011). Average quality scores of reads were checked with FastQC; length and quality filtration were carried out with USEARCH v8 (Edgar and Flyvbjerg, 2015)

setting the minimum length threshold at 70 b and 150b for microplankton and prokaryotes sequences respectively, and the quality threshold to a maximum allowed expected errors of 1 nucleotide each 100 bases. All sequences were deposited in GenBank (NCBI), the BiomProject accession numbers for 18S dataset is PRJNA305513 while for 16S dataset is PRJNA305512. Chimeras were removed performing UCHIME algorithm (Edgar et al., 2011): d*e-novo* chimera detection was chosen for microplankton dataset while prokaryote dataset was screened using GreenGenes v13.8 representative dataset clustered at 97% of similarity. OTUs picks for both cleaned sequence datasets were carried out in QIIME through open reference workflow strategy; singletons were removed and taxonomic assignation of the OTUs were performed with BLAST (Altschull et al., 1990) setting e-value > 10^{-20}; PR2 reference dataset was used as reference for sequences of microplankton while GreenGenes v13.8 reference dataset (clustered at 97% of similarity) was chosen for prokaryotes' dataset.

2.8 Statistical analysis

The ingestion rates (cells ind^{-1} d^{-1}) estimated for each ephyrae-treatments were standardized in relative ingestion rates (%) dividing the ingestion on each taxon by the sum of ingestion on all taxa. For all analytical replicates of T0 the relative initial abundance (%) of each taxa was obtained dividing by the total abundance of microplankton (cells L^{-1}). The correlation of relative ingestion rates with the relative initial abundances and with biovolumes were tested with Pearson (P) and Spearman (S) indexes.

Microplankton OTUs table was manually cleaned from multicellular organisms such as Archaeplastida, Metazoa, Amoebozoa and Fungi since the sampling method were not representative for these groups; therefore furthermore we have consider only protists. A multiple rarefaction step was applied to both protists and prokaryotes tables in order to minimize differences due to sequencing depth. Similarity matrices were calculated and constructed by the Bray-Curtis

similarity coefficient; hierarchical Cluster analyses (clustering on group average) were obtained in Primer 6® (PRIMER-E Ltd., Plymouth, UK).

In order to compare taxa composition among samples, relative abundance (RA) was calculated from OTUs abundance of both protists and prokaryotes; only OTUs present in all three replicates of T0, T24 controls or T24 ephyrae-treatments were kept and OTUs with <1% of RA were lumped in the category 'Others'. RA community profiles were plotted using Microsoft Excel®.

3. Results

The natural assemblage of microbes within this experiment was dominated by prokaryotes that constituted more than 80% of total biomass with 12.19 ± 1.13 µg C L^{-1} represented by heterotrophic bacteria (HB) and 5.37 ± 0.02 µg C L^{-1} by *Synechococcus*; nanoplankton (both heterotrophic and phototrophic fraction) biomass was 0.65 µg C L^{-1} and microplankton biomass 3.60 ± 0.58 µg C L^{-1}. After the 24h-incubation two different scenarios occurred. In the presence of ephyrae the HB biomass significantly increase up to 17.60 ± 0.70 µgC L^{-1} ($t = 6.26$, p-value < 0.01) for microplankton a remarkable decrease to 1.49 ± 0.26 µg C L^{-1} ($t = 5.78$, p-value < 0.01) was observed. In the controls *Synecococcus* increased reaching 7.59 ± 0.61 µg C L^{-1} while all other groups' biomass remained almost constant. Figure 1 shows the overall abundance of the major groups detected within microplankton community at T0 and after the incubation in all 6 microcosms. The natural assemblage was principally composed for 40% of Bacillariophyceae, 17% of Mediophyceae, 14% of dinoflagellates, 12 % of tintinnids and 7% of aloricate ciliates; within category 'Others' were grouped Dictyochophyceae, Metazoa, Coccolithophyceae, Coscinodiscophyceae, Fragilariophyceae whose abundances were lower than 4%. No significant variations were detected for total abundances among T0 and T24 controls, also in groups' composition. The comparison between T0 and T24 ephyrae-treatments revealed how there was remarkable decreases especially for tintinnids (-76%),

dinoflagellates (-65%) and aloricate ciliates (-61%) while Bacillariophyceae and Mediophyceae experienced a smaller decrease (-38% and -10% respectively).

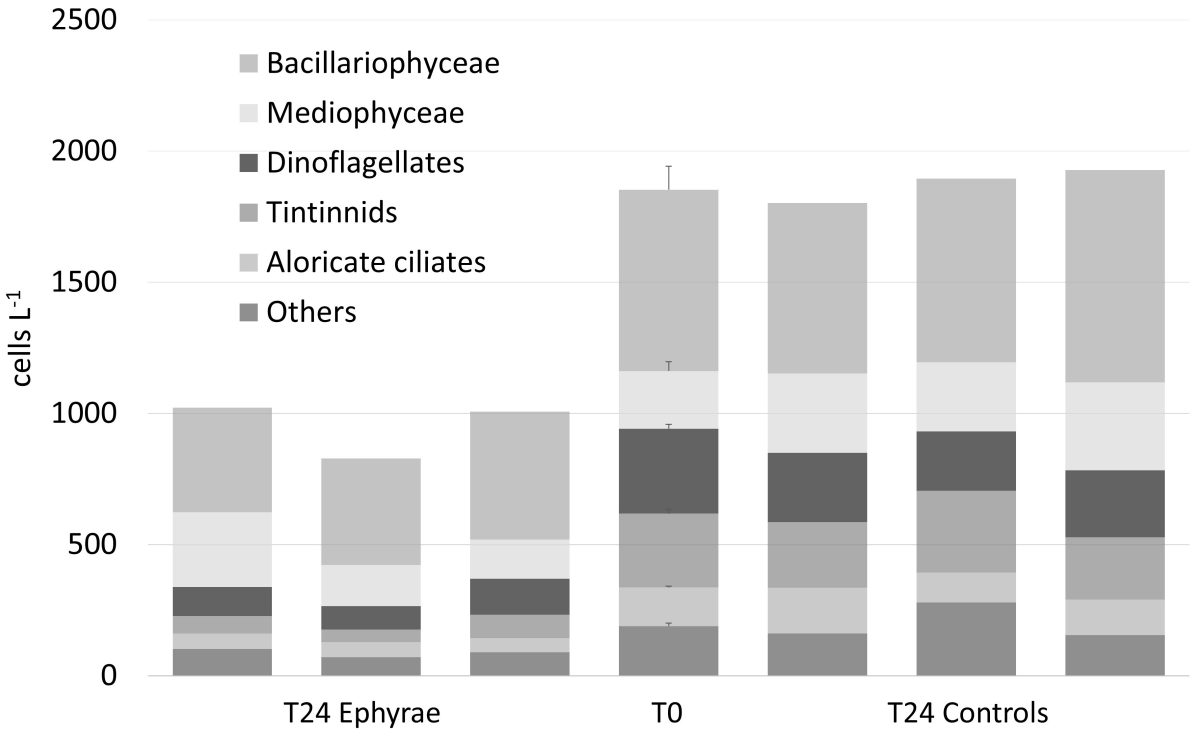

- **Figure 1**: Abundances overview of major microplanktonic groups at T0 and after the incubations in each microcosm. Dictyochophyceae, Metazoa, Coccolithophyceae, Coscinodiscophyceae and Fragilariophyceae were grouped as "Others".

Within aloricate ciliates and tintinnids groups, organisms belonging to Ciliophora, Strombidiidae and *Tintinnopsis* sp. taxa displayed a broad variability in size during microscopy counts and they were thus split in different size ranges (see Table 1; the numbers from 1 to 3 indicate an increase in size and the letters stand for the geometric shapes used to compute biovolumes: A = sphere, C = cone, E = cylinder). The mean ingestion rates exerted by a single ephyra during the grazing experiment (Table 1) shown as on overall the most impacted groups were Bacillariophyceae and tintinnids; they included several taxa that were strongly preyed such as Bacillariophyceae undetermined with an ingestion rate of 34.5 ± 11.3 cells ind^{-1} d^{-1} (corresponding to 0.15 ± 0.05 *x*10 µg C ind^{-1} d^{-1}),

- **Table 1:** Overview of biovolumes, initial (T0) cell abundances/biomasses (+ st.dev. computed on analytical replicates), and ingestion rates (+ st.dev. computed on experimental replicates) calculated on abundances/carbon contents for all preyed taxa.

	Bio-volumes	T0 cells L^{-1}	Ingestion cells ind^{-1} d^{-1}	T0 $x10$ µg C L^{-1}	Ingestion $x10$ µg C ind^{-1} d^{-1}
Dinoflagellates					
Ceratium furca	73236	31.5 ± 7.8	9.9 ± 1.0	2.52 ± 0.62	0.79 ± 0.08
Ceratium kofoidii	12747	151 ± 14.1	20.2 ± 5.7	2.34 ± 0.22	0.31 ± 0.09
Dinophysis fortii	80953	5 ± 1.4	1.0 ± 0.0	0.44 ± 0.12	0.06 ± 0.05
Gonyaulax sp	134628	17.5 ± 4.9	4.2 ± 0.8	2.48 ± 0.70	0.59 ± 0.11
Oxytoxum caudatum	8177	3.5 ± 0.7	0.9 ± 0.3	0.04 ± 0.01	0.01 ± 0.01
Prorocentrum micans	43960	19 ± 9.9	4.7 ± 1.7	0.94 ± 0.49	0.23 ± 0.08
Dinophyceae undet.	58875	4 ± 2.8	2.5 ± 0.4	0.26 ± 0.18	0.16 ± 0.03
Aloricate ciliates					
Ciliophora A1	14137	34.5 ± 13.4	5.0 ± 0.5	0.59 ± 0.23	0.09 ± 0.01
Ciliophora A2	65450	10.5 ± 2.1	2.5 ± 0.9	0.75 ± 0.15	0.18 ± 0.06
Strombidiidae C1	3142	20 ± 4.2	8.2 ± 0.7	0.08 ± 0.02	0.03 ± 0.00
Strombidiidae C2	14544	31 ± 9.9	12.1 ± 0.8	0.54 ± 0.17	0.21 ± 0.01
Tintinnids					
Favella sp	13901	60.5 ± 10.6	13.8 ± 3.0	1.02 ± 0.18	0.23 ± 0.05
Stenosemella nivalis	14137	101.5 ± 21.9	38.2 ± 2.4	1.73 ± 0.37	0.65 ± 0.04
Tinitinnopsis sp E1	4712	49.5 ± 9.2	14.6 ± 2.5	0.30 ± 0.06	0.09 ± 0.02
Tinitinnopsis sp E2	21817	19.5 ± 12.0	7.9 ± 1.2	0.50 ± 0.31	0.20 ± 0.03
Tinitinnopsis sp E3	59865	3.5 ± 2.1	1.9 ± 0.1	0.23 ± 0.14	0.13 ± 0.01
Metazoa					
Copepod nauplii	176625	10 ± 0.0	2.2 ± 0.5	1.83 ± 0.00	0.27 ± 0.24
Coccolithophyceae					
Calciosolenia murray	4091	50.5 ± 38.9	5.7 ± 0.4	0.12 ± 0.10	0.01 ± 0.00
Cocconeis sp	2322	38.5 ± 14.8	6.6 ± 2.1	0.06 ± 0.02	0.01 ± 0.00
Bacillariophyceae					
Diploneis sp	7800	29 ± 24.0	7.7 ± 0.4	0.12 ± 0.10	0.03 ± 0.00
Navicula sp	4377	85 ± 7.1	15.0 ± 0.5	0.22 ± 0.02	0.04 ± 0.00
Bacillariophyceae undet.	8450	248 ± 31.1	34.5 ± 11.3	1.09 ± 0.14	0.15 ± 0.05
Pseudonitzschia sp	2500	142 ± 39.6	36.4 ± 3.8	0.23 ± 0.06	0.06 ± 0.01
Pleurosigma sp	10838	126 ± 31.1	23.2 ± 7.9	0.68 ± 0.17	0.12 ± 0.04
Mediophyceae					
Chaetocheros sp	4352	11.5 ± 2.1	4.4 ± 1.6	0.03 ± 0.01	0.01 ± 0.00
Leptocylindrus sp	7850	167 ± 72.1	42.8 ± 0.5	0.69 ± 0.30	0.18 ± 0.00
Fragilariophyceae					
Fragilaria sp	1313	59 ± 38.2	28.1 ± 0.0	0.06 ± 0.04	0.03 ± 0.00
Coscinodiscophyceae					
Guinardia stiata	49063	11.5 ± 14.8	3.9 ± 0.3	0.21 ± 0.27	0.07 ± 0.01

Pseudonitzschia sp with an ingestion rate of 36.4 ± 3.8 cells ind^{-1} d^{-1} (0.06 ± 0.01 *x*10 µg C ind^{-1} d^{-1}), or *Stenosemella nivalis* with an ingestion rate of 38.2 ± 2.4 cells ind^{-1} d^{-1} (0.65 ± 0.04 *x*10 µg C ind^{-1} d^{-1}). High ingestion rates were found for some taxa of other groups like *Ceratium kofoidii* among dinoflagellates with 20.2 ± 5.7 cells ind^{-1} d^{-1} (0.31 ± 0.09 *x*10 µg C ind^{-1} d^{-1}), Strombidiidae C2 (sub-group of Strombidiidae characterized by larger size) among aloricate ciliates with 12.1 ± 0.8 cells ind^{-1} d^{-1} (0.21 ± 0.01 *x*10 µg C ind^{-1} d^{-1}), *Leptocylindrus* sp among the Mediophyceae with 42.8 ± 0.5 cells ind^{-1} d^{-1} (0.18 ± 0.00 *x*10 µg C ind^{-1} d^{-1}) and *Guinardia stiata* the only Coscinodiscophyceae for which an ingestion rate was detected and was of 28.1 ± 0.0 cells ind^{-1} d^{-1} (0.03 ± 0.00 *x*10 µg C ind^{-1} d^{-1}).

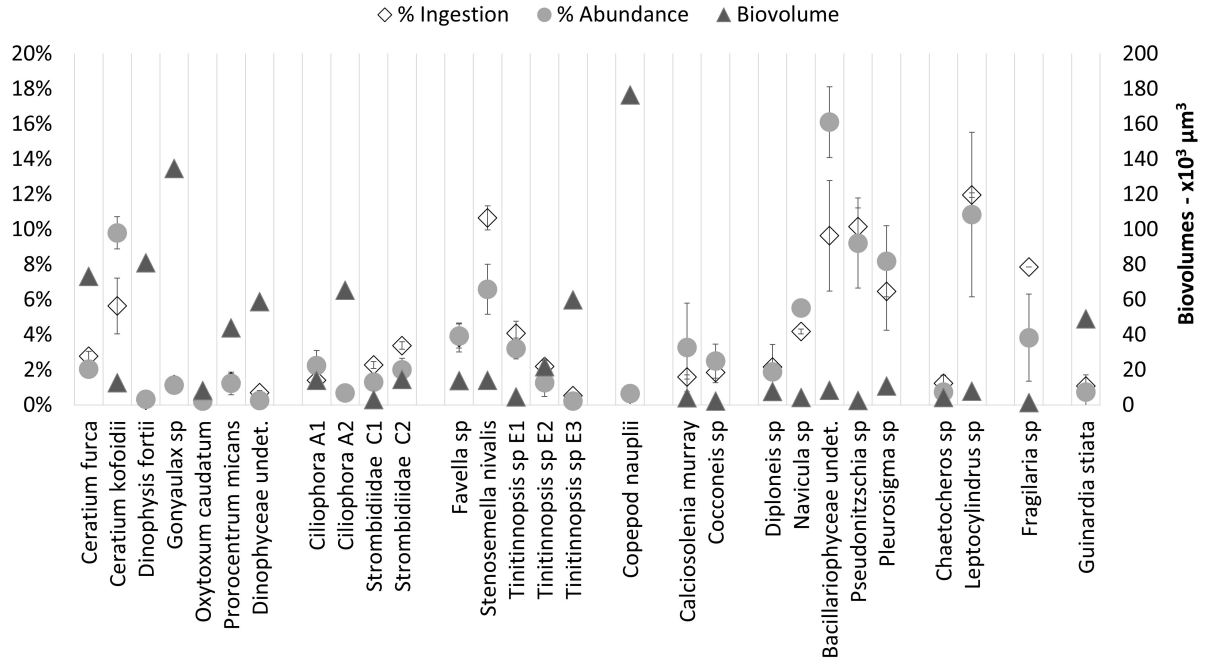

- **Figure 2:** Overview of relative ingestion rates, relative initial abundances and biovolumes among microplanktonic taxa.

The relative ingestion rates paralleled the relative initial abundances of preyed taxa (Fig. 2) with significant linear correlation (P = 0.87, *p*-value <<0.001) and rank-order correlation (S = 0.92, *p*-value = <<0.001). Conversely we did not observed any significant correspondence between ingestion and

biovolumes. *Cetarium kofoidii*, undetermined Bacillariophyceae, *Pseudonitzschia* sp, *Pleurosigma* sp and *Leptocylindrus* sp were the most abundant taxa and on them we registered the highest ingestions, although their biovolumes were among the smallest, being less than $15x10^3$ µm^3. Taxa such as *Ceratium furca*, *Dinophysis fortii*, *Gonyaulax* sp, *Ciliophora* A2, *Tinitinnopsis* sp E3 and Copepod nauplii that were characterized by higher biovolumes (values ranging from $60x10^3$ µm^3 and $177x10^3$ µm^3) were among the less ingested.

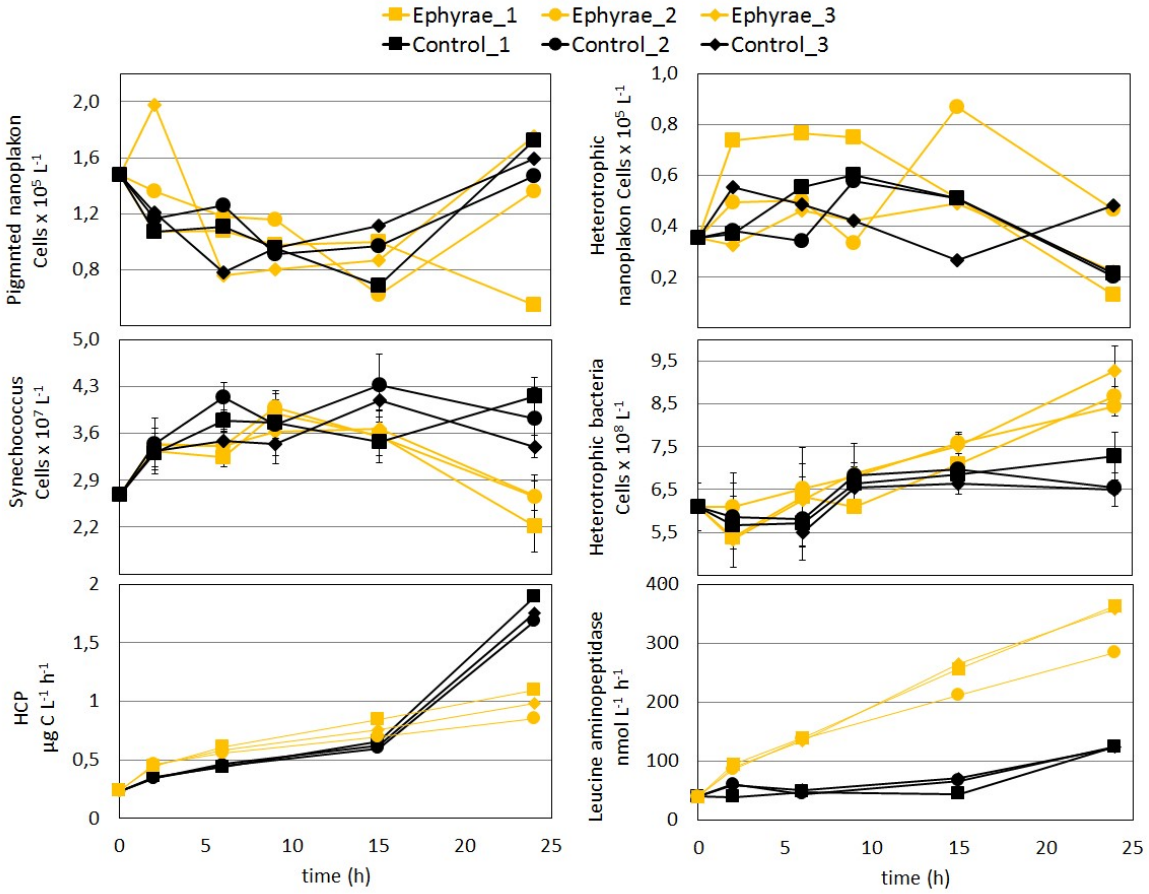

- **Figure 3:** Trends for pigmented nanoflagellates, heterotrophic nanoflagellates, Synechococcus, heterotrophic bacteria, heterotrophic carbon production (HCP), and leucine aminopeptidase over sampled time points.

Heterotrophic and pigmented nanoplankton abundance remained almost constant over the incubation both in controls and in microcosms with ephyrae (Fig. 3). About prokaryotes

Synechococcus displayed and increasing trend both in T24 control and T24 ephyrae microcosms during the first 9 hours of incubation; abundances in the T24 ephyrae decreased reaching the initial values while in T24 controls the number of cells increased to 2.22 ± 0.76 cells $x10^7$ L^{-1}. The abundance of heterotrophic bacteria similarly increased within the first 9 hours in both series of microcosms but at the end of the incubation in T24 controls the number of cells was slightly higher than at T0 while in T24 ephyrae the average abundance increased to 5.42 ± 0.85 cells $x10^7$ L^{-1}. Heterotrophic C production increased over time in all bottles, with the lowest values being measured at T0 (0.23 ± 0.01 µgC L^{-1} h^{-1}). The first 15 hours were characterized by a moderate uptake increase, slightly higher in the presence of ephyrae (average ± SD of values in all replicates = 0.77 ± 0.08 µgC L^{-1} h^{-1}) than in controls (average ± SD of values in all replicates = 0.62 ± 0.01 µgC L^{-1} h^{-1}). After 1 day, the highest values were measured in controls (1.78 ± 0.11 µgC L^{-1} h^{-1}), whereas ephyrae kept PCP around 0.98 (± 0.12) µgC L^{-1} h^{-1}. Leucine aminopeptidase activity increased linearly over time in ephyrae-treated bottles, starting from 39.01 ± 0.76 nM h^{-1} at T0 and reaching 334.56 ± 44.42 nM h^{-1} (average ± SD of values in all replicates) after 24h. On the contrary, polypeptide degradation in controls remained rather constant during the first 15 h (on average 49.61 ± 11.33 nM h^{-1}) and displayed a slight increase at T24 (132.52 ± 0.32 nM h^{-1}). At T24, leucine aminopeptidase activity performed by the prokaryotic consortium associated to ephyrae was 1083.47 ± 60.90 nM h^{-1} for each single animal.

The effect of ephyrae predation on protist communities were investigated analyzing the sequences obtained through parallel mass sequencing technique. This community in comparison with microplankton community described at the microscope, was lacking of Metazoa group that though represented only 1% in abundance. In natural assemblages (T0) the phylum of Alveolata clearly emerged as the most abundant with relative abundance (RA) ranging from 80.2% to 85.8%; it was mainly composed by the divisions Dinophyta (> 80%) and Ciliophora (>7%). The other detected phyla

were Stramenopiles (ranging from 3.0% to 23.7% in RA), Hacrobia (between 4.9% and 8.0% in RA), Rhizaria (between 2.0% and 4.2% in RA) and a low presence of Excavate (RA ≈ 0.1%). Within the phylum Alveolata we detected also sequences belonging to division Apicomplexa as well as Choanoflagellates were detected within the Opisthokonta phylum; these taxa plus other unclassified sequences were lumped in the category "other Alveolata" because of their low RA. Sequences that did not have a hit during BLAST and that remained unclassified were always less than 3.4% on the total sequences among all samples. Anyhow the Next-Generation Sequencing-based protist diversity was outstanding compared with the microscope-based one. For the most represented phylum we found 29 families of the Stramenopiles, 15 families of Ciliophoran and 21 families of Dinophyta; while the taxa of Excavate and Rizharia that harbored 2 and 16 families respectively, were completely missing from microscopy analysis. The cluster analysis on community profiles of all samples (Fig. 4) showed that replicates 2 and 3 of T0 and all replicates of T24 controls grouped together with a 73% similarity (this cluster will be so on referred as "EUK_1"); the replicates of T24 ephyrae-treatments grouped themselves at 80% similarity (the cluster will be so on referred to as "EUK_2"). T0 replicate 1 displayed a peculiar assemblage, mostly unrelated to the other replicates. Comparing the two clusters, the average RA of Dinophyta in EUK _1 was 67.6 ± 1.7%, higher than the RA of 57.3 ± 2.0% found in EUK_2. Also the average RA of Ciliophora was higher in for EUK_1 (7.3 ± 1.2%) than in EUK_2 (2.63 ± 0.2%). On the contrary, Stramenopiles RA in EUK_1 (9.3 ± 3.1%) was quite lower than RA in EUK_2 (22.5 ± 1.5%). The other taxa such as Hacrobia, Rhizaria and the category "other Alveolata" presented a variation among clusters comparable to the variation within each cluster. An insight analysis of taxa composition at family level was made for the phyla with the highest variation among EUK_1 and EUK_2 (Ciliophora, Dinophyta and Stramenopiles); the RA of taxa were recomputed for each phyla. Ciliophora presented the highest number of abundant taxa with 6 families having a RA > 5 % and 13 families having a RA > 1%; these

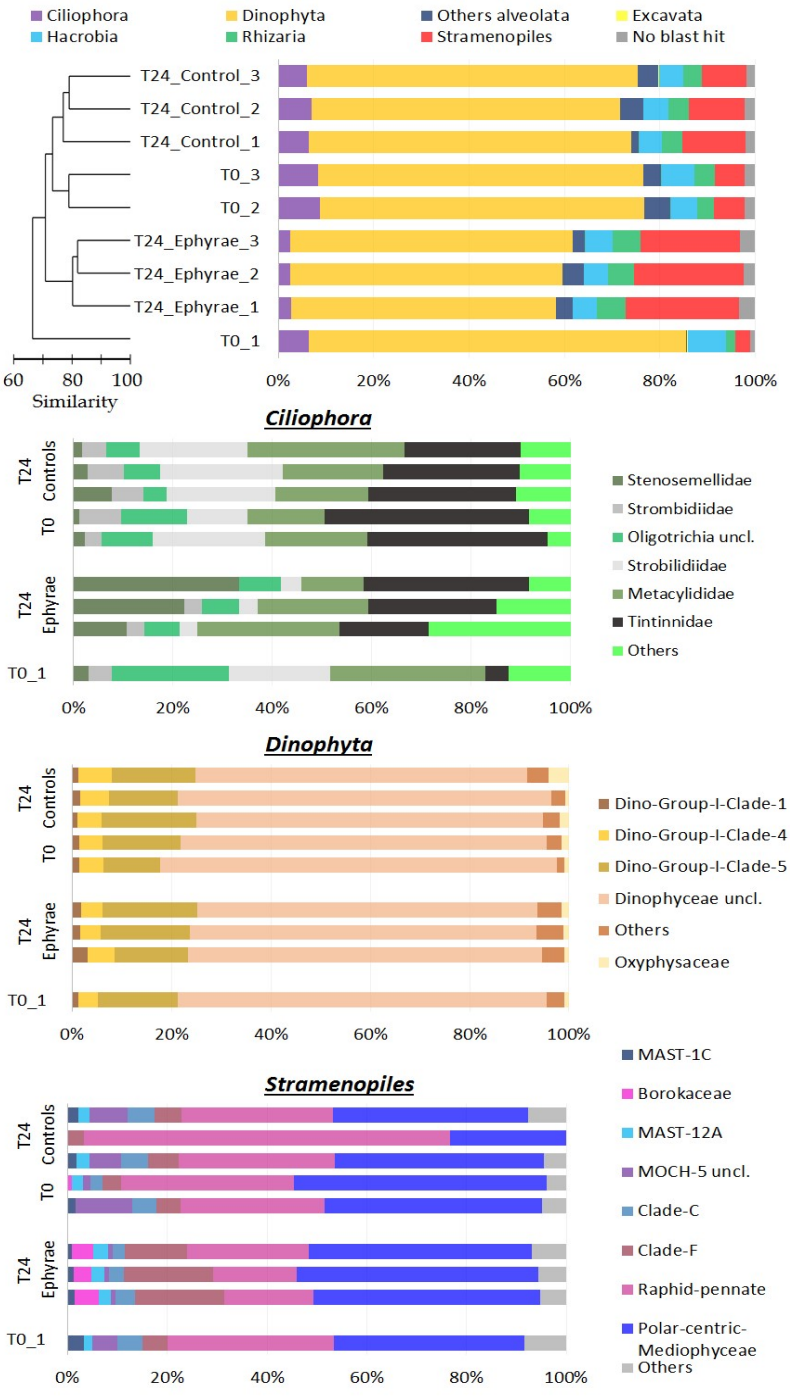

- **Figure 4:** Profiles of protists community obtained with NGS technique showing taxa with RA > 1%. The top chart represents the major phylum (major division for phylum Alveolata) among samples; profiles are ordered accordingly with cluster analysis reported along the Y axis. The three underlying bar plots show the family composition for Ciliophora, Dinophyta and Stramenopiles; taxa with RA < 1% were grouped as "Others" (RA < 5% for Ciliophora).

complexity combined to possible issue due to sampling depth - since RA of Ciliophora within protists community was very low - may led to the fuzzy variation in RA of these taxa. However comparing EUK_1 to EUK_2, Strombilidiidae shown a net decrease of RA, also Tintinnidae displayed a similar even if less clear trend while Stenosemellidae increased in RA. Dinophyta, despite the overall decrease of RA from EUK_1 to EUK_2, did not show any remarkable change in RA among its families; the Dinophyceae unclassified taxon was the most abundant among all profiles (RA of 47.2 ± 6.7% among all protists and of 72.1 ± 4.0% among Dinophyta taxa) so a further insight at genus level was tried in order to elucidate its composition. However from 58.3% to 73.4% of the reads remained still unclassified while among the more abundant genera found there were *Gyrodinium*, *Gonyaulax*, *Gymnodinium*, *Pentapharsodinium*, *Alexandrium* and *Prorocentrum* (RAs ranged from 2.5% to 5.9%). Stramenopiles presented variable RA values for some families in EUK_1 (especially the community profile of T24 control replicate 2); comparing EUK_1 with EUK_2 the Raphid-Pennate decreased in RA while clade-F (class Chrysophyceae-Synurophyceae) increased.

The profiles of prokaryotic communities shown as the most abundant taxa were: for Proteobacteria the classes Alphaproteobacteria (average RA of 43.5 ± 3.8%) and Gammaproteobacteria (average RA of 18.3 ± 1.4%), for Bacteroidetes the class Flavobacteriia (average RA 18.5 ± 1.6%), the phylum Verrucomicrobia (average RA 6.0 ± 1.1 %), the uncultured SAR406 (average RA 3.5 ± 1.9%) and Cyanobacteria (average RA 2.3 ± 0.6%); Planctomycetes, Actinobacteria and the uncultured SBR1093 were also detected with average RA of 1.0%, 0.6% and 0.3% respectively. Cyanobacteria included only the genus *Synechococcus*; sequences classified as chloroplast were lumped into category “others” that comprehend also the bulk of sequences unclassified during blast (their RA never overcame 0.1%). Cluster analysis on profiles of prokaryotic communities (Fig. 5) showed three main clusters at 75% similarity: T0, T24 controls (so on referred to as T24_C) and of T24 ephyra-treatments (so on referred as T24_E) that included their respective replicates. Comparing RA of the

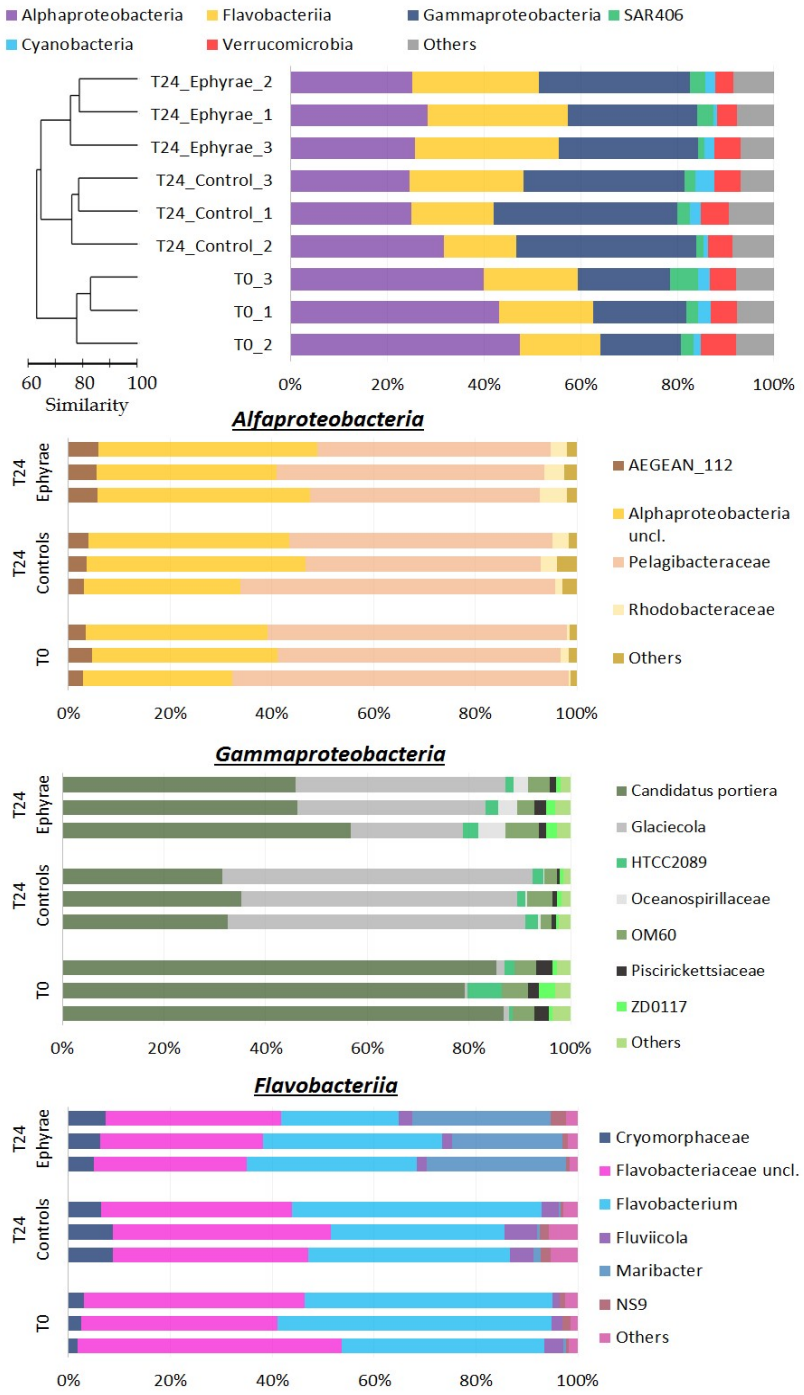

- **Figure 5:** Profiles of prokaryotic community obtained with NGS technique showing taxa with RA > 1%. Top chart report the most abundant phylum, for Proteobacteria and Bacteroidetes were reported the classes; profiles are ordered according with the cluster analysis. The three underlying bar plots are insight of taxa compositions for Alphaproteobacteria, Gammaproteobacteria and Flavobacteriia. Taxon with RA < 1% were grouped as “Others”.

most abundant taxa at T0 against T24_C and T24_E emerged how Alphaproteobacteria RA decrease similarly to values of 27.1 ± 4.0% in T24_C and of 26.5 ± 1.7% in T24_E; in T24_E Flavobacteriia RA increased to 28.2 ± 1.9% and Gammaproteobacteria RA increased to 28.9 ± 2.3%; in T24_C T24_C Gammaproteobacteria RA remarkably increased to 36.1 ± 2.5%. Verrucomicrobia, SAR406, Cyanobacteria and "others" had no significant variations in RA among clusters. Similarly to protists, an insight analysis was made on taxa composition for Alphaproteobacteria, Gammaproteobacteria and Flavobacteriia. The Gammaproteobacteria composition experienced large variations with a strong decrease of *Candidatus portiera* that at T0 had an average RA of 83.8 ± 4.0%, 49.6 ± 6.2% at T24_E and 33.0 ± 2.0% at T24_C; *Glaciecola* instead increased in RA from 1.1 ± 0.5% at T0 to 33.4 ± 10.2% at T24_E and 58.0 ± 3.4% at T24_C. The Flavobacteriia profiles of T0 and T24_C were quite similar while in T24_E largely increased the RA of Maribacter while decreased the RA of Flavobacteriaceae and unclassified *Flavobacterium*. No remarkable differences were detected for Alphaproteobacteria.

4. Discussion

4.1 Predation on microplankton

The feeding on microplankton organisms by adult stage of *Aurelia* was already been reported in literature although poorly studied (Stoecker et al., 1987; Båmstedt, 1990; Uye and Shimauchi, 2005; Malej et al.; 2007; Lo and Chen, 2008) because the majority of studies have addressed the impacts on larger organisms (e.g. Elliott and Leggett, 1997; Hansson et al., 2005; Titelman and Hansson, 2006; Moller and Riisgård, 2007; Riisgård and Madsen, 2011). Our microcosms grazing experiment was the first tentative to assess the capability of ephyrae of *Aurelia aurita* to prey on aloricate ciliates, tintinnids, micrometazoans, dinoflagellates, Coccolithophyceae, Coscinodiscophyceae, Fragilariophyceae, Dictyochophyceae, Mediophyceae and Bacillariophyceae communities. We tried

also to assess predation impact on both pigmented and heterotrophic fractions of nanoflagellates although we found no evidence of feeding activity. The estimated ingestion rates on microplanktonic taxa were quite high in comparison with prey availabilities and the 5 animals we added in each microcosm lead to a remarkable contraction in abundance and biomass of these communities in just 24 hours.

The correlation we found between relative ingestion rates and relative initial abundances and the lack of correlation between relative ingestion rates and biovolumes suggested that there was no selection based on prey sizes. Thus ephyrae seemed to prey preferentially upon what was more available. Furthermore, considering the ratios between ingestion rate and initial abundance, aloricate ciliates, tintinnids and dinoflagellates taxa exhibited values on average larger than 1 while micrometazoans, Coccolithophyceae, Bacillariophyceae and Coscinodiscophyceae had values lower than 1; only taxa belonging to Mediophyceae, Fragilariophyceae and genus *Pseudonitzschia* had ratios comparable with aloricate ciliates, tintinnids and dinoflagellates, but probably because they were in colonies of 2 organisms (a single capture's event might led to a double ingestion). We have no data on the growth rates for these organisms, however, comparing the abundances found at T0 and T24 controls with those found at T24 ephyrae-treatments we observed a stronger reduction for aloricate ciliates, tintinnids and dinoflagellates, whose average abundance value was more than halved.

This evidence suggests how ephyrae might prey selectively on some groups of organisms over others. This partially contradicts diffused evidences of *A. aurita* as generalist feeder due to its ability to exploit a wide range of marine organisms and the lack of clear evidence for patterns of prey selection (see the introduction for detailed references); nevertheless our data suggest a selective ingestion of aloricate ciliates, tintinnids and dinoflagellates for the juvenile stage of *Aurelia.* According to what reported by Suchman and Sullivan (2000) we hypothesize as possible explanation

for this evidence a differential vulnerability of the prey specifically due to difference in sizes, concentrations and motility.

Size, cells abundance and motility positively influence prey-predator encountering rate (Gerritsen and Strickler, 1976, Pastorok, 1981). About the size and the concentration, a clear difference emerged comparing the biovolumes of ingested taxa with their respective abundances: Bacillariophyceae, and Mediophyceae densities were higher than aloricate ciliates, tintinnids and dinoflagellates densities but the latter group included organisms quite larger than the former; however >75% of the ingested aloricate ciliates, tintinnids and dinoflagellates were smaller than $20x10^3$ μm^3 and thus of the same size range of Bacillariophyceae and Mediophyceae. Hence the selected prey was not the most abundant neither the largest.

The prey motility, in addition to the encounter rate, affects also the capture efficiency in agreement with the theory proposed by Costello and Colin (1994) of the marginal flow velocity; however while this theory worked for mesoplankton and micrometazoans that can exhibit relative fast swimming and thus escape strategy (Sullivan et al., 1994), it does not fit for other microplanktonic organisms whos swimming capabilities are limited. Anyhow dinoflagellates, aloricate ciliates and tintinnids are generally characterized by higher motility than Bacillariophyceae, Mediophyceae and Fragilariophyceae and prey motility may play a critical role during contact with tentacles and thus on prey recognition mechanism. Sullivan et al. (1997) demonstrated how copepod nauplii that "play-dead" after entrainment in the feeding current minimize their chance of contacting *Aurelia* ephyrae tentacles and were expelled from the subumbrella. Regula et al. (2009) hypothesize as only particles recognized as food trigger nematocyst and moreover the chemicals released form prey after contact with nematocyst stimulate the feeding behavior of scyphozoans (Arai, 1997); hydromedusa *Aglaura hematoma* that is able to prey on protists did not react to non-motile prey such as diatoms and dead nauplii (Colin et al., 2005). Hence even small differences in motility (almost no motility of

Bacillariophyceae, Mediophyceae versus relatively slow swimming of dinoflagellates, aloricate ciliates and tintinnids) might produce relevant differences in prey vulnerability and in prey selection. The analysis of protist diversity through Next-Generation Sequencing (NGS) approach allowed us to assess modifications in community compositions with a sharper resolution than with microscope analysis. This method is not free of flaws like the mismatch between the morphological concept of species and OTUs that results from a DNA segments comparison (Orsini et al., 2004); the low taxonomic accuracy of some taxa due to limitation of reference databases (we found a large amount of sequences belonging to 221 different OTUs that got lumped as "dinophyceae unclassified"); and the difficult to compare the number of sequences (NGS) with the number of organisms (microscope).

The cluster analysis made on protist OTU table shown how profiles of T0 (with the exception of T0_1) and T24 controls were more similar than profiles of T24 ephyrae-treatments; this outcome support the hypothesis that the predation exerted by ephyrae of *A. aurita* can affect protists community composition.

From the analysis of NGS data, the groups mostly impacted were ciliophora and dinophyta that incurred in a reduction of RA while stramenopiles' RA increased; these results are in accordance with what commented on the ingestion rates about the selective predation on aloricate ciliates, tintinnids and dinoflagellates. However the insight on family composition of dinophyta, ciliophora and stramenopiles revealed that although some families seemed to benefit from (*Stenosemellidae,* chrysophyceae-synurophyceae clade-F) or being disadvantaged by (*Strombilidiidae, Tintinnidae,* Raphid-Pennate) the presence of ephyrae, the variation in RA of higher taxonomic groups did not involve deep modification in their family level composition.

Against the exclusive availability of prey smaller than usual mesozooplankton, the ephyrae of *Aurelia aurita* were thus able to influence microplankton community. These small medusae likely

profit on different mechanic-physiologic features related with their small body size (5mm) that make them able to handle quite small prey (10-200 µm of size). Nevertheless this capability should be more specifically addressed also for adult stages of *Aurelia* in order to have a more detailed picture on medusae impacts during planktonic stages; furthermore ephyrae predation activity more than halve the communities of typical microplanktonic grazer with possible critical consequence on food web structure that may became even largest in light of increasing trends of abundance and blooms.

4.2 Shaping of prokaryote communities

The grazing experiment with ephyrae confirmed the influence of these animals on prokaryotic communities. During the 24h incubation the heterotrophic fraction showed an increase in abundance, especially in treated microcosms (up to +45% in terms of biomass); on the contrary *Synechococcus* abundance showed a slight decrease in the ephyrae- treatments and a slight increase at the end of controls' incubation, but differences were not statistically significant; these results are confirmed also by NGS data (mean RA varies from 2.3% at T0 to 2.4% at T24 controls and to 1.6% at T24 ephyrae-treatments). We found increasing trend within ephyrae-treatments also for heterotrophic carbon production (HCP) and the exoenzimatic activity of leucine aminopeptidase that fairly correlated and supported the growth of HB population.

These results agreed with experimental data of Turk et al. (2008) and field observation of Riemann et al. (2006); although in other experiments with longer incubation higher HCP values were achieved. Tinta et al. (2012) when exposing bacteria to jellyfish homogenate (12.5 g L^{-1} w/w) obtained an average HCP of 11.8 µgC L^{-1} h^{-1} after 3 days of incubation while Blanchet et al. (2014) providing DOM from jellyfish (more bioavailable) achieved HCP > 10 µgC L^{-1} h^{-1} already within the 1st day.

On the contrary, in our experiment medusae were alive and according with what reviewed by Pitt et al. (2009), they might have enriched the microcosms in organic matter (and inorganic nutrients)

through the production of mucus, faeces and excretions; also sloppy feeding and egestion of partially digested prey might play an important role although their effects are not yet studied. All these sources of organic matter can be used to sustain bacterial growth. It has been previously reported that excretion produces mainly labile or superlabile N-rich organic matter (Pitt et al., 2009). On the contrary, very few information are available on the potential utilization of jellyfish-derived mucus. Mucus of *Aurelia* has been shown to have the same biochemical composition of the animal's body (Ducklow and Mitchell, 1979), is produced in large quantity (Heeger and Möller, 1987; Arai, 1997) but it might not be immediately available. In fact, this matrix can be a complex and heterogeneous source of particulate (such as micro- or macro-aggregates) and dissolved organic matter (in the colloidal form) that can be slowly degraded by exoenzymes due to its biochemical and structural (3D) properties (Wells et al 2002; Pitt et al, 2009; Arnosti, 2014). Therefore, in our treated microcosms, the presence of ephyrae enhanced polysaccharide degradation by six to seven-fold the T0 value, which only doubled in controls. Moreover, we cannot exclude the influence of hydrolysis rates by prokaryotic consortia associated with the animals on the overall increase of leucine aminopeptidase activity in the treatments, since we detected exceptionally high proteolysis when testing this metabolic feature on single ephyrae (ca. 1 µmol ind^{-1} h^{-1}). Surprisingly, at T24 we detected a slower HCP and higher prokaryotic abundance in the treated microcosms. These data imply a 2.5-fold lower specific growth rate (HPC/HP biomass) than in controls. Since the community growth rate is the overall consequence of several drivers such as temperature (kept constant in this study), substrate availability (in terms of quantity and quality) and assemblage structure (Church, 2008), we speculate that shifts in community structure (see below) and the modified complexity of organic matter provided by ephyrae are the main causes of the observed growth rates. Indeed dissolved organic carbon concentration (DOC) at t24 did not significantly differ in the treatments (to

906.7 ± 55.0 µM) if compared to control microcosms (848.9 ± 83.7 µM) (C. Santinelli, personal communication).

The profile analysis of prokaryotic communities highlighted as modifications occurred in the natural assemblage after the incubation with ephyrae of *Aurelia*. Gammaproteobacteria and Flavobacteriia displayed an increase of RA coupled with a decrease of Alfaproteobacteria RA. The phyla that were favored by the presence of jellyfish are usually found in associations with particulate matter (Simon et al., 2002; Kirchman, 2002) and are able to degrade high-molecular weight organic compounds (Reichenbach, 1992); on the contrary the Alfaproteobacteria was composed mainly of Pelagibacteraceae (formerly known as SAR11; RA ranged from 45% to 66%) that are known to prefer oligotrophic conditions (Eiler et al., 2009).

The increment of Gammaproteobacteria was correlated with the increase of *Glaciecola* over *Candidatus Portiera*; the genus *Candidatus Portiera* is likely an error in the Greengenes database (McDonald and Hugenholtz 2014) however the taxon belongs to the order Oceanospirillales which shown the ability to degrade hydrocarbons (Mason et al., 2012; Lamendella et al. 2014). Genus *Glaciecola* grouped species usually correlated with algae (Uchida and Nakayama, 1993; Bowman et al. 1998) and thus likely able to exploit their exudates. The increment of Flavobacteriia was correlate with the increase of *Maribacter* over *Flavobacterium* and Flavobacteriaceae unclassified taxa; *Maribacter* genus is characterized by a heterotrophic metabolism (Barbeyron et al., 2008) and the capability to degrade macromolecule (Oh et al., 2011).

The reshape of prokaryotic community induced by the likely input of DOC released by living medusae is similar to the response described by Tinta et al. (2012) and Blanchet et al. (2014) to the input of organic matter derived from dead animals. Tinta et al. (2012) found a complete shift of bacteria community that resulted in final community composed only by Gammaproteobacteria and Flavobacteriia phyla; this is likely related with the lower number of 16S rRNA clone library sequences

analyzed, however it was the effect of 6 days of incubation. Blanchet and colleagues through pyrosequencing approach found that after two days of incubation the community was dominated by Gammaproteobacteria but the diversity of bacteria assemblage was unaffected; after 9 days, when the more labile fraction of organic matter was consumed, the Bacteroidetes (phylum that include Flavobacteriia) overwhelmed the community thanks to their ability to degrade polymeric compounds of organic matter (Fernández-Gómez et al. 2013).

Aurelia aurita's ephyrae were thus able to influence the occurrence of dominant bacterial taxa; the inferred alteration of DOC composition trigged a community reshape that favors clades more adapted and capable to exploit mucus-like organic matter. Since similar modifications of biodiversity were found when organic matter obtained directly from Aurelia body were provided, we can hypothesize that the lower HCP has to be imputed to a lover availability of easily utilizable DOC from live ephyrae. Interesting continuations of this topic would be to seek for a more detailed characterization of quality and liability of the organic matter excreted by medusea together with an insight into bacteria-DOC interactions.

Conflict of interest statement

The authors declare that there is no conflict of interest.

Acknowledgments

We are grateful to A Minetti, M Mavelli and T Diociaiuti who helped setting up the grazing experiment and processing samples at the optic and epifluorescence microscope. A special thanks to Dr. Alenka Malej (Marine Biology Station, Piran, Slovenia) that provided us the ephyrae of *Aurelia aurita*. This study was supported by the PERSEUS Project, managed by CONISMA, which provided the Ph. D. fellowship to LZ [grant numbers 287600]. Part of the research was funded by the project

RITMARE - La Ricerca Italiana per il Mare (coordinated by the National Research Council and funded by the Ministry for Education, University and Research within the National Research Programme 2011-2013).

References

Altschul SF, Gish W, Miller W, Myers EW, L. D. (1990). Basic Local Alignment Search Tool. *J. Mol. Biol.* 215, 403–410. doi:10.1016/S0022-2836(05)80360-2.

Arai, M. N. (1996). *A Functional Biology of Scyphozoa*. 1st ed. Springer Netherlands doi:10.1007/978-94-009-1497-1.

Arnosti, C. (2014). Patterns of Microbially Driven Carbon Cycling in the Ocean: Links between Extracellular Enzymes and Microbial Communities. *Adv. Oceanogr.* 2014, 1–12. doi:10.1155/2014/706082.

Avian, M., and Sandrini, L. R. (1994). History of scyphomedusae in the Adriatic Sea. *Bolletino della Soc. Adriat. di Sci.* 75, 5–12.

Azam, F., and Simon, M. (1989). Protein content and protein synthesis rates of planktonic marine bacteria. *Mar. Ecol. Prog. Ser.* 51, 201,213. doi:10.3354/meps051201.

Båmstedt, U. (1990). Trophodynamics of the scyphomedusae *Aurelia aurita*. Predation rate in relation to abundance, size and type of prey organism. *J. Plankton Res.* 12, 215–229. doi:10.1093/plankt/12.1.215.

Barbeyron, T., Carpentier, F., L'Haridon, S., Schüler, M., Michel, G., and Amann, R. (2008). Description of *Maribacter forsetii* sp. nov., a marine Flavobacteriaceae isolated from North Sea water, and emended description of the genus *Maribacter*. *Int. J. Syst. Evol. Microbiol.* 58, 790–797. doi:10.1099/ijs.0.65469-0.

Blanchet, M., Pringault, O., Bouvy, M., Catala, P., Oriol, L., Caparros, J., et al. (2014). Changes in bacterial community metabolism and composition during the degradation of dissolved organic matter from the jellyfish *Aurelia aurita* in a Mediterranean coastal lagoon. *Environ. Sci. Pollut. Res.* 22, 13638–13653. doi:10.1007/s11356-014-3848-x.

Bonnet, D., Molinero, J.-C., Schohn, T., and Daly-Yahia, M. N. (2012). Seasonal changes in the population dynamics of *Aurelia aurita* in Thau lagoon. *Cah. Biol. Mar.* 53, 343–347.

Bowman, J. P., Mccammon, S. a, Brown, J. L., and Mcmeekin, T. a (1998). *Glaciecola punicea* gen. nov., sp. nov. and *Glaciecola pallidula* gen. nov., sp. nov. : psychrophilic bacteria from Antarctic sea-ice habitats. *Int. J. Syst. Bacteriol.* 48, 1213–1222. doi:10.1099/00207713-48-4-1213.

Brotz, L., Cheung, W. W. L., Kleisner, K., Pakhomov, E., and Pauly, D. (2012). Increasing jellyfish populations: Trends in Large Marine Ecosystems. *Hydrobiologia* 690, 3–20. doi:10.1007/s10750-012-1039-7.

Di Camillo, C. G., Betti, F., Bo, M., Martinelli, M., Puce, S., and Bavestrello, G. (2010). Contribution to the understanding of seasonal cycle of *Aurelia aurita* (Cnidaria: Scyphozoa) scyphopolyps in the northern Adriatic Sea. *J. Mar. Biol. Assoc. United Kingdom* 90, 1105–1110. doi:10.1017/s0025315409000848.

Caron, D. a., Dam, H. G., Kremer, P., Lessard, E. J., Madin, L. P., Malone, T. C., et al. (1995). The contribution of microorganisms to particulate carbon and nitrogen in surface waters of the Sargasso Sea near Bermuda. *Deep Sea Res. Part I Oceanogr. Res. Pap.* 42, 943–972. doi:10.1016/0967-0637(95)00027-4.

Caron, D. A., Lim, E. L., Miceli, G., Waterbury, J. B., and Valois, F. W. (1991). Grazing and Utilization of Chroococcoid Cyanobacteria and Heterotrophic Bacteria By Protozoa in Laboratory Cultures and a Coastal Plankton Community. *Mar. Ecol. Prog. Ser.* 76, 205–217. doi:10.3354/meps076205.

Celussi, M., and Del Negro, P. (2012). Microbial degradation at a shallow coastal site: Long-term spectra and rates of exoenzymatic activities in the NE Adriatic Sea. *Estuar. Coast. Shelf Sci.* 115, 75–86. doi:10.1016/j.ecss.2012.02.002.

Christaki, U. (2001). Nanoflagellate predation on auto- and heterotrophic picoplankton in the oligotrophic Mediterranean Sea. *J. Plankton Res.* 23, 1297–1310. doi:10.1093/plankt/23.11.1297.

Church, M. J. (2008). "Resource Control of Bacterial Dynamics in the Sea," in *Microbial Ecology of the Oceans*, ed. D. L. Kirchman (John Wiley {&} Sons Inc., New York), 335–382. doi:10.1002/9780470281840.

Claesson, M. J., Wang, Q., O'Sullivan, O., Greene-Diniz, R., Cole, J. R., Ross, R. P., et al. (2010). Comparison of two next-generation sequencing technologies for resolving highly complex microbiota composition using tandem variable 16S rRNA gene regions. *Nucleic Acids Res.* 38,

e200. doi:10.1093/nar/gkq873.

Colin, S. P., Costello, J. H., Graham, W. M., and Higgins, J. (2005). Omnivory by the small cosmopolitan hydromedusa *Aglaura hemistoma*. *Limnol. Oceanogr.* 50, 1264–1268. doi:10.4319/lo.2005.50.4.1264.

Costello, J. H., and Colin, S. P. (1994). Morphology, fluid motion and predation by the scyphomeusa *Aurelia aurita*. *Adv. Mar. Biol.* 121, 327–334.

Decker, M. B., Brown, C. W., Hood, R. R., Purcell, J. E., Gross, T. F., Matanoski, J. C., et al. (2007). Predicting the distribution of the scyphomedusa *Chrysaora quinquecirrha* in Chesapeake Bay. *Mar. Ecol. Prog. Ser.* 329, 99–113. doi:10.3354/meps329099.

Ducklow, H. W., and Carlson, C. A. (1992). *Oceanic Bacterial Production*. , ed. K. C. Marshall US: Springer, US doi:10.1007/978-1-4684-7609-5{_}3.

Ducklow, H. W., and Mitchell, R. (1979). Composition of mucus released by coral reef coelenterates. *Limnology* 24, 706–714.

Edgar, R. C., and Flyvbjerg, H. (2015). Error filtering, pair assembly and error correction for next-generation sequencing reads. *Bioinformatics* 31, 3476–3482. doi:10.1093/bioinformatics/btv401.

Edgar, R. C., Haas, B. J., Clemente, J. C., Quince, C., and Knight, R. (2011). UCHIME improves sensitivity and speed of chimera detection. *Bioinformatics* 27, 2194–2200. doi:10.1093/bioinformatics/btr381.

Edler, L. (1979). Recomendations for marine biological studies in the Baltic sea. Phytoplankton and Chlorophyll. *Balt. Mar. Biol. 5 1-38.* 5, 1–38.

Eiler, A., Hayakawa, D. H., Church, M. J., Karl, D. M., and Rappé, M. S. (2009). Dynamics of the SAR11 bacterioplankton lineage in relation to environmental conditions in the oligotrophic North Pacific subtropical gyre. *Environ. Microbiol.* 11, 2291–2300. doi:10.1111/j.1462-2920.2009.01954.x.

Elliott, J. K., and Leggett, W. C. (1997). Influence of temperature on size-dependent predation by a fish (*Gasterosteus aculeatus*) and a jellyfish (*Aurelia aurita*) on larval capelin (*Mallotus villosus*). *Can. J. Fish. Aquat. Sci.* 54, 2759–2766. doi:10.1139/f97-190.

Fernández-Gómez, B., Richter, M., Schüler, M., Pinhassi, J., Acinas, S. G., González, J. M., et al. (2013). Ecology of marine Bacteroidetes: a comparative genomics approach. *Isme J.* 7, 1026–

1037. doi:10.1038/ismej.2012.169.

Frost, B. W. (1972). Effects of size and concentration of food particles on the feeding behavior of the marine planktonic copepod *Calanus pacificus*. *Limnol. Oceanogr.* 17, 805–815. doi:10.4319/lo.1972.17.6.0805.

Gerritsen, J., and Strickler, J. R. (1977). Encounter Probabilities and Community Structure in Zooplankton: a Mathematical Model. *J. Fish. Res. Board Canada* 34, 73–82. doi:10.1139/f77-008.

Hansson, L. J., Moeslund, O., Kiørboe, T., and Riisgård, U. (2005). Clearance rates of jellyfish and their potential predation impact on zooplankton and fish larvae in a neritic ecosystem (Limfjorden, Denmark). *Mar. Ecol. Prog. Ser.* 304, 117–131. doi:10.3354/meps304117.

Heeger, T., and Möller, H. (1987). Ultrastructual observations on prey capture and digestion in the scyphomedusa *Aurelia aurita*. *Mar. Biol.* 96, 391–400. doi:10.1038/470444a.

Hoppe, H.-G. (1993). Use of fluorogenic model substrates for extracellular enzyme activity (EEA) measurement of bacteria. *Handb. methods Aquat. Microb. Ecol.*, 423–431.

Kirchman, D., K'nees, E., and Hodson, R. (1985). Leucine incorporation and its potential as a measure of protein synthesis by bacteria in natural aquatic systems. *Appl. Environ. Microbiol.* 49, 599–607.

Kirchman, D. L. (2002). The ecology of Cytophaga-Flavobacteria in aquatic environments. *FEMS Microbiol Ecol* 39, 91–100.

Kogovšek, T., Bogunović, B., and Malej, A. (2010). Recurrence of bloom-forming scyphomedusae: Wavelet analysis of a 200-year time series. *Hydrobiologia* 645, 81–96. doi:10.1007/s10750-010-0217-8.

Lamendella, R., Strutt, S., Borglin, S., Chakraborty, R., Tas, N., Mason, O. U., et al. (2014). Assessment of the Deepwater Horizon oil spill impact on Gulf coast microbial communities. *Front. Microbiol.* 5, 130. doi:10.3389/fmicb.2014.00130.

Lo, W. T., and Chen, I. L. (2008). Population succession and feeding of scyphomedusae, *Aurelia aurita*, in a eutrophic tropical lagoon in Taiwan. *Estuar. Coast. Shelf Sci.* 76, 227–238. doi:10.1016/j.ecss.2007.07.015.

Lynam, C. P., Lilley, M. K. S., Bastian, T., Doyle, T. K., Beggs, S. E., and Hays, G. C. (2011). Have jellyfish in the Irish Sea benefited from climate change and overfishing? *Glob. Chang.*

Biol. 17, 767–782. doi:10.1111/j.1365-2486.2010.02352.x.

Malej, a., Turk, V., Lučić, D., and Benović, A. (2007). Direct and indirect trophic interactions of *Aurelia* sp. (Scyphozoa) in a stratified marine environment (Mljet Lakes, Adriatic Sea). *Mar. Biol.* 151, 827–841. doi:10.1007/s00227-006-0503-1.

Martin, M. (2011). Cutadapt removes adapter sequences from high-throughput sequencing reads. *EMBnet.journal* 17, 10–12. doi:10.14806/ej.17.1.200.

Mason, O. U., Hazen, T. C., Borglin, S., Chain, P. S., Dubinsky, E. A., Fortney, J. L., et al. (2012). Metagenome, metatranscriptome and single-cell sequencing reveal microbial response to Deepwater Horizon oil spill. *Isme j* 6, 1715–1727. doi:10.1038/ismej.2012.59.

McDonald D., and Hugenholtz, P. (2014). "Pelagibacteraceae" (and SAR86 clade) [Online forum comment]. Available at: https://groups.google.com/forum/{#}!msg/qiime-forum/8QfE3ta{_}NiE/Npwf6xJUFzgJ.

Menden-Deuer, S., and Lessard, E. J. (2000). Carbon to volume relationships for dinoflagellates, diatoms, and other protist plankton. *Limnol. Oceanogr.* 45, 569–579. doi:10.4319/lo.2000.45.3.0569.

Mills, C. E. (2001). Jellyfish blooms: Are populations increasing globally in response to changing ocean conditions? *Hydrobiologia* 451, 55–68. doi:10.1023/A:1011888006302.

Møller, L. F., and Riisgård, H. U. (2007). Feeding, bioenergetics and growth in the common jellyfish *Aurelia aurita* and two hydromedusae, *Sarsia tubulosa* and *Aequorea vitrina*. *Mar. Ecol. Prog. Ser.* 346, 167–177. doi:10.3354/meps06959.

Oh, H.-M., Kang, I., Yang, S.-J., Jang, Y., Vergin, K. L., Giovannoni, S. J., et al. (2011). Complete genome sequence of strain HTCC2170, a novel member of the genus *Maribacter* in the family Flavobacteriaceae. *J. Bacteriol.* 193, 303–304. doi:10.1128/JB.01207-10.

Olenina, I., Hajdu, S., Edler, L., Wasmund, N., Busch, S., Göbel, J., et al. (2006). Biovolumes and size-classes of phytoplankton in the Baltic Sea. *HELCOM Balt.Sea Environ. Proc.* 106, 1–44.

Omori, M., Ishii, H., and Fujinaga, A. (1995). Life history strategy of *Aurelia aurita* (Cnidaria, Scyphomedusae) and its impact on the zooplankton community of Tokyo Bay. *ICES J. Mar. Sci.* 52, 597–603. doi:10.1016/1054-3139(95)80074-3.

Orsini, L., Procaccini, G., Sarno, D., and Montresor, M. (2004). Multiple rDNA ITS-types within the diatom *Pseudo-nitzschia delicatissima* (Bacillariophyceae) and their relative abundances

across a spring bloom in the Gulf of Naples. *Mar. Ecol. Ser.* 271, 87–98. doi:10.3354/meps271087.

Pastorok, R. a (1981). Prey Vulnerability and Size Selection by Chaoborus Larvae. *Ecology* 62, 1311–1324.

Pitt, K. a., Welsh, D. T., and Condon, R. H. (2009). Influence of jellyfish blooms on carbon, nitrogen and phosphorus cycling and plankton production. *Hydrobiologia* 616, 133–149. doi:10.1007/s10750-008-9584-9.

Porter, K. G., and Feig, Y. S. (1980). The Use of Dapi for Identifying and Counting Aquatic Microflora. *Limnol. Oceanogr.* 25, 943–948.

Purcell, J. E. (2012). Jellyfish and Ctenophore Blooms Coincide with Human Proliferations and Environmental Perturbations. *Ann. Rev. Mar. Sci.* 4, 209–235. doi:10.1146/annurev-marine-120709-142751.

Regula, C., Colin, S. P., Costello, J. H., and Kordula, H. (2009). Prey selection mechanism of ambush-foraging hydromedusae. *Mar. Ecol. Prog. Ser.* 374, 135–144. doi:10.3354/meps07756.

Reichenbach, H. (1992). "The Order Cytophagales," in *The prokaryotes*, ed. D. M. H. W. S. K. H. Balows A. Trüper H. G. (Springer-Verlag, New York), 549–590. doi:10.1007/0-387-30747-8.

Richardson, A. J., Bakun, A., Hays, G. C., and Gibbons, M. J. (2009). The jellyfish joyride: causes, consequences and management responses to a more gelatinous future. *Trends Ecol. {&} Evol.* 24, 312–322. doi:10.1016/j.tree.2009.01.010.

Riemann, L., Titelman, J., and Båmstedt, U. (2006). Links between jellyfish and microbes in a jellyfish dominated fjord. *Mar. Ecol. Prog. Ser.* 325, 29–42. doi:10.3354/meps325029.

Riisgård, H. U., and Madsen, C. V (2011). Clearance rates of ephyrae and small medusae of the common jellyfish *Aurelia aurita* offered different types of prey. *J. Sea Res.* 65, 51–57. doi:10.1016/j.seares.2010.07.002.

Shan, Z., Xiaoxia, S. U. N., Yantao, W., and Song, S. U. N. (2015). Significance of Different Microalgal Species for Growth of Moon Jellyfish Ephyrae, *Aurelia* sp . 1. *J. Ocean Univ. China* 14, 823–828. doi:10.1007/s11802-015-2775-x.

Simon, M., Grossart, H., Schweitzer, B., and Ploug, H. (2002). Microbial ecology of organic aggregaes in aquatic ecosystems. *Aquat. Microb. Ecol.* 28, 175–211. doi:10.3354/ame028175.

Smith, D. C., and Azam, F. (1992). A simple, economical method for measuring bacterial protein synthesis rates in seawater using ^{3}H-leucine. *Mar. Biol. Res.* 6, 107–114.

Stoeck, T., Bass, D., Nebel, M., Christen, R., Jones, M. D. M., Breiner, H. W., et al. (2010). Multiple marker parallel tag environmental DNA sequencing reveals a highly complex eukaryotic community in marine anoxic water. *Mol. Ecol.* 19, 21–31. doi:10.1111/j.1365-294X.2009.04480.x.

Stoecker, D. K., Michaels, A. E., and Davis, L. H. (1987). Grazing by the jellyfish, *Aurelia aurita*, on microzooplankton. *J. Plankton Res.* 9, 901–915. doi:10.1093/plankt/9.5.901.

Suchman, C. L., and Sullivan, B. K. (2000). Effect of prey size on vulnerability of copepods to predation by the scyphomedusae *Aurelia aurita* and *Cyanea* sp. *J. Plankton Res.* 22, 2289–2306. doi:10.1093/plankt/22.12.2289.

Sullivan, B. K., Garcia, J. R., and Klein--MacPhee, G. (1994). Prey selection by the scyphomedusan predator *Aurelia aurita*. *Mar. Biol.* 121, 335–341.

Sullivan, B. K., Suchman, C. L., and Costello, J. H. (1997). Mechanics of prey selection by ephyrae of the scyphomedusa *Aurelia aurita*. *Mar. Biol.* 130, 213–222. doi:10.1007/s002270050241.

Tinta, T., Kogovšek, T., Malej, A., and Turk, V. (2012). Jellyfish Modulate Bacterial Dynamic and Community Structure. *PLoS One* 7, e39274. doi:10.1371/journal.pone.0039274.

Titelman, J., and Hansson, L. J. (2006). Feeding rates of the jellyfish *Aurelia aurita* on fish larvae. *Mar. Biol.* 149, 297–306. doi:10.1007/s00227-005-0200-5.

Turk, V., Lucic, D., Flander-Putrle, V., and Malej, A. (2008). Feeding of *Aurelia* sp . (Scyphozoa) and links to the microbial food web. *Mar. Ecol.* 29, 495–505. doi:10.1111/j.1439-0485.2008.00250.x.

Uchida, M., and Nakayama, A. (1993). Isolation of Laminaria-frond Decomposing Bacteria from Japanese Coastal Waters. *Nippon Suisan Gakkaishi* 59, 1865–1871. doi:10.2331/suisan.59.1865.

Utermöhl, H. (1958). Zur Vervollkommnung der quantitativen Plankton-Methodik. *Mitt. Int. Ver. Theor. Angew. Limnol.* 9, 1–38.

Uye, S., and Shimauchi, H. (2005). Population biomass, feeding, respiration and growth rates, and carbon budget of the scyphomedusa *Aurelia aurita* in the Inland Sea of Japan. *J. Plankton Res.* 27, 237–248. doi:10.1093/plankt/fbh172.

Walters, W. A., Caporaso, J. G., Lauber, C. L., Berg-Lyons, D., Fierer, N., and Knight, R. (2011). PrimerProspector: de novo design and taxonomic analysis of barcoded polymerase chain reaction primers. *Bioinformatics* 27, 1159–1161. doi:10.1093/bioinformatics/btr087.

Wells, M. L. (2002). "Marine colloids and trace metals," in *Biogeochemistry of Marine Dissolved Organic Matter*, eds. D. A. Hansell and C. A. Carlson (Academic Press, San Diego), 367–404. doi:http://dx.doi.org/10.1016/B978-012323841-2/50009-9.